People's Democratic Republic of Algeria

Ministry of Higher Education and Scientific Research

University M'Hamed BOUGARA- Boumerdes

Institute of Electrical and Electronic Engineering

Department of Power and Control

Project Report Presented in Partial Fulfilment of

the Requirements of the Degree of

'MASTER'

In Electrical and Electronic engineering

Option: Power Engineering

Title:

CONTROL DESIGN OF PUC5-BASED MULTIFUNCTION SOLAR ACTIVE FILTER

Presented By:

- **DJELLOUL Ammar**
- **SAHLI Mohamed Rafik**

Supervisor:

Prof. KHELDOUN Aissa

Registration Number:……/2022

Dedication

This work is dedicated to my darling parents, who have been a wonderful supporter until the end of my project, to my brothers, sisters, family and friends, who has been encouraging me diligently with their fullest and truest attention to complete my work.

To IGEE's staff

Thank you all

Ammar

This work is dedicated to my dear parents, who has been nicely my supporters until my research was fully finished, to my beloved sisters for the inspiring words of encouragement and push, to my family and my friends.

to the teachers and all the staff of IGEE.

Thank you all

Mohamed Rafik

Acknowledgement

Alhamdulillah, all praises to Allah for the strengths and His blessing in completing this thesis.

We would like to express our gratitude to our supervisor ***Pr. A.Kheldoune****, who guided us throughout this project and made this work possible. His guidance and advice carried us through all the stages of writing our project.*

A special thanks goes to the PhD student ***Mr. AYACHI AMOR Yacine*** *for the help with useful tips and remarks.*

Abstract

This work presents a Solar Photovoltaic Active Power Filter system (PV-APF) whose architecture basically consisted of a PV generator as primary renewable source three-phase double stage power converters (DC-DC, DC-AC), utility grid and non-linear load connected through Point of Common Coupling (PCC). In addition to the PV power injection the system intended to operate as an Active Power Filter (APF) to filter the harmonic pollution form the non-linear load. Based on the p-q theory, the PV-APF extracts the fundamental and harmonics information from the polluted load current in order to estimate a compensating reference current that should be injected along with a maximum photovoltaic power extracting (P_{PV}).

Moreover, we have investigated the use of new topology inverter that is the packed U-cell 5 levels (PUC5) inverter and compared with the conventional two-level inverter. The comparable simulations of the PV-APF based on each inverter revealed the superiority of the PUC5 inverter in terms power quality improvement and achieved THD levels. According to obtained results of simulation, under standard test condition (STC) with a disconnected nonlinear load, the classical inverter measures THD of 1.24% in output current, whereas in case of using the PUC5 inverter and under the same conditions the THD was 0.19%.

Keywords–Shunt active power filter (SAPF), Photovoltaic (PV), Maximum power point tracking (MPPT), instantaneous active and reactive power theory (p-q), Total harmonic distortion (THD), Packed U-cell 5 levels inverter (PUC5), Perturb and observe (P&O), Model predictive control (MPC).

Table of Contents

Dedication I

Acknowledgment II

Abstract III

List of figures VII

List of tables IX

List of abbreviations X

General introduction 1

Chapter I: ***Power System and Challenges***

1.1 Chapter overview 3

1.2 Electrical Power generation 3

1.3 Power quality 3

1.4 Grid Connected PV System 4

1.5 General types of Power Quality Problems 4

1.6 Harmonics 7

1.6.1 Voltage and Current Harmonics 8

1.6.2 Harmonic Sources in Power System 8

1.6.3 Harmonics effect 9

1.6.4 Harmonics solution 9

1.6.4.1 Conventional solution 9

1.6.4.1.1 Passive Harmonic Mitigation Techniques 9

1.6.4.2 Advanced techniques for harmonics mitigation 11

1.6.4.2.1 Active filter 11

1.6.4.2.2 Hybrid harmonic mitigation techniques 12

1.7 Conclusion 12

Chapter II: ***Modeling of Solar Active Filter***

2.1 Introduction 13

2.2 Structure of photovoltaic system 13

2.2.1 PV cell 13

2.2.2 PV module 15

2.2.3 PV array 15

2.3 Maximum power point of solar array 16

2.3.1 Effect of solar irradiance and temperature on photovoltaic array 16
2.3.1.1 Effect of solar irradiation on characteristic curves 17
2.3.1.2 Effect of solar irradiation on characteristic curves 17
2.3.2 Maximum Power Point Tracking (MPPT) 18
2.4 Boost Converter 18
2.4.1 Overview of Boost Converter 18
2.4.2 Working of DC-DC Boost Converter 19
2.5 DC Link Capacitor & Voltage 21
2.6 DC-AC Inverter 21
2.6.1 Classical Two-Level Inverter 21
2.6.2 Packed U-Cell 5-level inverter (PUC5) 22
2.7 Synchronization 24
2.8 Non-Linear Loads 24
2.9 Filters 25
2.9.1 L Passive Filters 25
2.9.2 Active Power Filters (APF) 26
2.10 Conclusion 27

Chapter III: *System Control Strategy*

3.1 Introduction 28
3.2 PQ Theory 28
3.3 Classical three phase Inverter (2-Level) 30
3.3.1 p-q Modified Power Injection 30
3.3.2 Voltage Regulator: 31
3.3.3 Hysteresis Current Controller (HCC) 31
3.3.4 Active and Reactive Power Flow 32
3.4 Perturb & Observe (P&O) 33
3.5 Packed U-Cell Three Phase Inverter (5-Level) 34
3.5.1 Model Predictive Control (MPC) 35
3.5.2 Active and Reactive Power Management 37
3.5.3 Modified pq theory for three-phase PUC5 inverter: 38
3.6 Conclusion 39

Chapter IV: *Simulation and Results*

4.1 Introduction 40
4.2 Solar-AF using MATLAB environment 40
4.2.1 Solar-AF Parameters 41
4.2.2 Environment condition 42
4.3 Solar-AF with Classical Three-phase inverter 43
4.3.1 Simulation Results 44
4.3.1.1 System under STC 45
4.3.1.2 System performance under decreasing of irradiance 46
4.3.1.3 System performance at irradiance of 500 W/m^2 47
4.3.1.4 System performance at irradiance of 600 W/m^2 48
4.3.1.5 System performance under increased load demand 48
4.3.1.6 System performance during a decreasing irradiance 50
4.3.1.7 System performance at irradiance of 0 W/m^2 50
4.3.1.8 System with an increasing irradiance 51
4.3.1.9 System performance at irradiance of 1000 W/m^2 with extra load demand 52
4.3.1.10 System performance without load 52
4.4 PUC5 Three-phase inverter-based Solar-AF 53
4.4.1 Simulation Results 55
4.4.1.1 System performance at irradiance of 1000 W/m^2 [0s,0.5s] 58
4.4.1.3 System performance at irradiance of 0 W/M^2 [3.75s,4.5s] 59
4.4.1.2 System performance at irradiance of 1000 w/m^2 with additional load demand [5.5s,5.75s] 59
4.4.1.4 System performance without Load [5.75s,7s] 60
4.5 Comparison and Evaluation 61
4.6 Results Discussion 62
4.7 Conclusion 62
General conclusion and future work 62
Appendix XI
Appendix A: Sim power diagram of solar-AF XI
Appendix B: MPC of solar-AF XII
Appendix C: PV module datasheet XIII
References

List of figures

Figure 1. 1 Grid connected PV system 4
Figure 1. 2 voltage waveform during voltage sag..... 5
Figure 1. 3 Voltage waveform during an interruption 5
Figure 1. 4 Voltage waveform during spike 6
Figure 1. 5 Voltage waveform during swell 6
Figure 1. 6 Voltage waveform during harmonics 6
Figure 1. 7 Voltage waveform during noise 7
Figure 1. 8 Voltage waveform during fluctuation 7
Figure 1. 9 Voltage waveform during voltage unbalance. 7
Figure 1. 10 Sinusoidal 50 Hz waveform with 3rd, 5th and 7th Harmonics. 8
Figure 1. 11 Parallel APF..... 11
Figure 1. 12 Series APF. 12
Figure 2. 1: photovoltaic cell, module and array 13
Figure 2. 2: Basic operation of a photovoltaic cell diagram..... 14
Figure 2. 3: a) Double and b) single diode models equivalent circuits 14
Figure 2. 4: Current vs voltage (I-V) characteristics of PV cell and power vs voltage (P-V) characteristics of PV cell. 15
Figure 2. 5: Series connected PV cells..... 15
Figure 2. 6: Connections of solar panels (modules) 16
Figure 2. 7: V-I characteristics of PV array..... 16
Figure 2. 8: I-V characteristics for different irradiation values 17
Figure 2. 9: I-V Characteristics for different temperature values..... 18
Figure 2. 10: Boost Converter 19
Figure 2. 11: Current flow across boost converter according to the switching states 19
Figure 2. 12: DC-DC boost converter with MPPT..... 20
Figure 2. 13: Two-level three-phase inverter 21
Figure 2. 14: Single-phase PUC Inverter..... 22
Figure 2. 15: First order low pass filter and second order low pass filter 25
Figure 2. 16: Frequency response of 1st order and 2nd order low pass filter..... 26
Figure 2. 17 Active filters 26
Figure 3. 1: Calculations for the constant instantaneous supply power control strategy 28
Figure 3. 2: Compensation of power components $\tilde{p}$,q, $\tilde{p}0$ and $\overline{p}0$ in a-b-c coordinates 29
Figure 3. 3: p-q modified power injection 31
Figure 3. 4: Description of the hysteresis controller..... 32
Figure 3. 5: Active and reactive power flow of system 33
Figure 3. 6: Workflow of P&O algorithm in P-V characteristics 33
Figure 3. 7: Flowchart of P&O algorithm 34
Figure 3. 8: PUC5 Three Phase Inverter Topology 35

Figure 3. 9: Flowchart of the proposed MPC 37
Figure 3. 10: Blocks Diagram of PQ Reference Current Measurement And MPC.. 38
Figure 3. 11: Modified PQ theory for three-phase PUC5 inverter 39
Figure 4. 1: General scheme of the system..... 40
Figure 4. 2: The I-V and P-V characteristics of the used PV module (under STC) . 41
Figure 4. 3: irradiance profile 42
Figure 4. 4: load demand profile..... 42
Figure 4. 5: the simulated system of the classical inverter-based Solar-AF 43
Figure 4. 6: Demonstration PV Output Voltage, Current, Power and The DC Link for All the Simulation using the classical inverter. 44
Figure 4. 7: Active power curves of source, load and inverter during the simulation time using classical inverter..... 44
Figure 4. 8: A) Source, load and inverter reactive power in all the simulation using classical inverter 45
Figure 4. 9: Display of grid current, load current and filter current under 1000W/m^2 46
Figure 4. 10: FFT analysis tool for the source current under 1000W/m^2 46
Figure 4. 11: Display of grid current, load current and filter current under 500W/m^2 47
Figure 4. 12: FFT analysis tool for the source current under 500W/m^2 47
Figure 4. 13: Display of grid current, load current and filter current under 600W/m^2 48
Figure 4. 14: FFT analysis tool for the source current under 600W/m^2 48
Figure 4. 15: Display of grid current, load current and filter current with additional load demand..... 49
Figure 4. 16: FFT analysis tool for the source current under 600W/m^2 with extra load demand..... 49
Figure 4. 17: Display of grid current, load current and filter current under zero irradiance. 50
Figure 4. 18: FFT analysis tool for the source current under 0 W/m^2 51
Figure 4. 19: Display of grid current, load current and filter current during increasing irradiance condition. 51
Figure 4. 20: FFT analysis tool for the source current System under 1000 W/m^2 with extra load demand..... 52
Figure 4. 21: Display of grid current, load current and filter current under no load condition. 53
Figure 4. 22: FFT analysis tool for the source current of the system without load .. 53
Figure 4. 23: the simulated system of the three phase PUC5 inverter-based Solar-AF 54
Figure 4. 24: Demonstration PV Output Voltage, Current, Power and The DC Link of phase A for All the Simulation using PUC5..... 55
Figure 4. 25: Display of the output power of phases A, B and C..... 55

Figure 4. 26: Active power curves of source, load and inverter during the simulation time using PUC5 inverter 56
Figure 4. 27: Source, nonlinear load and inverter reactive power in all the simulation using PUC5 inverter..... 56
Figure 4. 28: Source current and source voltage 57
Figure 4. 29: The DC link voltages at each phase in all the simulation 57
Figure 4. 30: demonstration of a one phase output voltage of PUC5 inverter 57
Figure 4. 31: demonstration of grid current, load current and filter current under 1000W/m^2 (PUC5 inverter)..... 58
Figure 4. 32: FFT analysis tool for the source current of the system under 1000 W/m^2(PUC5 inverter) 58
Figure 4. 33: Demonstration grid current, load current and filter current under 0 W/m^2 (PUC5 inverter)..... 59
Figure 4. 34: FFT analysis tool for the source current of the system under 0 W/m^2 (PUC5 inverter)..... 59
Figure 4. 35: FFT analysis tool for the source current of the system under 1000 W/m^2 (PUC5 inverter)..... 60
Figure 4. 36: Demonstration grid current, load current and filter current without load 60
Figure 4. 37: FFT analysis tool for the source current of the system without load (PUC5 inverter)..... 61

List of tables

Table 2. 1: The switching states in a two-level three-phase inverter..... 22
Table 2. 2: Switching States and Voltage Levels of the PUC Inverter..... 23
Table 3. 1: Switching states and voltage levels of the MPUC5 Inverter. 36
Table 4. 1: the general parameters values of the Sola-AF. 41
Table 4. 2: Comparison in terms of THD, power factor and power loss between Classical inverter and PUC5 inverter-based Solar-AF systems..... 61

List of abbreviations

IEEE	Institute of Electrical and Electronic Engineers
UPS	Uninterruptible Power Supply
GPV	Grid Connected PV System
LED	Light Emitting Diode
RMS	Root Mean Square
PQ	Power Quality
PF	Power Factor
APF	Active Power Filters
SMPS	Switch Mode Power Supplies
PV	Photo Voltaic
AC	Alternative Current
MPPT	Maximum Power Point Tracking
DC	Direct Current
HVDC	High Voltage Direct Current
VSD	Variable Speed Drive
VSI	Voltage Source Inverter
HF	Hybrid Filter
THD	Total Harmonic Distortion
IGBT	Insulated Gate Bipolar Transistor
PWM	Pulse Width Modulation
SAPF	Shunt Active Power Filter
P & O	Perturbation and Observation
STC	Standard Test Condition
HC	Hill Climbing
SVPWM	Space Vector Pulse Width Modulation
IC	Incremental Conductance
MOSFET	Metal Oxide Semiconductor Field Effect Transistor
PUC	Packed U Cell Inverter
PLL	Phase Locked Loop
p – q	Instantaneous Active and Reactive Power
PCC	Point of Common Coupling
HB	Hysteresis Band
MPC	Model Predictive Control
HCC	Hysteresis Current Control

General Introduction

Energy is playing a vital role for a sustainable economy of nations and the driving force for social and financial growth [1]. The electric energy demand in the world is increasing every year [2], and most of the energy is produced by conventional sources that contribute in the environment pollution. In the recent years, the renewable energy resources have been found to have a significant role in electrical power generation systems for being environment-friendly, secure and for other desirable features that give it advantage comparing to conventional fuels [3], thus renewable energy resources meet around 13.5% of the global energy demand [4], and the solar photovoltaic (PV) renewable energy system has gained a major importance [5].

A grid connected PV system as proposed in this project injects power to the network without any need of an energy storage device. A three-phase grid connected photovoltaic systems is to be studied. The most common components of grid connected PV system (GPV) includes PV array, DC-DC converter and a voltage source inverter (VSI). The DC-DC converter ensures the extraction of the maximum power from the PV array.

In the system under consideration, A double stage GPV has been adopted where a perturb and observe (P&O) based algorithm has been used for the maximum power point tracking operation (MPPT). In a double stage GPV, where the DC-DC boost converter ensures the maximum power point tracking (MPPT) in addition to VSI which converts the DC into AC power, whereas in a single stage system the DC-DC converter could be eliminated, by including the MPPT control in VSI control. Both single stage and double stage three-phase VSC based GPV systems perform the control of active power, reactive power compensation and DC voltage regulation features and other power quality issues are covered too.

The power quality deterioration is dramatically affected by harmonics, which are one of the most important challenges in the power system network. The harmonic pollution is a result of drawing harmonic currents from the distribution system, the non-linear loads are the main source of it. A variety of nonlinear loads have become largely used in residential and industrial domains. The domestic loads like, TVs, computers, uninterruptible power supply (UPS) equipments and battery chargers…etc, and industries like arc rectifiers, furnaces and welding machines etc.

Also, the use of power electronic Chas been extended due to its achieved developments, but the use of power electronic devices that produce harmonics and distort the source current and voltage waveforms should be put under consideration too. These power electronics are considered as non-linear loads, such as variable-speed drives, light-emitting diode (LED) lamps, switch-mode power supplies and uninterruptible power supplies. [6] [7].

Thus, harmonic elimination is a serious concern in power systems. Passive filter (LC) and active power filters (APFs) have been proposed to eliminate harmonics in the distribution system. LC filters are employed to filter out the undesirable harmonics produced by VSI; However, they cannot effectively mitigate the harmonics produced by the non-linear loads. APFs are designed for harmonic issues in power systems APFs thanks to its rapid response to the load variations. We distinguish two categories of

APFs, series APFs which are applied to fix harmonic problems for voltages, and shunt APFs which provide a better harmonic compensation for currents non-linear loads. [8]

The SAPF acts as a controlled current source connected in parallel with the non-linear load, the control technique is used to compensate harmonic pollution along the power line caused by a three-phase diode bridge rectifier followed by passive load (RL).[9][10] The control strategy is known as pq theory which takes part in providing the APF with the reference signal, in order to generate the compensating load current.

Two categories of APF have been employed in this report, the first is based on Classical 2-level 3-phase inverter while the other is based on Packed U-Cell 5-level three phase inverter. Both the inverters differ in topology, their strategies of control and performance.

In this report, the project is presented in four chapters:

- Chapter I: This chapter covers an overview about power generation that nowadays necessitates the conversion into renewable resources. In addition to the concept of power related problems which are briefly classified in this chapter. Harmonics in the main concern of this project, with quick description of the harmonic's mitigation methods.
- Chapter II: This chapter gives the needed background to understand the power circuit of the proposed system, providing detailed descriptions of the components involved in the Solar-AF.
- Chapter III: An investigation into the adopted control strategies is conducted in this chapter such MPPT, voltage regulators and two different controllers for two different inverters.
- Chapter IV: In this chapter, the simulation of Solar-AF with changeable modes of operation based on distinct inverters provides disparate results, where a comparison between the two is handled.

Chapter 01

Power System and Challenges

1.1 Introduction

The deep integration of renewable energy resources particularly solar photovoltaic (PV), is dependent on low-cost technological improvements in worldwide emissions and precise power quality techniques. The Power quality (PQ) issues in power utility distribution systems are not modern, but their consequences have recently gained attention.

The power electronics-based equipment which involve adjustable-speed motor drives, electronic power supplies, battery chargers, DC motor drives and electronic ballasts appear to be major causes of harmonic distortion in a distribution system, causing an increase in PQ-related issues. Harmonics have a variety of undesirable distribution system consequences. In grid-connected systems, several current and voltage harmonics affect the system performances.

Passive filters (PFs) and active power filters (APFs) are effective solutions to several of these problems. The passive filtering is the simplest conventional solution to mitigate the harmonic distortion, however, PFs increase the cost, size, and weight of a high-power system. On the other hand, APFs have a number of advantages over the passive filters [11].

1.2 Electrical Power generation

The apparent increase in demand for electricity in recent years has been related to quality measures of 1 and social economic progress. According to current forecasts, the global electrical energy consumption will keep rising [12]. Energy sector planning is becoming increasingly important to satisfy the requirement to grow power generation.

On the other side, the socioeconomic scenario and critical environmental effects resulting from the development of large-scale conventional power plants, in addition to the usage of fossil-fuel-based energy sources which include coal, gas and oil have motivated governments and researchers around the world to search for advanced solutions and techniques to fulfill growing electricity demand. Electric energy generation from alternative and renewable sources has been regarded a viable method for increasing energy supply in this setting [13], and promote global energy diversification by combining electrical power system modernization, environmental aggression reduction and financial economics [14].

1.3 Power quality

The Power Quality (PQ) has become a principal issue to electricity consumers at all levels of usage. The PQ issue is defined as “Any power problem manifested in voltage, current, or frequency deviations that results in failure or disoperation of

customer equipment". The development of power electronics based equipment has a significant impact on quality of electric power supply. The switch mode power supplies (SMPS), dimmers, current regulator, frequency converters, low power consumption lamps, arc welding machines…etc, are some out of the many vast applications of power electronics-based devices. The operation of this loads generates harmonics, thus pollutes the modern distribution system.

The growing interest in the utilization of renewable energy resources for electric power generation is making the electric power distribution network more susceptible to power quality problems. In such conditions both electric utilities and end users of electric power are increasingly concerned about the quality of electric power. Many efforts have been taken by utilities to achieve consumers requirement; some consumers require a higher level of power quality than the level provided by modern electric networks [15].

1.4 Grid Connected PV System

Grid connected PV systems in the world account for about 99% of the installed capacity compared to stand alone systems, which use batteries. Battery-less grid connected PV system are cost effective and require less maintenance. The generated power is uploaded to the grid for direct transmission, distribution and consumption. This eases the burden on other sources supplying power to the grid.

The network consists of grid, load and PV array, which generates a certain amount of power. A DC/DC converter, which is also used as a power optimizer, is equipped with control functions such as Maximum Power Point Tracking (MPPT). The PV system is integrated to the grid by means of a DC/AC inverter. [16]

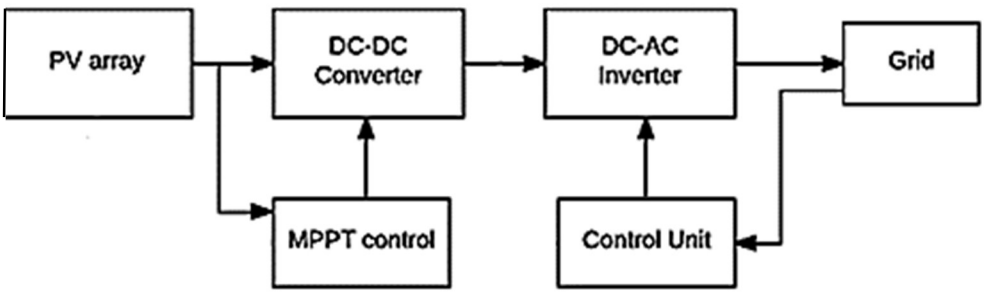

Figure 1. 1 Grid connected PV system

1.5 General types of Power Quality Problems

Power quality (PQ) problems are presently among the highest concerns. The increased utilization of electronic devices and power electronics has caused a large change in electric loads. These loads are at once the main source and the main victims

of power quality issues. All these loads cause various types of disturbances in the voltage waveform due to their non-linearity. The purpose for categorizing power quality disturbances is the existence of many strategies to manage them depending on the specific variation in concern, and categorizing will also benefit in the implementation of the correct technique and analysis.

The following are the most common types of Power Quality issues:

- Voltage sag (or dip) :

A decrease of the normal voltage level between 10% and 90% of the nominal rms voltage at the power frequency, for durations of 0,5 cycle to 1 minute [17].

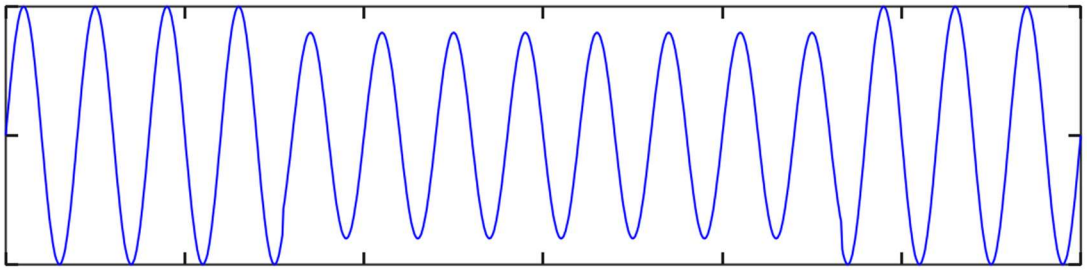

Figure 1. 2 voltage waveform during voltage sag

- Interruptions:

Short interruptions: Total interruption of electrical supply for duration from few milliseconds to one or two seconds [17].

Long interruptions: Total interruption of electrical supply for duration greater than 1 to 2 seconds [17].

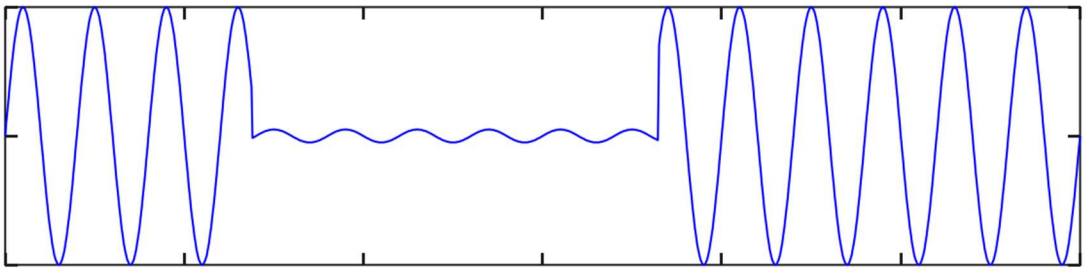

Figure 1. 3 Voltage waveform during an interruption

- Voltage spike:

Very fast variation of the voltage value for durations from a several microseconds to few milliseconds. These variations may reach thousands of volts, even in low voltage [17].

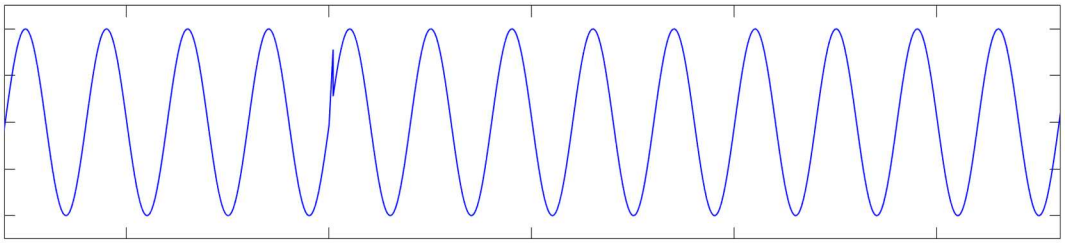

Figure 1. 4 Voltage waveform during spike

- Voltage swell :

A temporary rise in voltage outside of usual limits at the power frequency, lasting more than one cycle and often less than a few seconds [17].

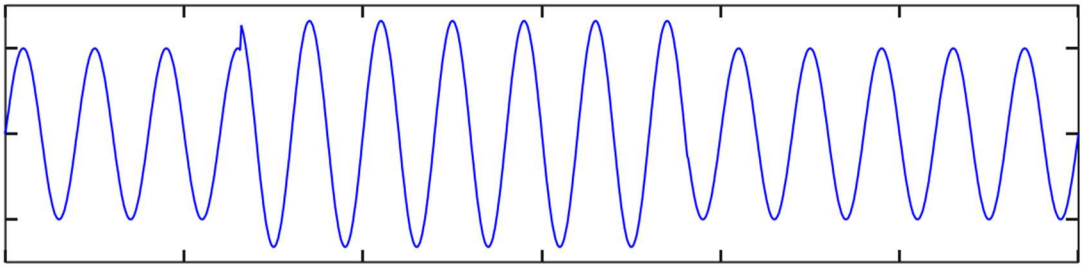

Figure 1. 5 Voltage waveform during swell

- Harmonic distortion :

Voltage or current waveforms assume non-sinusoidal shape. The waveform corresponds to the sum of different sinewaves with different magnitude and phase, having frequencies that are multiples of power-system frequency [17].

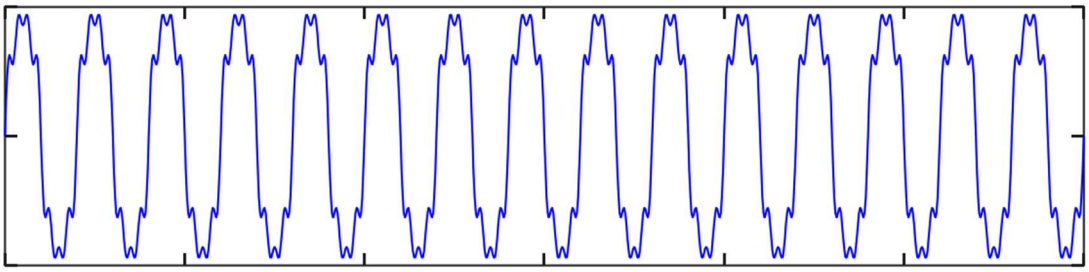

Figure 1. 6 Voltage waveform during harmonics

- Noise:

An unwanted electrical signal of high frequency from other equipment [17] .

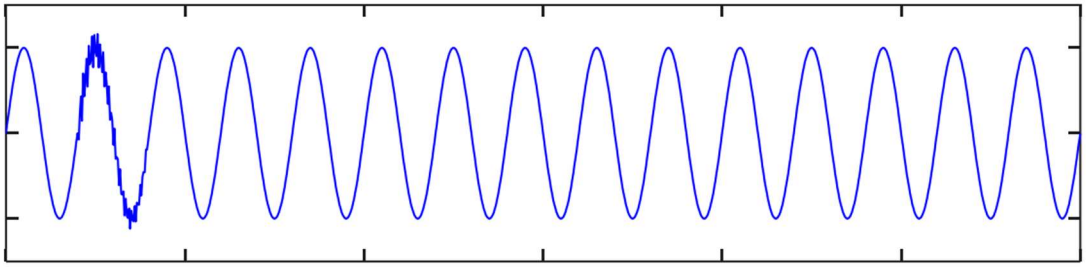

Figure 1. 7 Voltage waveform during noise

- Voltage fluctuation :

Oscillation of voltage value, amplitude modulated when device or equipment requiring a higher load are used [17].

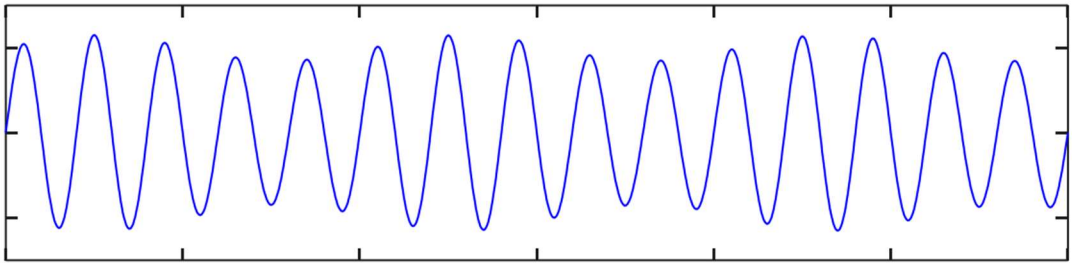

Figure 1. 8 Voltage waveform during fluctuation

- Voltage unbalance :

A voltage variation in a three-phase system in which the three voltage magnitudes or the phase-angle differences between them are not equal. [17]

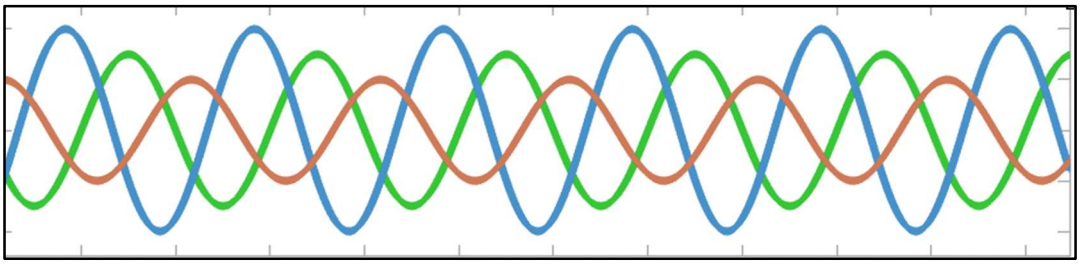

Figure 1. 9 Voltage waveform during voltage unbalance.

1.6 Harmonics

Harmonic source describes a load that returns normal power to the source at harmonic frequencies. [18]

Harmonics are produced as a result of voltage and current waveform distortion. A part of a waveform that is the integral multiple of the fundamental frequency is referred to as harmonics.

1.6.1 Voltage and Current Harmonics

The effects of voltage and current harmonics are distinct, yet they are also connected. Harmonic currents appear to be injected into the power system by non-linear loads at the consumer end. As a result, they are sometimes considered as harmonic current sources. In addition to that the harmonic voltages are the consequence of harmonic current times the control system's linear impedances. The voltage drops across the system resistances caused by the harmonic current passing through it results in voltage harmonics. Thus, voltage harmonics are a function of current harmonics and the power system's linear impedances. Fig 1.10 shows a voltage waveform of peak value equal to the secondary distribution level i.e 220 V. Likewise, it also depicts the harmonics mechanisms with amplitudes of (1/3) to (1/5) and (1/5) to (1/7) of 220V and having the frequencies three, five and seven times the essential frequency correspondingly. Assuming the voltage harmonics are due to the passage of harmonic current through a system resistance.

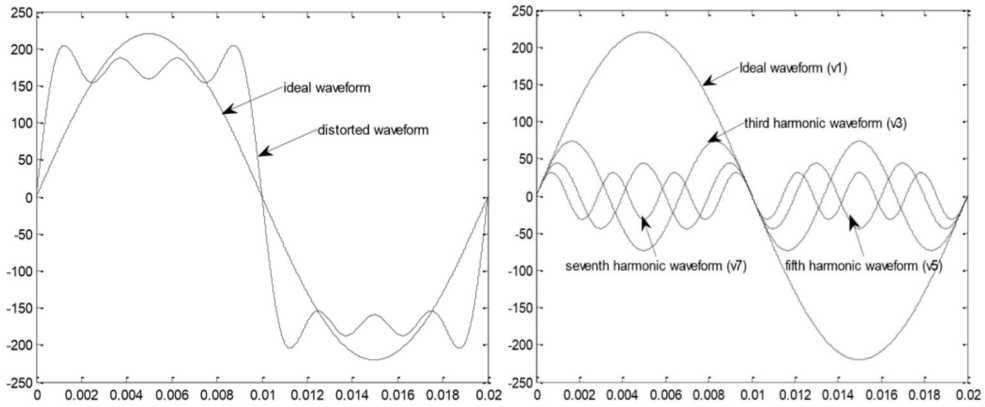

Figure 1. 10 Sinusoidal 50 Hz waveform with 3rd, 5th and 7th Harmonics.

1.6.2 Harmonic Sources in Power System:

In the electrical power system, sources of harmonics can be transformers, powerful motors and generators based on renewables, such as wind and solar energy, are connected in all voltage levels of the system and also inject current harmonics. HVDC power lines and their adjacent converter stations are considered as main source of harmonics, too. [19]

1.6.3 Harmonics effect

Harmonics are extremely harmful to the remaining power system and the equipment connected to it. The following are the primary effects of voltage and current harmonics in the power system [18]:

- The possibility of harmonic level amplification due to series and parallel resonances
- Power factor degradation
- Overheating of the phase and neutral conductors
- Efficiency of the generators is reduced day by day due to harmonics
- Eddy current and hysteresis losses in transformers
- Overheating of the system components e.g. generators, motors and transformers …etc
- Flow of additional current through power capacitors
- Decrement in the useful lives of the incandescent lamps
- Increase skin and proximity effects
- Interference problem with telecommunication
- Effects the relay protection system for the adverse effects of harmonics on the power system.

It is the major demand of the today's power system that these harmonics should be mitigated by appropriate designing of the filters either active or passive.

1.6.4 Harmonics solution

As mentioned before harmonics distortion becomes a modern concern due to the rapid development and the increase utilization of semiconductor material. In order to mitigate harmonics, effect many conventional and modern solution are proposed:

1.6.4.1 Conventional solution

Passive filtering techniques that employ single-tuned or band-pass filters are one of the most frequent ways for controlling harmonic distortion in industry. Passive harmonic filters can be designed as single-tuned elements that provide a low impedance path to harmonic currents at a punctual frequency or as band-pass devices that can filter harmonics over a certain frequency bandwidth. [20].

1.6.4.1.1 Passive Harmonic Mitigation Techniques

Harmonic pollution in an electrical network can be reduced using a variety of passive techniques, including the use of series line reactors, tuned harmonic filters, and higher pulse number converter circuits such as 12-pulse, 18-pulse, and 24-pulse rectifiers. In these approaches, undesired harmonic currents are avoided from entering the system by either adding a high series impedance to block their flow or redirecting it through a low-impedance parallel channel. [21]

- **Series Line Reactors**

The employment of series AC line reactors is a frequent and cost-effective means of raising the source impedance relative to a load, such as the input rectifier in a motor drive system. The harmonic mitigation performance of series reactors varies with load; nonetheless, when current through them decreases, their effective impedance decreases proportionally [22].

- **Tuned Harmonic Filters**

A tuned LC and high-pass filter circuit are connected in series or parallel to provide a low-impedance path for a given harmonic frequency in passive filters (PF). The tuned frequency harmonic current is diverted away from the power source by connecting the filter in parallel or series with the nonlinear load. Harmonic filters remove a single harmonic frequency from the supply current waveform rather than attenuating all harmonic frequencies.

The most efficient approach of reducing harmonic losses in the isolated power system has been found to be eliminating harmonics at their source. However, the higher initial cost of this approach implies is a deterrent. More daily expenses will build if the parallel-connected filter is connected farther upstream in the power network due to I^2R losses in the conductors and other plant items that carry the harmonic currents. In contrast, there are increasing losses in the filter itself for series-connected filters at the load. These losses are caused by the high series impedance, which blocks harmonics from flowing but increases line loss due to the flow of the remaining load current components [22, 23].

- **Higher Pulse Converters**

Low frequency current harmonics are generated by three-phase, six-pulse static power converters, such as those used in variable speed motor drive (VSD). These are mostly the 5th, 7th, 11th, and 13th harmonics, with additional higher order harmonics present but at lower levels. Harmonics of the order 6k, where k = 1, 2, 3, 4… will be present in the supply current waveform with a 6-pulse converter circuit. AC-DC converters based on the multipulse concept, particularly 12, 18 or 24 pulses, are used in high-power applications to minimize harmonics in AC supply currents. They are referred to as a multipulse converters. To generate the appropriate supply current waveforms, they use either a diode bridge or a thyristor bridge, and a phase shifting magnetic circuit [24, 25–31].

When adopting a multipulse converter, harmonics of certain orders are avoided; The 5th and 7th harmonics disappear from line current waveforms when utilizing a 12-pulse system, leaving the 11th as the first to appear. The supply current waveform will only contain harmonics of the order 12k, where k= 1, 2, 3, 4…, resulting in a high-power factor and low THD [32].

1.6.4.2 Advanced techniques for harmonics mitigation

1.6.4.2.1 Active filter

Active power filter based on injecting equal but-opposite current or voltage distortion into the network, thereby canceling the original distortion. Active harmonic filters (APFs) utilize fast-switching insulated gate bipolar transistors (IGBTs) to produce an output current of the required shape such that when injected into the AC lines, it cancels the original load-generated harmonics. To achieve pure sinusoidal wave in source (Grid) side.

Also, it could be classified as parallel or series APF according to the circuit configuration

- **Parallel APF**

This is the most widely used type of APF (preferable than series APF in terms of form and function). As the name implies, it is connected in parallel to the main power circuit as shown in Figure 1.11. The load harmonic currents are cancelled out by the filter, in order to achieve pure sine wave in source side. Parallel filters have the advantage of carrying the load harmonic current components only and not the full load current of the circuit [33–38].

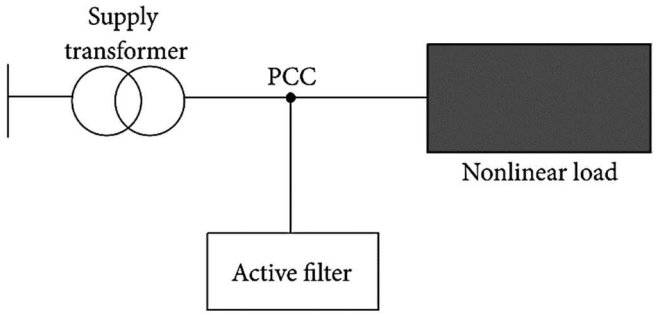

Figure 1. 11 Parallel APF.

- **Series APF**

The main circuit configuration for this type of APF is shown in Figure 1.12. The aim is to reduce voltage harmonic distortions and enhance the voltage quality delivered to the load. This is achieved by producing a sinusoidal pulse width modulated (PWM) voltage waveform across the connection transformer, which is added to the supply voltage to compensate the distortion across the supply impedance and deliver a sinusoidal voltage across the load. Series APF must carry the full load current increasing their current ratings and I^2R losses compared with parallel filters, especially across the secondary side of the coupling transformer [37].

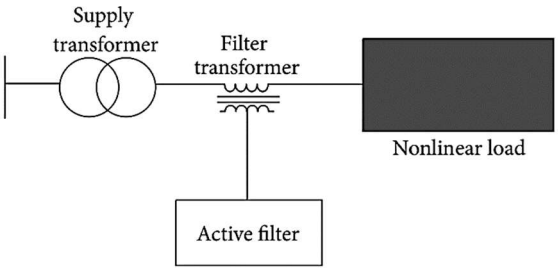

Figure 1. 12 Series APF.

1.6.4.2.2 Hybrid harmonic mitigation techniques

As shown in figure1.13 hybrid connections of Series and Parallel APF are also employed to reduce harmonics distortion levels in the network, where the PF with fixed compensation characteristics is ineffective to filter the current harmonics. APF overcomes the drawbacks of the PF by using the switching-mode power converter to perform the harmonic current elimination. However, the APF construction cost in an industry is too high, its power rating is exceptionally large. These bound the applications of APF used in the power system. Hybrid filter (HF) topologies have been developed [39–44] to solve the problems of reactive power and harmonic currents effectively. When low-cost PF is used in the HF, the active converter's power rating is lowered when compared to APF.

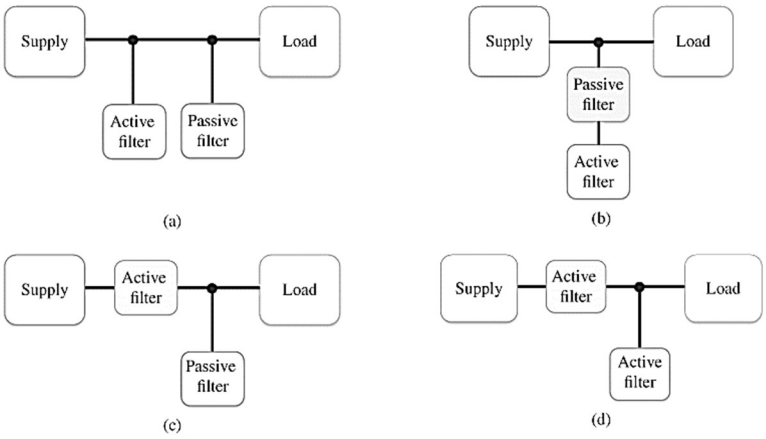

FIGURE 1. 13 Hybrid connections of active and passive filters.

1.7 Conclusion

At the end of the chapter, power quality relates to the constancy of the energy being consumed. Critical equipment can be damaged or malfunctioned because of power disturbances, including harmonics that originate within the power system. This can result in lower productivity as well as expensive repairs or replacement. Understanding power quality issues and mitigation techniques can help in the selection of an affordable system. The next chapter will cover the system description.

Chapter 02

Modeling of Solar Active Filter

2.1 Introduction

The proposed system presents a solar active power filter tied photovoltaic system, which is intended to perform current harmonic mitigation and maximum power extraction from PV source.

The system combines photovoltaic array, boost DC-DC converter, DC link capacitor, DC-AC inverter, AC grid supply and nonlinear load which involves full bridge rectifier with passive loads. The DC-DC boost converter is controlled based on P&O algorithm for a maximum power point tracking (MPPT) method. Therefore, the PV array is responsible for producing the power to be integrated to the grid, and simultaneously feeding the inverter based SAPF.

2.2 Structure of photovoltaic system

PV systems are rated based on their PV modules (cells) maximum DC power output under Standard Test Conditions (STC). Standard Test Conditions include a module (cell) operating temperature of 25°C, incident solar irradiance of 1000 W/m2, and spectral distribution of Air Mass 1.5. Since these circumstances are not typically indicative of how PV modules and arrays behave in the field, real performance is usually about 85% of the STC rating.

To reach larger voltages, currents, and power levels, photovoltaic cells are electrically connected in series and/or parallel circuits. Photovoltaic modules are the main components of PV systems, which are constructed of PV cell circuits sealed in an environmentally friendly laminate. In photovoltaic panels, one or more PV modules are structured as a pre-wired field-installable unit. [45]

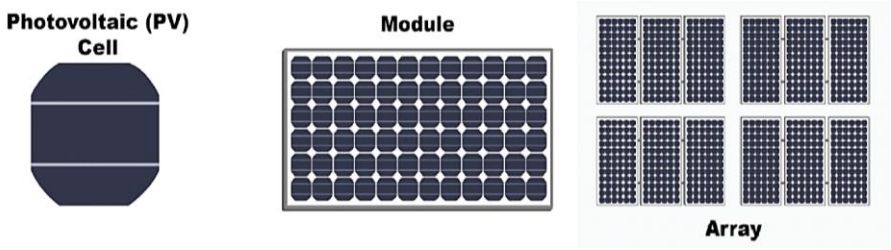

Figure 2. 1: photovoltaic cell, module and array

2.2.1 PV cell

Solar cells are devices in which sunlight is transformed directly into energy. Sunlight releases electric charges, allowing them to freely move in a semiconductor and eventually flow through an electric load. This process is known as photovoltaic effect.

The most common semiconductor material used in solar cells is silicon. When the semiconductor is exposed to light, it absorbs the energy and converts it to negatively charged particles called electrons. This increased energy permits electrons to flow as an electrical current through the material. A simple PV cell diagram is

shown in Figure 2.2. The cell's efficiency in converting energy from one form to another is measured by the ratio of electrical power produced by the cell to the energy released by the shining light.

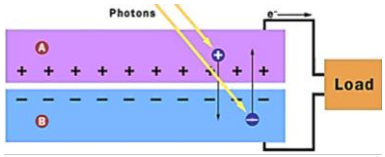

Figure 2. 2: *Basic operation of a photovoltaic cell diagram*

To model the PV cell, a double and single based equivalent circuit are widely used as shown in Figure 2.3. The shunt and series resistances R_{sh} and R_p are the internal resistances of the PV Cell.

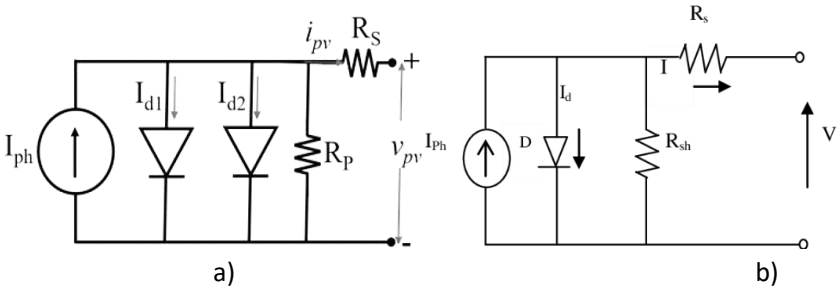

Figure 2. 3: a) Double and b) single diode models equivalent circuits

The current I_{PV} *ge*nerated by the PV cell, can be computed by:
For single diode model:

$$I_{PV} = I_{Ph} - I_D - I_{sh} \quad (2.1)$$

For double diode model:

$$I_{PV} = I_{Ph} - I_{D1} - I_{D2} - I_{sh} \quad (2.2)$$

Where I_D, I_{D1} and I_{D2} can be computed by:

$$I_D = I_S\left(e^{\left(\frac{V_{PV}+I_{PV}R_S}{V_T}\right)} - 1\right) \quad (2.3)$$

And:

$$I_{PH} = A_{Ph} \times J_{SC} \times \frac{G}{G_{sh}} \quad (2.4)$$

Where:

V_{PV}: Output voltage across the PV cell.
I_{PV}: Output current across the PV cell.
I_{ph}: Total photon current of the PV module.
R_{sh}: Shunt resistor.
R_S: Series resistor.
A_{ph}: Area of PV cell.
J_{SC}: Short-circuit current density.
V_T: Thermal voltage = AKT/q.
A: Diode ideality constant.
K: Boltzmann's constant.
q: The charge constant.
I_S: Diode saturation current.
G: Solar irradiation data.
G_{Sh}: Shaded solar irradiation data.

The current vs. voltage (I-V) and power vs. voltage (P-V) characteristics obtained for a single PV cell is shown in Figure 2.4**.** Knowing the electrical I-V

characteristics of a solar cell, or panel is critical in determining the device's output performance and solar efficiency.[46]

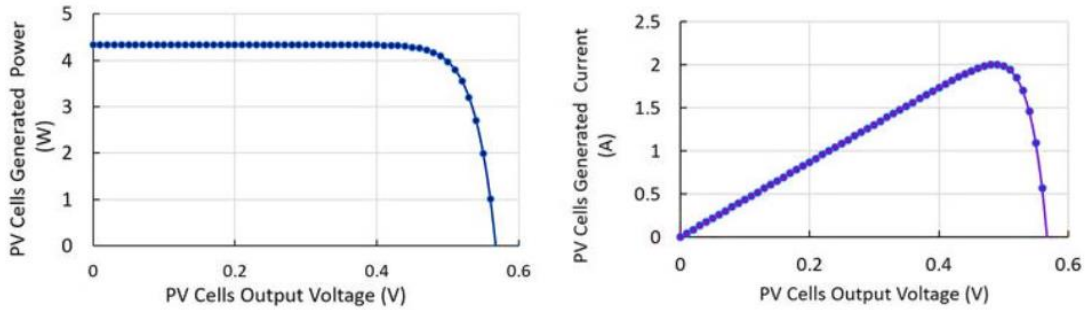

Figure 2. 4: Current vs voltage (I-V) characteristics of PV cell and power vs voltage (P-V) characteristics of PV cell.

2.2.2 PV module

A single solar PV cell produces a relatively small quantity of power, ranging from 0.1 to 2 watts. However, using such a low-power device as a system building block is not practical. Several PV cells must be connected to increase the output power of a PV system. A solar module is generally composed of a sufficient number of solar cells connected in series to generate the necessary output voltage and power. Because a solar cell's typical output voltage is around 0.5 V, if 36 of them are connected in series, the module's output voltage will be 0.5×36 = 18 Volt. The power output of a single solar module can range from 3 to 300 watts. As a result, the necessary number of such cells are assembled to make a commercially viable solar module, also known as a PV module.

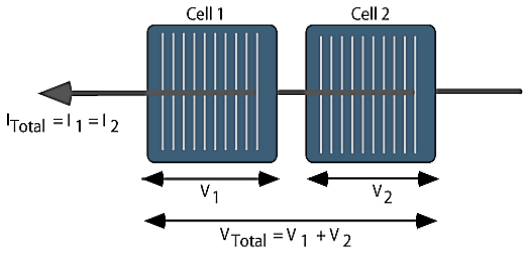

Figure 2. 5: Series connected PV cells

2.2.3 PV array

A single photovoltaic panel or module cannot provide enough solar energy for wide usage. A PV array is a complete energy-generating system formed by different numbers of PV module panels. Since PV array is connected, the PV module can function and produce power.

Consequently, A photovoltaic array is a collection of solar panels that have been electrically connected to make a much bigger PV system. The greater the array's overall surface area, the more solar power it will produce. By connecting many single PV panels in series; for a higher voltage requirement, and in parallel; for a higher current requirement, the PV array will produce the desired power output. The panels

in an array can be electrically connected in either a series, a parallel, or a mixture of the two.

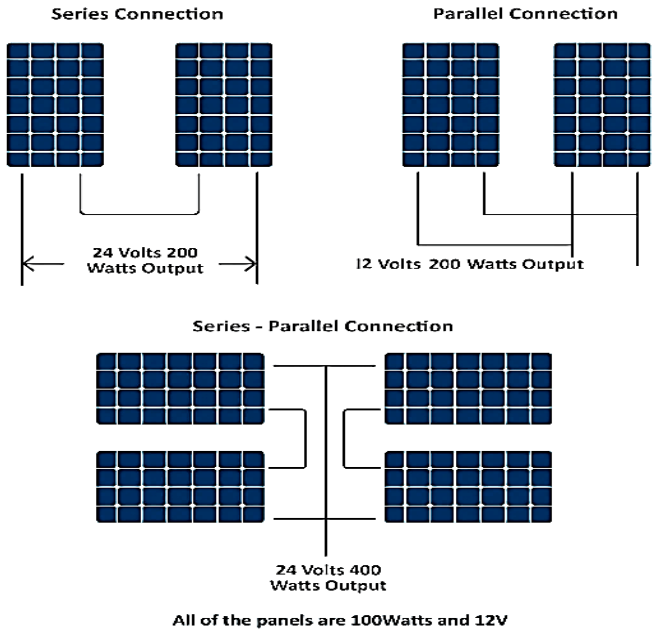

Figure 2. 6: Connections of solar panels (modules)

2.3 Maximum power point of solar array

At its STC, if we draw the V-I characteristics of a solar cell, the maximum power will appear at the bend point of the characteristic curve. The maximum electrical power the solar array can deliver is shown in the V-I characteristics of solar cell by P_m.

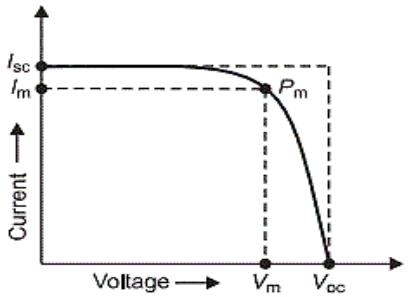

Figure 2. 7: V-I characteristics of PV array

In the V-I characteristics of a solar cell, I_m represents the current at maximum power point, while V_m represents the voltage at which maximum power occurs.

2.3.1 Effect of solar irradiance and temperature on photovoltaic array

Temperature, solar irradiation, dust accumulation, wind speed, PV array configuration, tilt angle and shading pattern all have an impact on the amount of power extracted from the PV array. Generally, variations in solar irradiance and temperature will be recognized as the most important influencing elements for PV generating systems.

2.3.1.1 Effect of solar irradiation on characteristic curves

The term irradiance refers to the measurement of the power density of sunlight received at a certain area on the earth, it is measured in W/m^2. The total irradiance of typical solar spectrum on the earth surface on a clear day is 1 kW/m2.[47] However, the availability of the irradiance is variable, and is usually considerably less than 1kW/m2 due to the rotation of the earth and the weather condition.

The solar irradiance effect on electrical characteristics of PV module is simulated under solar irradiance of 200 W/m2, 400 W/m2, 600 W/m2, 800 W/m2, 1000 W/m^2 and constant temperature. The current-voltage characteristic of PV module in the Figure 2.8 shows that under constant temperature with the increasing solar irradiance both the open circuit voltage and the short circuit current increases and therefore the maximum power point varies. Hence, the higher the irradiance, the greater the output current, and as a result, the greater the power generated.

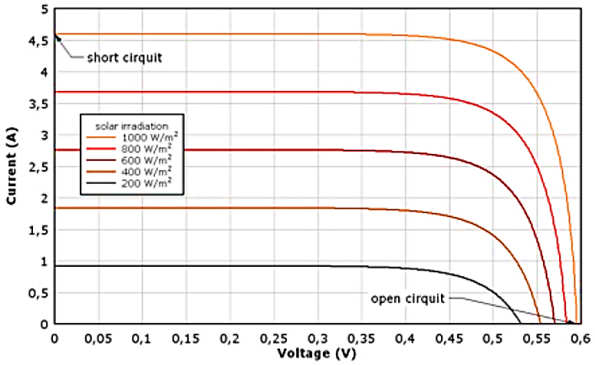

Figure 2. 8: I-V characteristics for different irradiation values

2.3.1.2 Effect of solar irradiation on characteristic curves

The temperature is one of the most important factors affecting the amount of power we get from a solar system. When solar panels absorb sunlight, their temperature rises because of the sun's heat. Although the amount of sunlight absorbed by a solar cell is unaffected by temperature, the amount of power produced differs.

Under constant solar irradiance and temperatures of -25^{o}C, 0^{o}C, 25^{o}C, 50^{o}C, and 75^{o}C, the effect of temperature on the electrical characteristics of PV arrays is simulated. Figure 2.9 illustrates the current-voltage curve.

By varying the temperature, the open circuit voltage and short circuit current of PV module will be influenced significantly and slightly, respectively. The maximum point power follows the changes of open circuit voltage and short circuit current. The raise in temperature causes the maximum power of PV module to decrease, while colder temperatures increase the voltage of solar cells and consequently the maximum power improves.

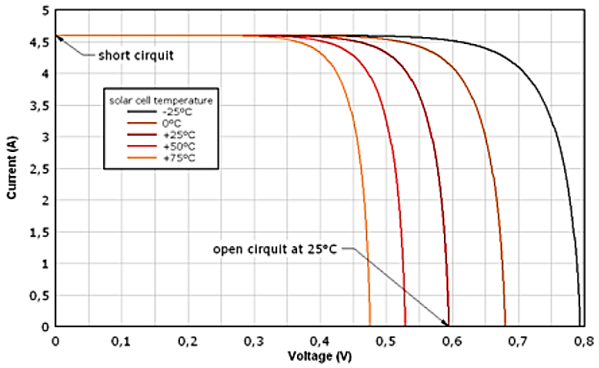

Figure 2. 9: I-V Characteristics for different temperature values

2.3.2 Maximum Power Point Tracking (MPPT)

Maximum power point tracking is a controller algorithm that extracts the maximum possible power from a PV module under specific situations. Several algorithms of maximum power point tracking (MPPT), such as perturb and observe (P&O), incremental conductance (IC), and hill-climbing (HC), have been proposed.

Due to its accuracy in obtaining the maximum power point in a short time with a simple implementation, the perturb and observe (P&O) method is a popular MPPT technique with a simple implementation. [48]. The DC-DC boost converter is to be controlled in this work to ensure MPPT. The duty cycle of the boost converter is decided by comparing the DC link voltage with the PV output voltage generated by MPPT algorithm.

2.4 Boost Converter

2.4.1 Overview of Boost Converter

The presented system is a double stage grid connected PV system; it consists of P&O based boost converter to extract the greatest PV power. Across a PV inverter, a DC-DC boost converter is used to connect the solar generator to the grid.

The system connected to grid consists of PV array, followed by the boost converter to raise the voltage to the desired voltage level and perform with maximum power tracking. Based on the MPPT control method, the boost converters drain energy from PV arrays and feed the DC bus capacitor. A boost converter is a DC/DC switch mode power supply that is needed to increase (or boost) the input voltage of DC supply (PV array) to a stabilized higher output voltage.

It consists of inductor, semiconductor switch (MOSFET), diode and capacitor.

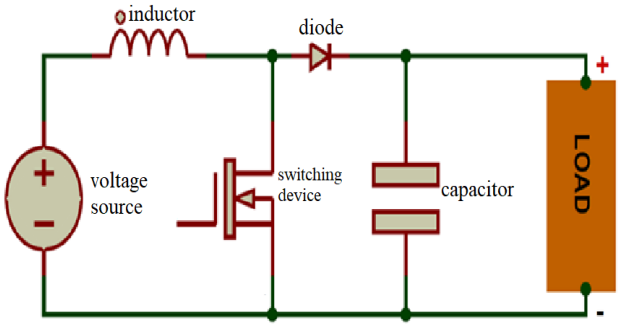

Figure 2. 10: Boost Converter

2.4.2 Working of DC-DC Boost Converter

Using the knowledge above, we can go through the working of the boost converter step by step. The simplified circuit diagram below indicates the current flow across the circuit during the boost converter's switching states.

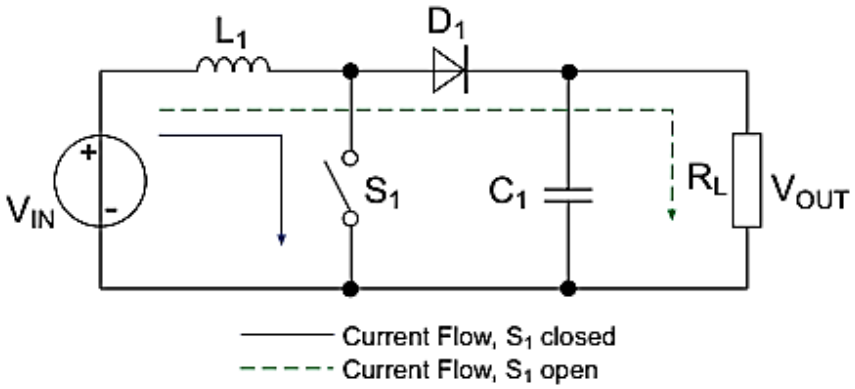

Figure 2. 11: Current flow across boost converter according to the switching states

Step 1:

Here the switching device (S_1) is opened, the input voltage (V_{in}) minus one diode drop is used to charge the output capacitor (C_1).

Step 2:

When the switch (MOSFET) is turned on, the inductor (L_1) diverts all the current from the source to the MOSFET. Since the inductor slows the current ramp up, the power source is not immediately short-circuited.

Note that as the output capacitor cannot discharge through the presently back-biased diode, it remains charged.

Step 3:

When the MOSFET is switched off, the current to the inductor is suddenly stopped. The inductor's nature is to keep the current flowing smoothly; it prevents sudden changes in current. Using the energy stored in the magnetic field, it generates a large voltage with opposite polarity to the voltage previously fed to it. The inductor now acts like a voltage source in series with the supply voltage. This means that the anode of the diode is now at a higher voltage than the cathode and is forward biased.

Eventually, the output capacitor is charged to a higher voltage than before (in step 1), which ensures that the DC voltage has been successfully boosted to a higher one.[49]

The boost converter is controlled using MPPT (P&O) method to achieve the MPP by varying the PV panel output voltage. A PI controller compares the actual dc-link voltage with the reference provided by the P&O MPPT technique in order to establish the dc-link voltage**.** Figure 2.2 demonstrates a PV DC-DC boost converter with MPPT.

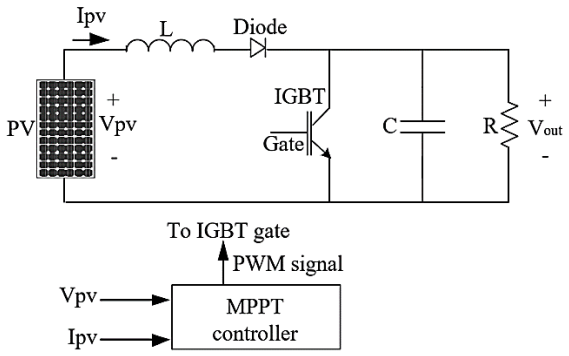

Figure 2. 12: DC-DC boost converter with MPPT

The relationship of the converter output voltage $V_{dc\text{-}link}$ to its input voltage V_{PV} and the duty ratio D of the MOSFET are expressed by Equation (2.5) [50].

$$V_{DC_{link}} = \frac{V_{PV}}{1-D} \tag{2.5}$$

The DC converter output depends on its input voltage and MOSFET duty ratio. The ratio is modulated in form of a PWM switching signal and fed to the gate of the MOSFET.

To allow the converter to work in continuous current mode, the inductor, capacitor, and switching frequency need all be appropriately chosen. This setting keeps the minimum inductor current above zero and the output current ripple to a minimal [51]. Therefore, the minimum value of the required inductor L_{min} is described by:

$$C = \frac{DV_o}{Rf\Delta V_o} \tag{2.6}$$

$$L_{min} = \frac{D(1-D)^2 R}{2f} \tag{2.7}$$

The input DC link capacitor *C*, which determines the peak-to-peak voltage ripple, is selected based on:

$$C = \frac{DV_o}{Rf\Delta V_o} \tag{2.8}$$

where ΔVo is peak-to-peak voltage ripple of the capacitor voltage

2.5 DC Link Capacitor & Voltage

The DC voltage fed by the boost converter into the inverter is called the DC link voltage, this voltage is measured across a DC-link capacitor. The DC-link capacitor, as its name indicates, connects these two devices and is connected in parallel to reduce the effects of voltage changes. The DC-link capacitor is chosen to limit the ripples in the DC-link voltage, the selection of its value depends on the desired voltage and current ripples. it is derived as [52]:

$$C_{dc} = \frac{I_{dc}}{2\omega V_{dcr}} \quad (2.8)$$

where I_{dc} is the current through the capacitor taken equal to the MPP current, ω is the nominal grid frequency, and V_{dc} is the permissible voltage deviation (such as 3% of the nominal value)

2.6 DC-AC Inverter

In a solar energy system, an inverter is one of the most crucial components. It is the interconnection of a solar renewable energy system with the grid at the distribution level.

An inverter converts the DC voltage, which is what a PV array generates, to an AC voltage equals to the grid supply voltage and at the same frequency, this is achieved using controlled switching devices such as MOSFETs, which are continuously turned on and off, and by which the grid interfacing inverter gets additional responsibilities of shunt active power filter in our system.

2.6.1 Classical Two-Level Inverter

The two-level three-phase voltage source inverter is extensively being used due to its simple structure, such as in motor drives and active filters to generate controllable frequency and ac voltage magnitudes using various pulse width modulation (PWM) control strategies as illustrated in Figure 2.12.

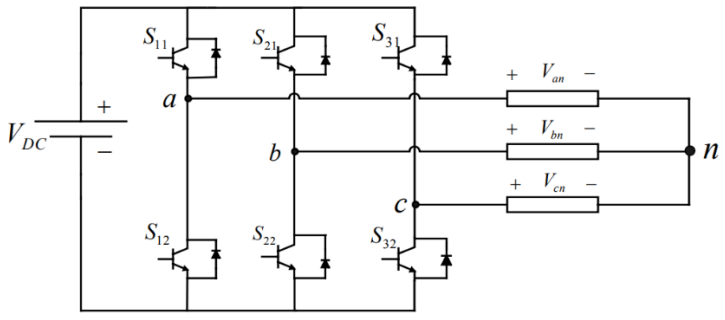

Figure 2. 13: Two-level three-phase inverter

The inverter has eight switch states given in Table 2.1. both switches in the same leg cannot be turned ON at the same time, as it would short the input. Thus, the relationship of switches S_{11}, S_{21} and S_{31} with S_{12}, S_{22} and S_{32}, respectively, is complementary. [53]

Table 2. 1: The switching states in a two-level three-phase inverter.

S11	S21	S31	Vab	Vbc	Vca
0	0	0	0	0	0
0	0	1	0	$-V_{DC}$	V_{DC}
0	1	0	$-V_{DC}$	V_{DC}	0
0	1	1	$-V_{DC}$	0	$-V_{DC}$
1	0	0	V_{DC}	0	$-V_{DC}$
1	0	1	V_{DC}	$-V_{DC}$	0
1	1	0	0	V_{DC}	$-V_{DC}$
1	1	1	0	0	0

Where, the line-to-line voltage are obtained as in Eq (2.6):

$$V_{ab} = V_{an} - V_{bn}$$
$$V_{bc} = V_{bn} - V_{cn} \quad (2.9)$$
$$V_{ca} = V_{cn} - V_{an}$$

2.6.2 Packed U-Cell 5-level inverter (PUC5)

PUC inverter has been first introduced by Al-Haddad as a 7-level topology [54]. It includes six active switches, one isolated DC supply and one DC capacitor as second DC source, which is shown in Figure 2.13. It has a promising feature of generating multi-level voltages using single-DC-source and at reduced number of components comparable to other topologies, thanks to the auxiliary capacitor which should be voltage controlled. [55]

The less switches there are, the lower power losses, the fewer gate drives, the less distortion there is, and the cheaper the system cost. Therefore, it could explain that the PUC advantage is to decrease the load voltage harmonics by dividing the DC bus voltage in multi levels. This procedure reduces the required filters size at the inverter's output.

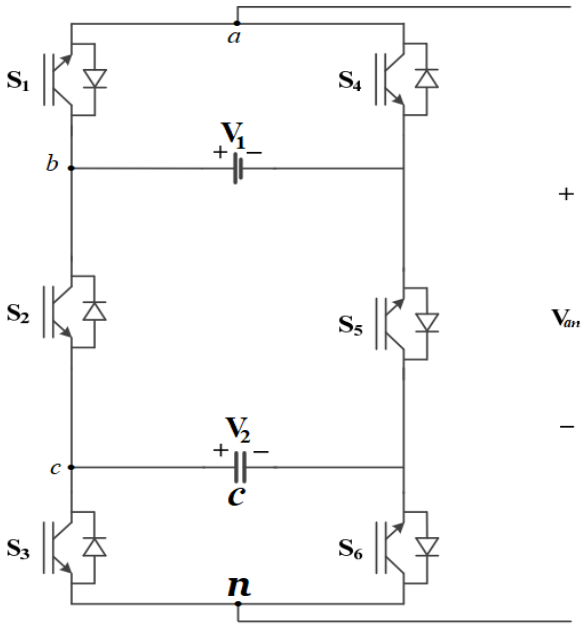

Figure 2. 14: Single-phase PUC Inverter

To have 5 level at the output voltage waveform, the capacitor voltage (V_2) should be half of the DC bus voltage V_1 ($V_1=2V_2$), so the output voltage levels would be 0, $\pm V_2$, $\pm 2V_2$. [56] The output voltage levels of the single-phase inverter topology of Figure 2.13 are listed in Table 2.1 under voltage V_{an}.

The single-phase PUC converter topology depicted in Figure 2.13 consists of six switches labeled S_X where x=1,2,3,4,5,6, one capacitor and one isolated DC source [57]. As it is clear, the PUC inverter cannot produce voltage level more than the DC bus voltage amplitude which is its prominent limitation. It should be noted that switches S_4, S_5 and S_6 are working in complementary of S_1, S_2 and S_3, respectively, so each pair of (S_1, S_4), (S_2, S_5) and (S_3, S_6) cannot conduct simultaneously.

The output voltage can be defined as:

$$V_{an} = V_{ab} + V_{bc} + V_{cn} \tag{2.10}$$

Table 2. 2: Switching States and Voltage Levels of the PUC Inverter

State	S1	S2	S3	V_{an}	Capacitor Voltage
1	1	0	0	V_1	No Effect
2	1	0	1	V_1-V_2	Charging
3	1	1	0	V_1	Discharging
4	1	1	1	0	No Effect
5	0	0	0	0	No Effect
6	0	0	1	-V_1	Discharging
7	0	1	0	V_2-V_1	Charging
8	0	1	1	-V_1	No Effect

All of the switching states, output voltage levels, and capacitor voltage variation ($\Delta V2$) of PUC5 converter are listed in Table I. The values of 1 and 0 represent ON and OFF states of power switch S_X. As presented in Table I, there are eight switching states to generate five staircase voltage levels in PUC5 converter. Hence, there are several redundancy switching states to provide balanced capacitor charging and discharging period to generate three voltage levels of $-V2$, 0 , and $+V2$. Using the presented method in [58], the capacitor is charged during positive half cycle and discharged in negative half cycle of the output voltage waveform. Hence, the charging and discharging of capacitor is balanced in each output voltage fundamental period. Therefore, the capacitor size strongly depends on the load current, PF and fundamental frequency. Moreover, due to the fact that the capacitor is charged and discharged at low frequency, the capacitor size is large[59].

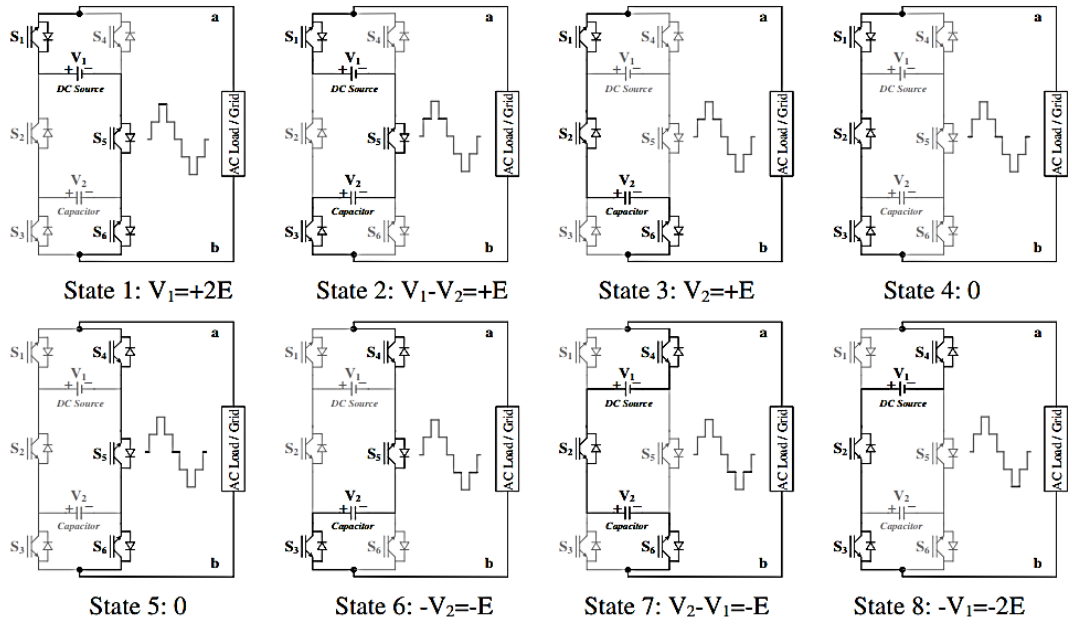

Figure 2. 14: PUC5 configuration, switching states and conducting paths

2.7 Synchronization

Certain parameters must be regarded while connecting two power systems. Synchronizing is the process of connecting two AC power sources in an electrical power system with the least amount of disruption We can connect different power systems by using a circuit breaker. In order to connect two power systems certain factors must be considered like the magnitude of the voltage must be the same, both the voltages must be in phase, and the frequencies should be equal. Collectively, matching of frequency and voltage is called synchronization [60].

It is important to estimate the grid voltage phase angle and frequency properly and precisely inside the grid-connected converter control algorithm in order to establish synchronization, besides separate management of active and reactive power flow between the converter side and the grid. Phase locked loop (PLL) and the p-q theory are among the most important control techniques for synchronization between a grid-tied system and the utility grid.

2.8 Non-Linear Loads

In a power system, a nonlinear load is defined by the introduction of a switching action and, as a result current interruption. This behavior generates current with various components that are multiples of the system's fundamental frequency, known to cause serious problems in electric power systems. Harmonics is the name for these components. The second order harmonic of a fundamental power frequency of 50 Hz is 100 Hz, the third order harmonic is 150 Hz, and so on. Some examples of nonlinear loads are computers, fax machines, printers, PLCs, TVs and electronic lighting ballasts [61].

The most challenging Power electronics devices are used in nonlinear loads, such as phase regulated thyristor bridges, insulated-gate bipolar transistors (IGBTs), and diodes as in bridge. All these devices produce harmonic current distortion, which distorts the applied AC voltage waveform [62].

Consequently, the recent increase in the utilization of non-linear (NL) loads has caused major harmonics and reactive power difficulties in electrical energy distribution networks. To address these issues, harmonic and reactive power adjustment is necessary to improve power quality [63].

2.9 Filters

Power rectifiers are widely applied in a variety of industrial applications for supplying DC power to many types of loads. These rectifiers behave as nonlinear loads, injecting harmonic currents into the AC main source, impacting negatively on both the utility grid and the load. As is mentioned in the previous chapter, the growing number of harmonic mitigation techniques are now available, including L passive filter and active power filter (APF).

2.9.1 L Passive Filters

Capacitors, inductors, and resistors are often used in passive harmonic filters. A passive filter can be connected in series, parallel or hybrid. To reduce harmonic distortion, the filter L parameters are appropriately set to make the circuit resonance at a specific frequency. Passive filters are considered as one of the cheapest ways of mitigating harmonics [64].

Filters are named according to the frequency range of signals that they let pass through while blocking the rest, where:

- Low pass filter only allows low frequency signals from 0Hz to its cut-off frequency, while blocking those any higher.
- High pass filter only allows high frequency signals from its cut-off frequency to infinity to pass through, while blocking those any lower.
- Band pass filter allows signals falling within a certain frequency band to pass through, while blocking frequencies out of this frequency band.

Filters are also classified by their order, the order of a passive filter is an integer number, is determined by the number of used elements, also called the number of poles. In general, the higher the order of the filter, the more closely in approximates an ideal filter and the complex the circuitry required to construct it.

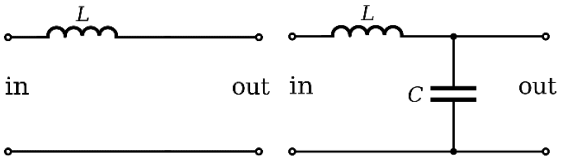

Figure 2. 15: First order low pass filter and second order low pass filter

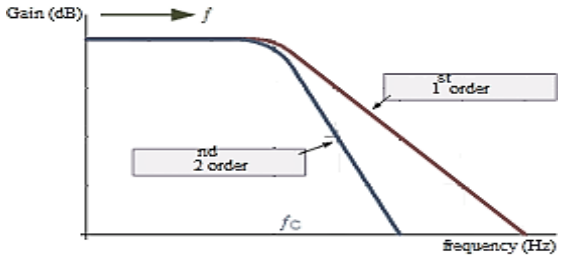

Figure 2. 16: Frequency response of 1st order and 2nd order low pass filter

2.9.2 Active Power Filters (APF)

A growing concept in the domain of grid-connected PV systems is to give the grid interfacing inverter the extra responsibility of active power filtering. The operation of active filters requires the use of an external power source. Passive components such as resistors and capacitors are also included, except inductors. It features a modest size and a compact design.

In this system, a device comprising an inverter and a solar panel is known as active power filter (APF), it is integrated into a system of three-phase power source and nonlinear load. Three configurations of APFs have been mostly adopted: series, shunt and hybrid.

The series active filter is connected through a coupling transformer and injects a compensating voltage component in series with the supply voltage to eliminate the voltage harmonics.

A shunt active filter (SAPF) is designed to detect the harmonic components of the load current and to inject compensating current to nullify the effect of harmonics at the point of common coupling. SAPF injects a current that opposes the harmonic current emitted by the load to mitigate the effect of harmonics currents and reactive power, so that the delivery of the current by the power source remains sinusoidal.

The hybrid connection is a combination of shunt and series configurations of an active filter and passive filter.

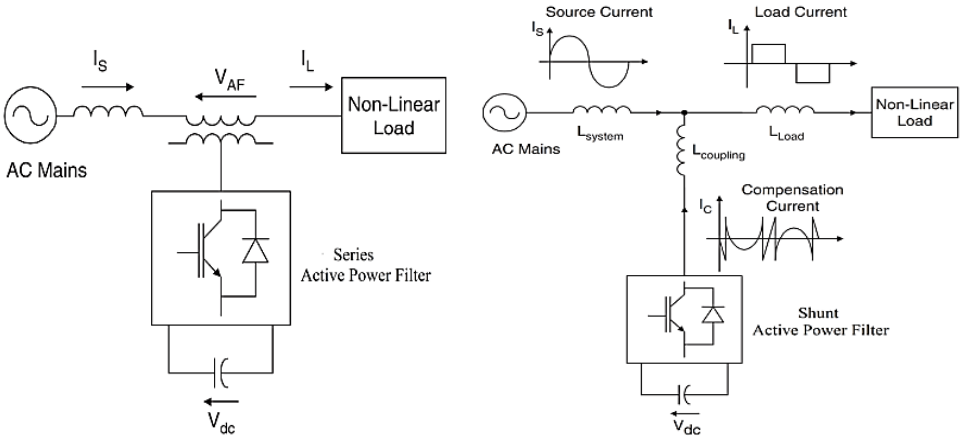

a) Series active power filter b) Shunt active power filter

Figure 2. 17 Active filters

2.10 Conclusion

In this chapter, the main devices and components used in the power circuit modeling of the Solar-AF have been discussed, passing through the photovoltaic power generation, maximum power extraction, DC-AC inversion and active filtering. The next chapter will cover the control strategies of the system.

Chapter 03

System Control Strategy

3.1 Introduction

The proposed Solar-AF is capable of peak power extraction from a photovoltaic (PV) array along with harmonics currents elimination, reactive power compensation, grid currents balancing and adaptive DC link voltage control. In the control system that is in use, the DC-DC converter control necessitates PV array voltage and PV current as inputs, while VSIs control needs grid currents, load currents, PCC voltages and the DC link voltage for the estimation of reference grid currents in proposed technique.

The based Solar-AF controllers of both 2-level classical and 5-level packed U-cell (PUC5) inverters are presented in this chapter.

3.2 PQ Theory

One of multiple ways that can be utilized in control active filters is the p-q theory [65]. It has several impressive features, including:

- It's a three-phase system theory.
- It works with any three-phase system (balanced or unbalanced, with or without harmonics in both voltages and currents).
- It is based on real-time values, which allows for exceptional dynamic responsiveness.
- Its computations are simple and direct (it only includes algebraic expressions that can be implemented using standard processors).
- It supports two control strategies: constant instantaneous power supply and sinusoidal current supply.

The p-q theory consists of an algebraic transformation (Clarke transformation) of three-phase voltages and currents in the a-b-c coordinates to the αβ0 coordinates (Figure 3. 1), followed by the calculation of the p-q theory instantaneous power components expression.

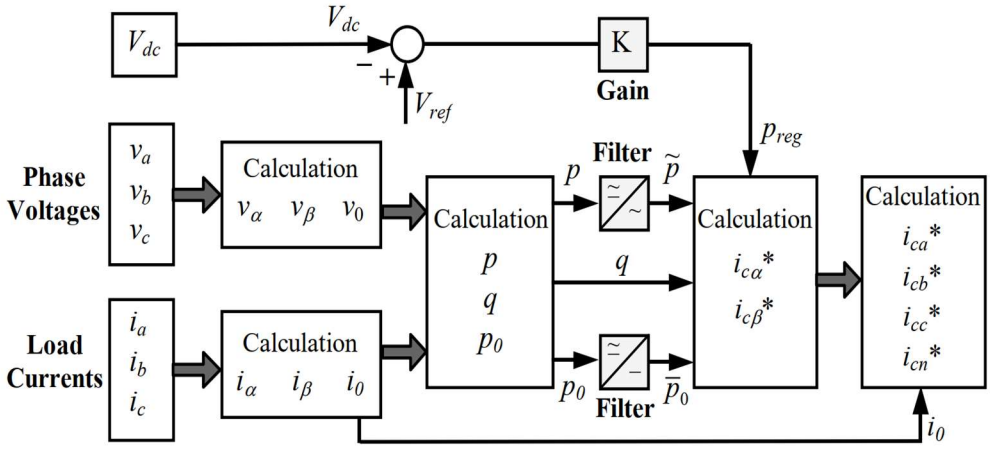

Figure 3. 1: Calculations for the constant instantaneous supply power control strategy

$$\begin{bmatrix} v_0 \\ v_\alpha \\ v_\beta \end{bmatrix} = \sqrt{\frac{2}{3}} \cdot \begin{bmatrix} 1/\sqrt{2} & 1/\sqrt{2} & 1/\sqrt{2} \\ 1 & -1/2 & -1/2 \\ 0 & \sqrt{3}/2 & -\sqrt{3}/2 \end{bmatrix} \cdot \begin{bmatrix} v_a \\ v_b \\ v_c \end{bmatrix} \quad \begin{bmatrix} i_0 \\ i_\alpha \\ i_\beta \end{bmatrix} = \sqrt{\frac{2}{3}} \cdot \begin{bmatrix} 1/\sqrt{2} & 1/\sqrt{2} & 1/\sqrt{2} \\ 1 & -1/2 & -1/2 \\ 0 & \sqrt{3}/2 & -\sqrt{3}/2 \end{bmatrix} \cdot \begin{bmatrix} i_a \\ i_b \\ i_c \end{bmatrix} \tag{3.1}$$

If the system is three-phase with three wires, there are no zero sequence current components (no neutral conductor), so i_0 can be removed from the above equations, simplifying them. The current analysis will concentrate on three-wire systems. As a result, there is no zero-sequence voltage or current [66].

In this situation, the real and imaginary powers are given by:

$$\begin{bmatrix} p \\ q \end{bmatrix} = \begin{bmatrix} v_\alpha & v_\beta \\ -v_\beta & v_\alpha \end{bmatrix} \cdot \begin{bmatrix} i_\alpha \\ i_\beta \end{bmatrix} \tag{3.2}$$

$\bar{p}$: mean value of the instantaneous real power, corresponds to the energy per time unity which is transferred from the power supply to the load, through the *a-b-c* coordinates, in a balanced way (it is the desired power component).

$\tilde{p}$: alternated value of the instantaneous real power. It is the energy per time unity that is exchanged between the power supply and the load, through the *a-b-c* coordinates.

q: the instantaneous imaginary power, equal to the conventional reactive power ($q = 3 \cdot V \cdot I \cdot sin\varphi$).

$p0$ = zero-sequence power.

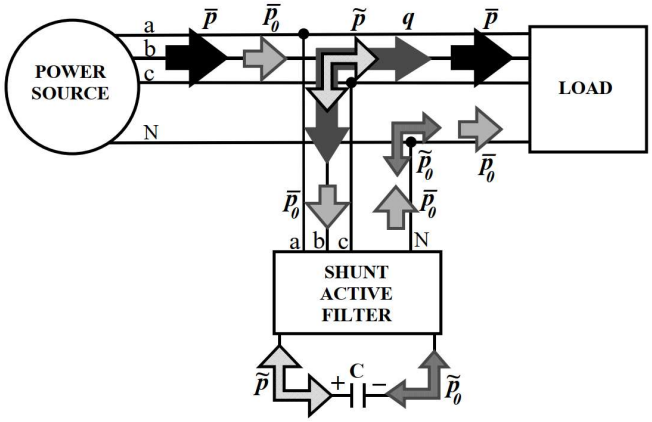

Figure 3. 2: Compensation of power components $\tilde{p}$,q, $\tilde{p}0$ and $\bar{p}0$ in a-b-c coordinates

The reference compensation currents in α-β-0 coordinates can be calculated from the following:

$$\begin{bmatrix} i_{c\alpha}{}^* \\ i_{c\beta}{}^* \end{bmatrix} = \frac{1}{v_\alpha{}^2 + v_\beta{}^2} \cdot \begin{bmatrix} v_\alpha & -v_\beta \\ v_\beta & v_\alpha \end{bmatrix} \cdot \begin{bmatrix} \tilde{p} - \bar{p}_0 \\ q \end{bmatrix} \tag{3.3}$$

In order to obtain the reference compensation currents in the *a-b-c* coordinates the inverse of the transformation given in Eqs (3.4) and (3.4) is applied:

$$\begin{bmatrix} i_{ca}* \\ i_{cb}* \\ i_{cc}* \end{bmatrix} = \sqrt{\frac{2}{3}} \cdot \begin{bmatrix} 1/\sqrt{2} & 1 & 0 \\ 1/\sqrt{2} & -1/2 & \sqrt{3}/2 \\ 1/\sqrt{2} & -1/2 & -\sqrt{3}/2 \end{bmatrix} \cdot \begin{bmatrix} i_{c0}* \\ i_{c\alpha}* \\ i_{c\beta}* \end{bmatrix} \tag{3.4}$$

$$i_{cn}* = -\left(i_{ca}* + i_{cb}* + i_{cc}*\right) \tag{3.5}$$

The calculations presented so far are synthesized in Figure 3.3 and correspond to a shunt active filter control strategy for constant instantaneous supply power. This approach, when applied to a three-phase system with balanced sinusoidal voltages, produces the following results:

- the phase supply currents become sinusoidal, balanced, and in phase with the voltages. (In other words, the power supply “sees” the load as a purely resistive symmetrical load).

- the neutral current is made equal to zero (even 3rd order current harmonics are compensated).

- the total instantaneous power supplied.

To generate the harmonic reference currents, the AC component ($\tilde{p}$) of the active power and the total reactive power (q) are required. The shunt active power filter takes a small amount of real power (Ploss) from the three-phase AC source or an external power supply to recompose the voltage source inverter switching losses and to maintain the DC-link voltage at the desired level. Therefore, the AC component ($\tilde{p}$) of the active power is measured as in Equation (3.6) [67]

$$\tilde{p} = P - \overline{p} - \overline{p}_{loss} \tag{3.6}$$

3.3 Classical three phase Inverter (2-Level)

3.3.1 p-q Modified Power Injection

In addition to harmonics mitigation, we are going to inject active power from the PV array that will be connected to the inverter through a boost converter, therefore we need a certain feedback signal to force control circuit to include power in its output along with harmonics.

The chosen signal is the power calculated from the PV array output as demonstrated expression (3.8) which should be added to reference active power *p** (negative sign “- Ppv”) as shown in Figure 3.3.

$$P_{PV} = V_{pv} \times I_{pv} \tag{3.7}$$

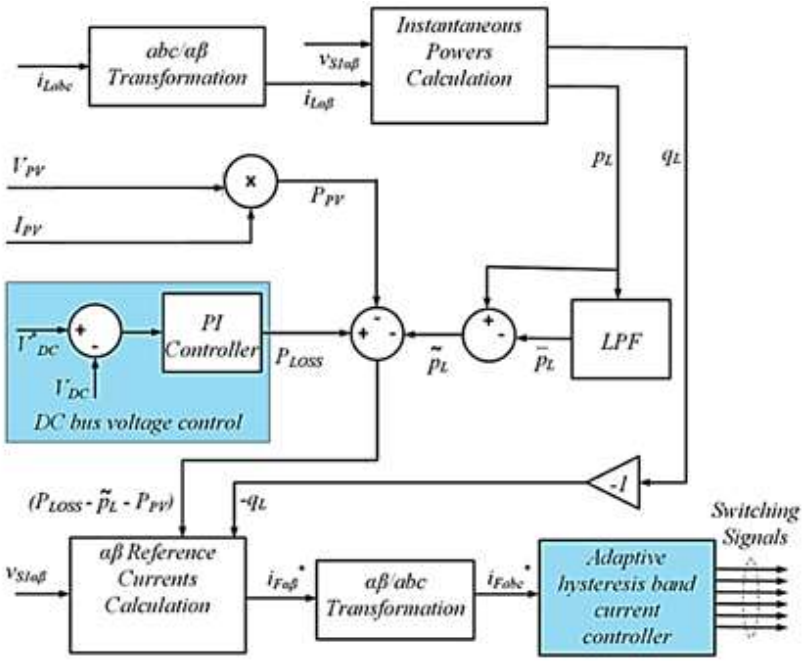

Figure 3. 3: p-q modified power injection

3.3.2 Voltage Regulator:

The energy should be injected into the AC source is controlled by the signal Ploss appropriately eq (3.8). where the DC bus voltage regulator determines the amount of generated power [68].

The difference between DC reference and bus voltages passes through a PID controller and then it is added to the power calculated by p-q theory. As presented in Figure 3. 3 then if overvoltage is obtained, PID sends an appropriate positive signal to decrease the generated power until reach the specified reference voltage, and the vice versa.

$$v_e = V_{dc}^{ref} - v_{dc} \tag{3.8}$$

$$P_{loss} = K_P v_e + K_I \int v_e dt + K_D \frac{dv_e}{dt} \tag{3.9}$$

To achieve DC bus stability, the entire procedure is processed withing fractions of a second.

3.3.3 Hysteresis Current Controller (HCC)

Hysteresis control schemes are based on a nonlinear feedback loop with two level hysteresis comparators, it makes sure that sensed grid currents follow reference grid currents. As is explained in Figure 3. 4 [69]. The switching signals S1 and S2 are produced directly when the error exceeds an assigned tolerance band HB. such that:

- If i_{sa}^{error}<HB, the upper switch S1 is off and the lower switch S2 is on.
- If i_{sa}^{error}>HB, the upper switch S1 is on and the lower switch S2 is off.

Note that the upper band and the lower band differ by 2HB,

The hysteresis controller is used to force the inverter current to track the reference current within the hysteresis band. The inverter currents are sensed instantaneously and compared with the reference currents and switching pulses are generated using HCC for switching on and off the IGBT of the inverter. If the inverter current crosses the upper hysteresis limit, the switch in the upper switch in the inverter arm is turned off and lower switch is turned on. The upper switch is switched on and the lower switch is turned off if the inverter current falls below the lower hysteresis limit.

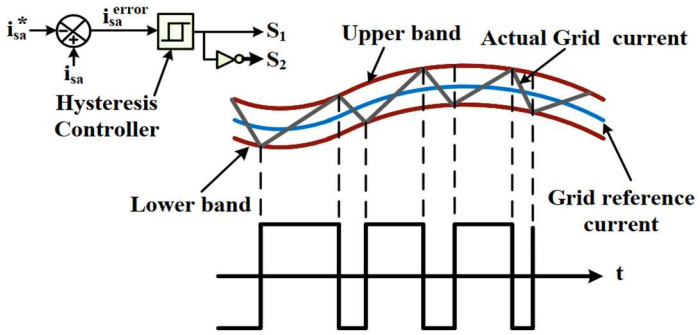

Figure 3. 4: Description of the hysteresis controller

3.3.4 Active and Reactive Power Flow

An important aspect related to the PV system connected to the electric grid is that it can operate as both active power generator and reactive power compensator. The DC-AC inverter's control method ensures proper power transmission and regulation between the AC source and Solar AF. Figure 3.6 illustrates the system's active and reactive power flow [70]. The load is absorbing the active power (P_{Ls}) and reactive power (q_{Ls}). Operation of the proposed system can be divided into daytime and nighttime operation modes.

In the daytime mode, if the Solar AF starts to inject active power (p_f), clearly the active power supplied by the AC source P_s will decrease. When the PV power is greater than the load demand throughout the system, the excessive power of PV will be injected to the AC source. If the available PV power is insufficient for load, the AC grid will supply the rest to the load. In the nighttime mode, P_f is equal to zero and the load will be totally supplied by the AC source.

In both modes, the reactive power of AC loads must be compensated by APF. If $|q_f|$ is equal to $|q_{Ls}|$, then the source power factor can be kept equal to unity under different load conditions.

Shortly, we have:
$P_{Ls} = P_f + P_{s*}$
and
$P_f = P_{dc} = P_{pvs}$
Also:
$|q_{Ls}| = |q_f|$ and $q_s = 0$

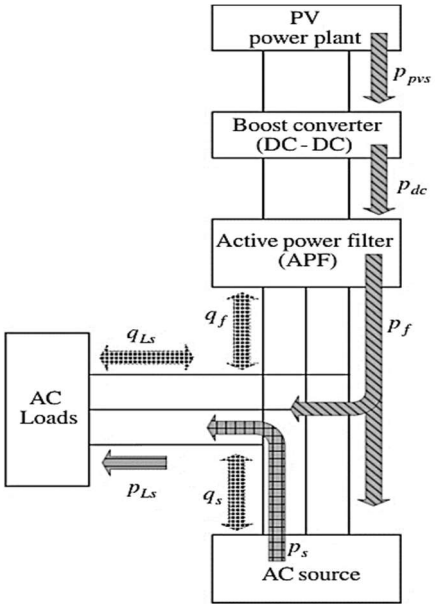

Figure 3. 5: Active and reactive power flow of system

3.4 Perturb & Observe (P&O)

In this thesis, the boost converter is used to ensure the transfer of the maximum power delivered by the PV generator to the load.

The module voltage is perturbed on a regular basis, and the output power is compared to the preceding perturbing cycle. As seen in Figure 3. 5, on the left side of the MPP, when the voltage increase (decreases) the power increases (decreases), while on the right side of the MPP when the voltage increases (decreases) the power increases (increases). As consequence, in order to obtain the MPP, the perturbation direction must remain constant as the power is increased. Whereas it is reversed if the power is reduced.

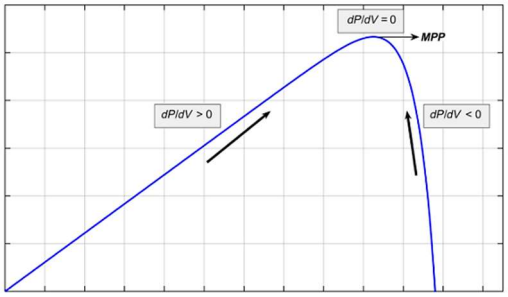

Figure 3. 6: Workflow of P&O algorithm in P-V characteristics

This strategy essentially searches for a difference in PV cell power(dP) and then a change in PV cell voltage (dV). D is perturbed as a function of the obtained values. According to $\frac{dP_{pv}}{dV_{pv}}$ the actual point can be located as follows:

$\frac{dP_{pv}}{dV_{pv}} = 0$, At MPP

$\frac{dP_{pv}}{dV_{pv}} > 0$, Left side of MPP

$\frac{dP_{pv}}{dV_{pv}} < 0$, Right side of MPP

P&O's advantages include excellent tracking capabilities, as well as a simple and quick dynamic oscillation around the MPP [71]. Figure 3. 6 shows the flowchart of P&O technique.

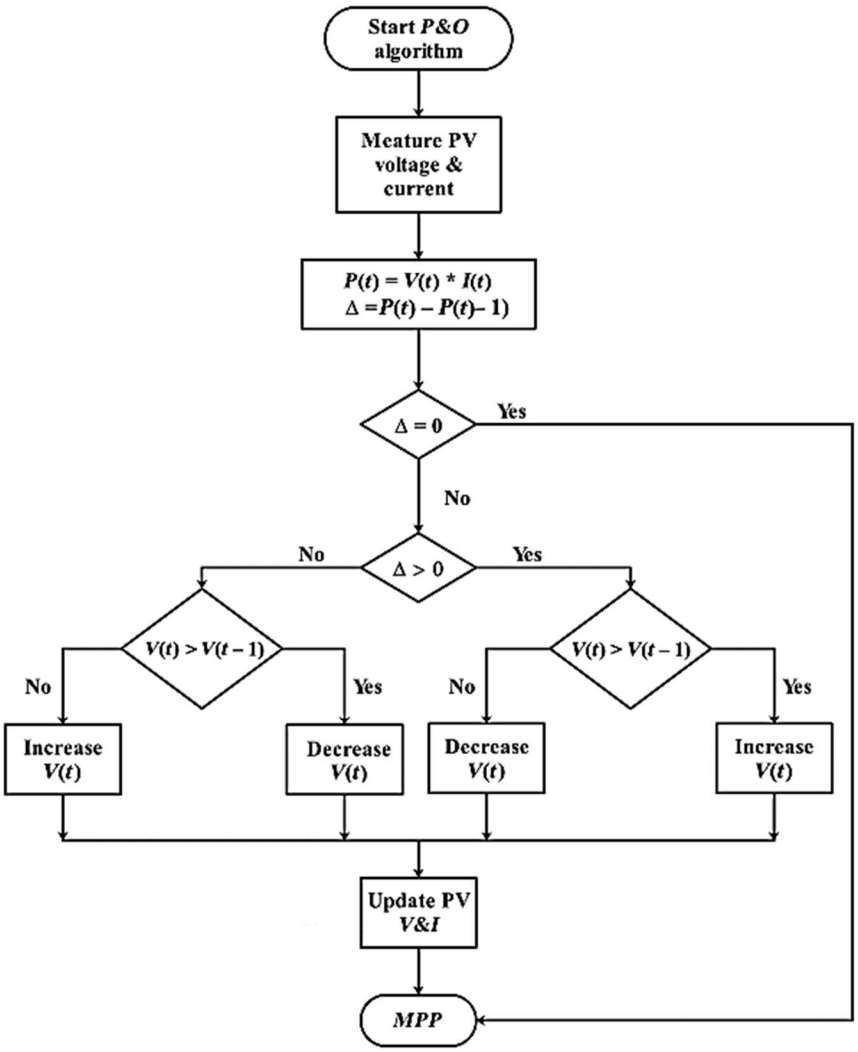

Figure 3. 7: Flowchart of P&O algorithm

3.5 Packed U-Cell Three Phase Inverter (5-Level)

The three-phase PUC5 is simply derived by connecting three single-phase PUC5 as shown in Figure 3.7. In every leg the capacitors must be controlled in such a way that to maintain Vbus = 2 Vaux. Instead of having one DC bus, A PV array connected to each phase of the three phases PUC5 inverter at Vbus through DC/DC boost converter, with the help of an auxiliary capacitor which should be voltage controlled so that the system benefits from a low THD rate.

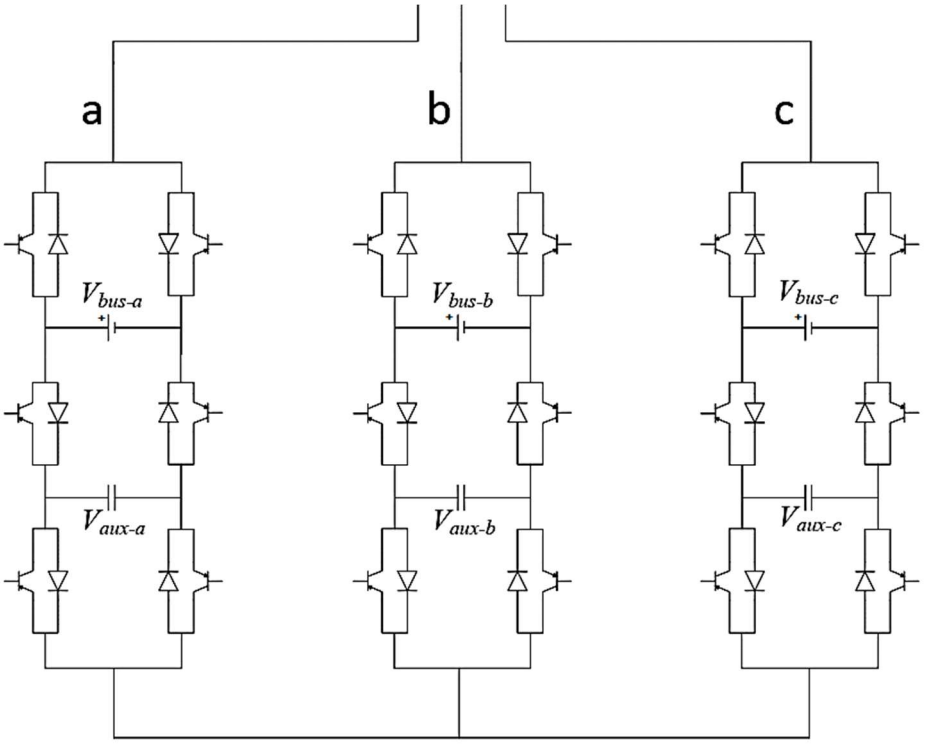

Figure 3. 8: PUC5 Three Phase Inverter Topology

3.5.1 Model Predictive Control (MPC)

Among the advanced control techniques, that is, more advanced than standard PID control, MPC is one that has been successfully used in industrial applications. In general, MPC is an advanced and effective strategy to control the power converters. it is based on the mathematical model of the studied system in order to predict the future behavior of the controlled variables [72,73].

The proposed predictive control strategy is based on the fact that only a finite number of possible switching states can be generated by a static power converter and that models of the system can be used to predict the behavior of the variables for each switching state. For the selection of the appropriate switching state to be applied, a selection criterion must be defined. This criterion consists of a cost function that will be evaluated for the predicted values of the variables to be controlled. Prediction of the future value of these variables is calculated for each possible switching state and then the state that minimizes the cost function is selected.

The flowchart of the proposed MPC applied to PUC5 inverter is shown in Figure 3.8. Using the measured values of the filter current *if* , the grid voltage *Vs*, the filter reference current *if_ ref* estimated from the pq theory, the DC bus voltage (V_{dc1}), and the capacitor voltage (V_{dc2}), the predicted value of filter current *if* (k +1) is calculated for all switching states cases; the predicted voltages are also calculated for the switching states which has an effect on capacitor voltage (charging or discharging), otherwise, the predicted capacitor voltages remain the same in the other states.

Moreover, a cost function is evaluated in order to compute the optimal value which is applied during the next sampling time. The corresponding switching pulses are generated according to the selected state from switching Table 3.1.

Table 3. 1: Switching states and voltage levels of the MPUC5 Inverter.

Switching state (x)	S_a	S_b	S_c	$\bar{S}_a$	$\bar{S}_b$	$\bar{S}_c$	Voltage levels generated by PUC5 (*Vin*)
State 1	0	1	0	1	0	1	*Vin=-2E*
State 2	1	0	1	0	1	0	*Vin=+2E*
State 3	1	1	1	0	0	0	*Vin=0*
State 4	0	0	0	1	1	1	*Vin=0*
State 5	0	1	1	1	0	0	*Vin=-E*
State 6	1	1	0	0	0	1	*Vin=-E*
State 7	0	0	1	1	1	0	*Vin=+E*
State 8	1	0	0	0	1	1	*Vin=+E*

In order to reduce the computation burden, two variables *S*1 and *S*2 are introduced to simplify the use of switching states *Sa*, *Sb* and *Sc*. They are calculated by using Eqs (3.10) and (3.11) [74].

$S_1=S_a-S_b$ (3.10)

$S_2=S_c-S_b$ (3.11)

The voltage vector generated by the 5-level MPUC inverter can be calculated as follows:

$V_{in}=S_1.V_{dc1}+S_2.V_{dc2}$ (3.12)

The two DC voltages are given as:

$$V_{dc1}(k+1) = V_{dc1}(k) - ((T_s \cdot S_1)/C) \cdot i_f(k) \quad (3.13)$$

$$V_{dc2}(k+1) = V_{dc2}(k) - ((T_s \cdot S_2)/C) \cdot i_f(k) \quad (3.14)$$

Where C is the DC link capacitor.

The cost function g is derived as Eq(3.15)

$$g = abs(i_{f\_ref}(k) - i_f(k+1) + \lambda \cdot abs(V_{dc1}(k+1) - V_{dc2}(k+1)) \quad (3.15)$$

Where λ is the weighting factor, *if_ref(k) and if (k+1)* are the reference and future behavior of filter current respectively, *Vdc*1(*k*+1) and *Vdc*2(*k*+1) are the future behavior of DC voltages.

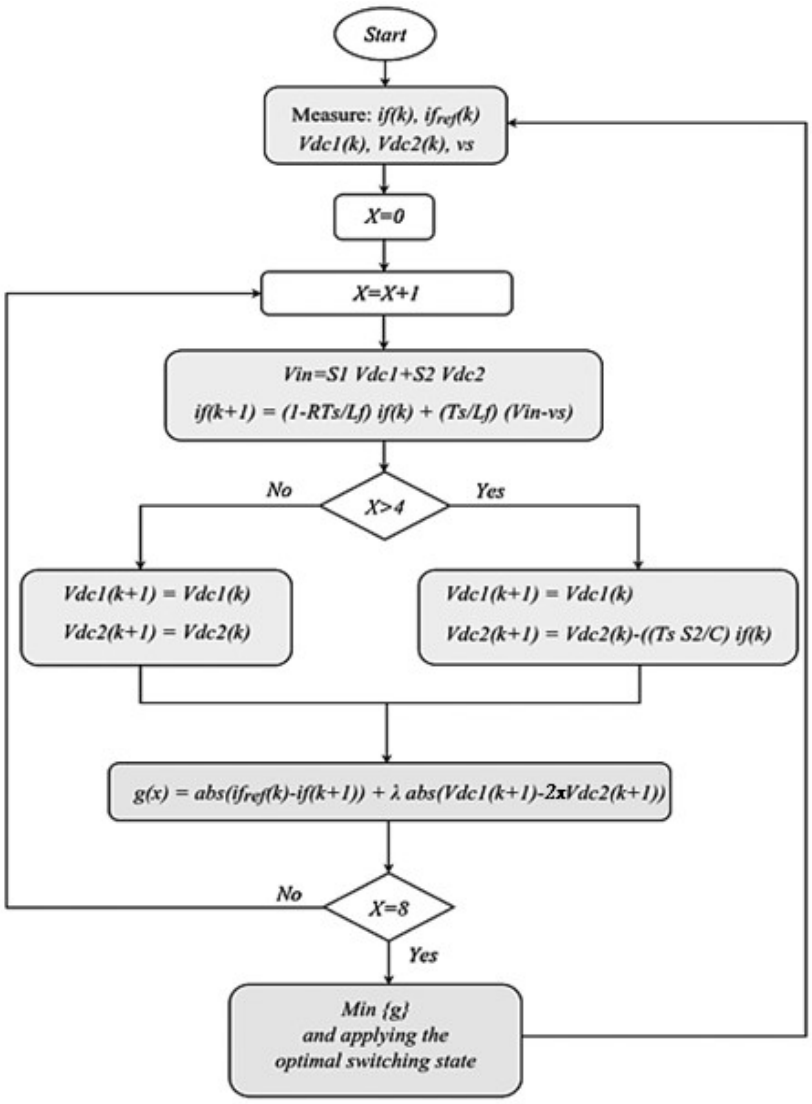

Figure 3. 9: Flowchart of the proposed MPC

3.5.2 Active and Reactive Power Management

The typical controller designed to control the amplitude and phase-shift of i_s results in delivering active power and exchanging reactive power desirably with the grid by means of PUC5 inverter.

In this purpose, the instantaneous power theory known as pq theory (also discussed previously in this chapter, Figure 3.3) this theory uses the Clarke transformation of currents and voltages to calculates the instantaneous active and reactive power and that flows through a three-phase system. The calculated active and reactive powers p and q of the nonlinear load can be separated into average parts and oscillating parts. The compensating powers (P_{osc} and q) are negated in order to affirm that the APF generates a compensating current that produces exactly the inverse of the undesirable powers drawn by the nonlinear load.

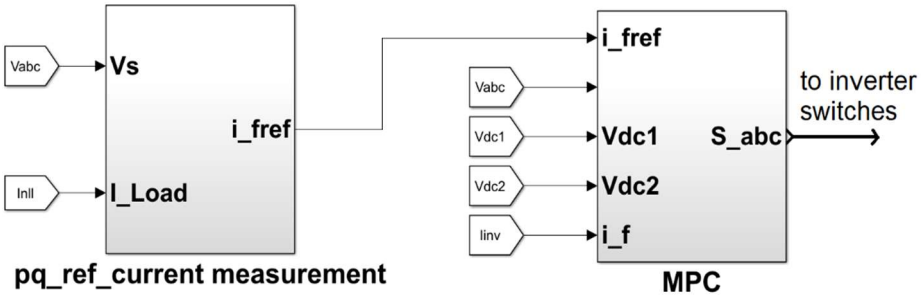

Figure 3. 10: Blocks Diagram of PQ Reference Current Measurement And MPC

After that, using the inverse Clarke's transformation (αβ to abc) the current reference signal (*if_ref*) that should be generated by the PUC inverter is obtained, and is ready to be sent to MPC to create the switching pulses.

3.5.3 Modified pq theory for three-phase PUC5 inverter:

To attain best voltage regulation and accurate power injection we proposed some modifications to pq theory diagram:

- The PV power measurements are summed together and called Ppv, therefore, the total Ppv power will be considered in reference power calculation.
- In order to regulate DC voltages of the inverter legs we have used the same technique as previous with slight modification, since we have three DC buses, we have used three PIDs instead of one. The errors of the three DC buses are processed by three PIDs, then, the outputs are combined in one signal (Ploss).

The above explanation is demonstrated in the following Figure:

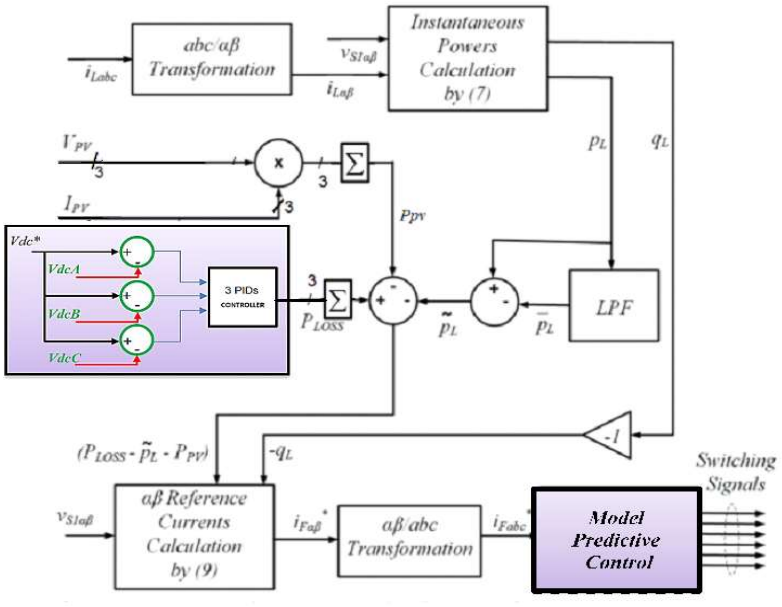

Figure 3. 11: Modified pq theory for three-phase PUC5 inverter

3.6 Conclusion

This chapter covers the design of APF using both two level and PUC5 inverters, the technique used to control is known as MPC algorithm, the principal of this technique has been shown. In order to ensure the second function of APF which is power injection the control circuit has been modified and explained in this chapter. The next chapter covers the design and simulation of the proposed system using MATLAB/Simulink.

Chapter 04

Simulation and Results

4.1 Introduction

This chapter tests the control functionality and the performance of the proposed Solar-AF system. Different perturbations in the system have been considered, including variation of solar irradiance and load demand. the implementation and modeling were conducted by MATLAB/Simulink.

4.2 Solar-AF using MATLAB environment

Figure 4.1 describes the general circuit of the system; it represents the proposed Solar-AF which is arranged in parallel with a nonlinear load and the grid supply. The system consists of the PV array of 238 modules and delivering up to 50kW (under STC) where it is constructed of 14 modules in series and 17 in parallel. The maximum power is extracted across the boost converter at voltage of 406 V and at current of 124 A. In addition to the SAPF which is first built based on the 2-level classical inverter then using the 5-level PUC inverter, and it is also the interconnection between the system and the grid utility.

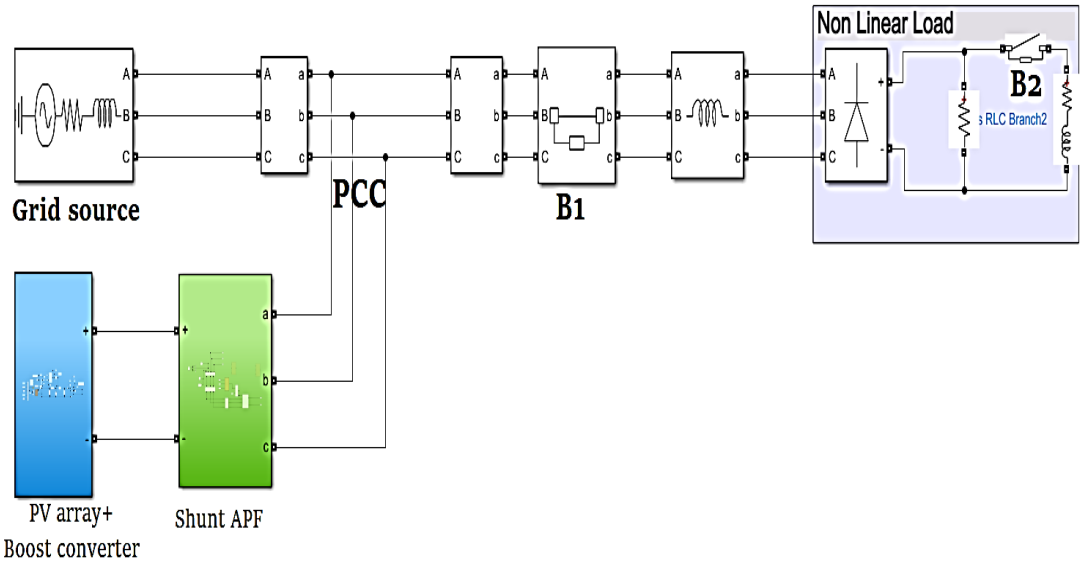

Figure 4. 1: General scheme of the system

4.2.1 Solar-AF Parameters

The values of the used components, elements and other parameters are indicated in the table below (**Table 4.1**).

Table 4. 1: the general parameters values of the Sola-AF.

Grid	Phase to phase RMS Voltage	380 V
	Internal inductance	0.15 µH
	Internal resistance	0.001 Ω
	Frequency	50 Hz
PV generator	Maximum power (STC)	50 kW
	Voltage at MPP	406 V
	Current at MPP	124.9 A
Boost converter	Capacitor	50 µF
	Inductor	6 mH
	DC-link Capacitor	3.5 mF
	DC-link voltage	1000 V
Low-pass filter	Lf (inverter output)	15 mH
	Lf (load input)	10 mH
Load	3-ph Bridge rectifier load	60 Ω
	Additional parallel load	50 Ω, 15 mH

The I-V and P-V characteristics corresponding to the used (user-defined) PV module are shown in Figure 4.2

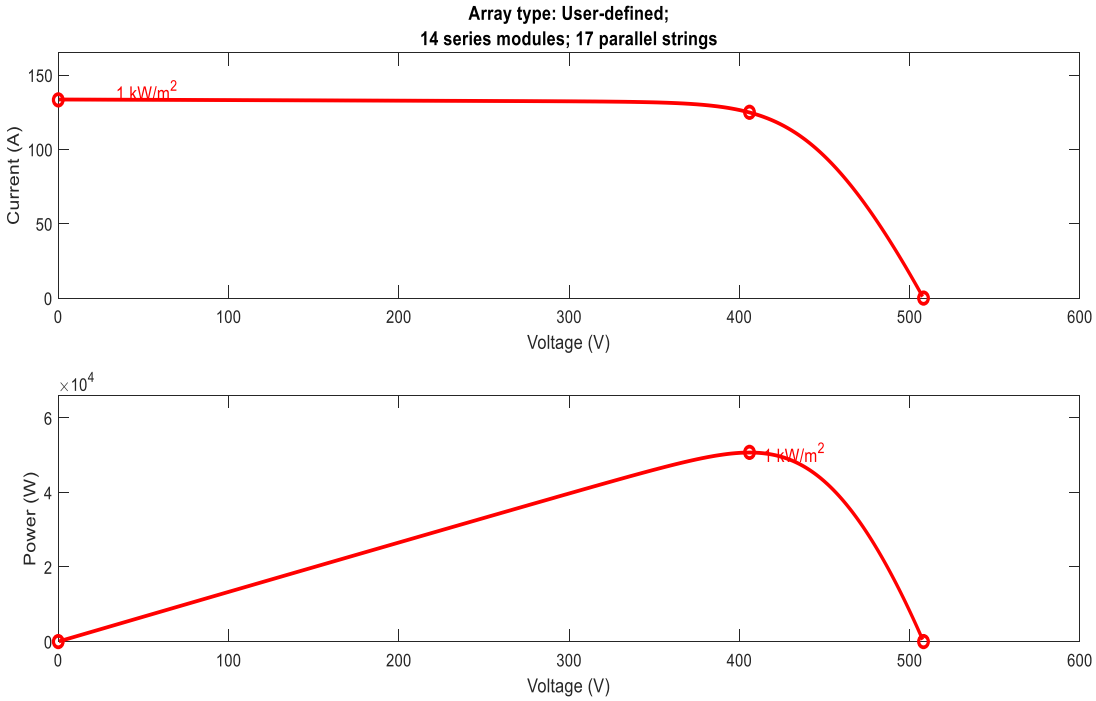

Figure 4. 2: The I-V and P-V characteristics of the used PV module (under STC)

4.2.2 Environment condition

In order to view the performance of the proposed Solar-AF, it is tested under certain conditions, which comes as combinations of solar irradiance and load demand variations.

The different perturbations occurring during the time of simulation are given as profiles, the irradiance variation profile is shown in Figure 4. 3 while load profile is given in Figure 4. 4

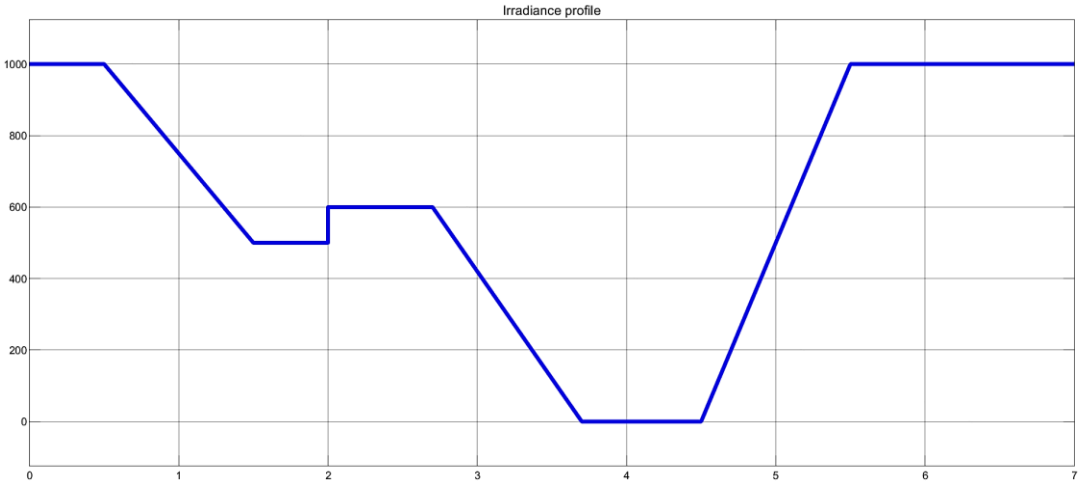

Figure 4. 3: irradiance profile

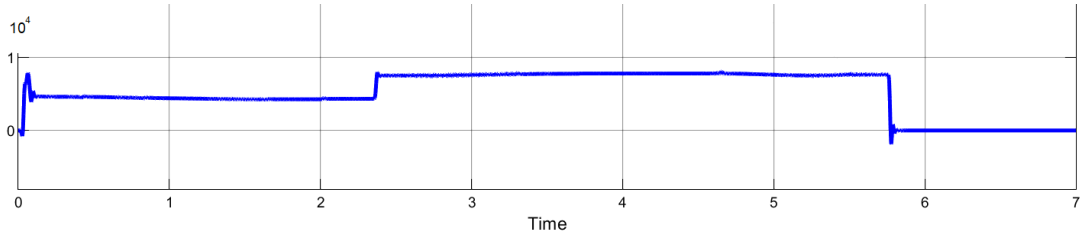

Figure 4. 4: load demand profile

4.3 Solar-AF with Classical Three-phase inverter

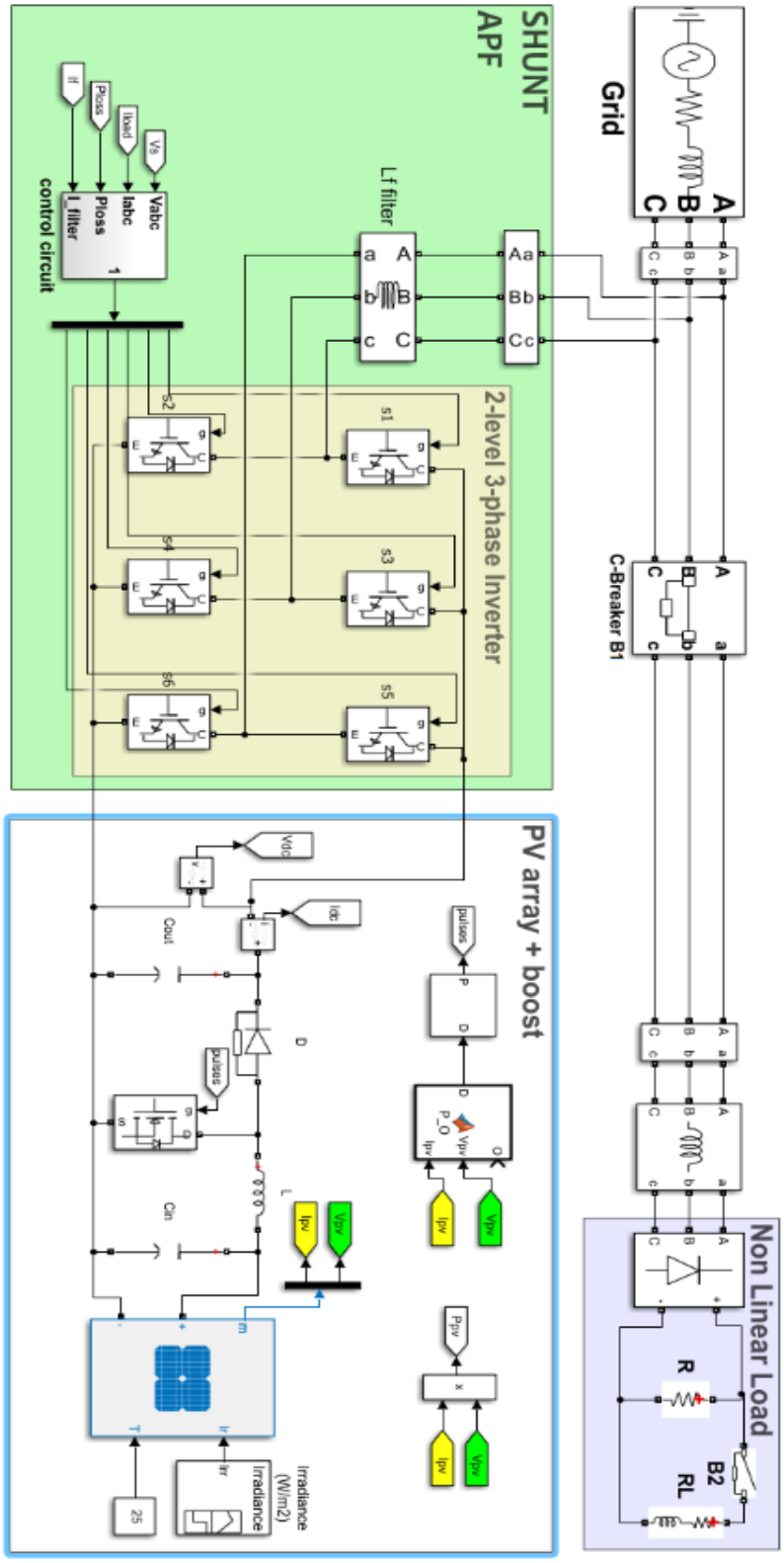

Figure 4. 5: the simulated system of the classical inverter-based Solar-AF

4.3.1 Simulation Results

The results of PV output voltage, current, power and the DC link voltage are shown in Figure 4.6.

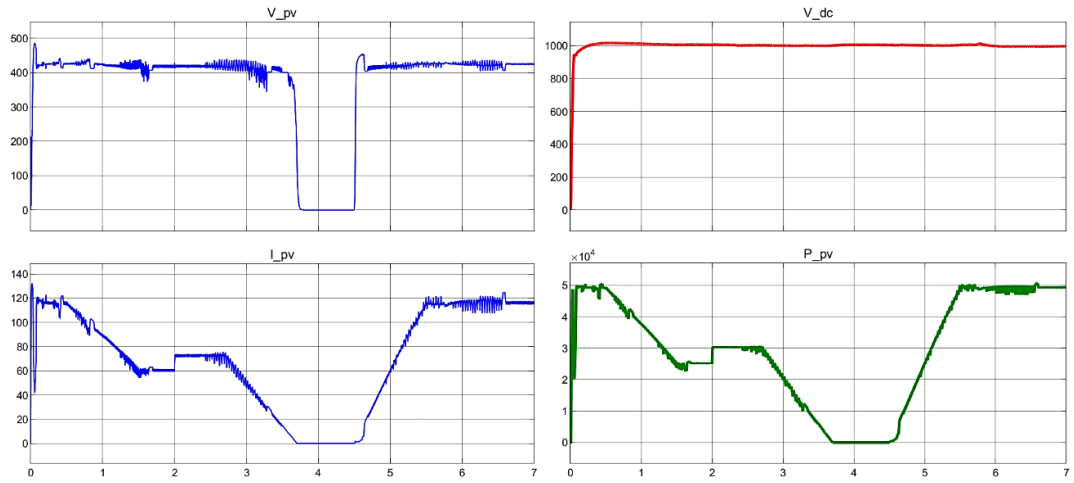

Figure 4. 6: Demonstration PV Output Voltage, Current, Power and The DC Link for All the Simulation using the classical inverter.

The resulting curves of active power and the curves of reactive power are depicted in Figure 4.7 and Figure 4.8, respectively.

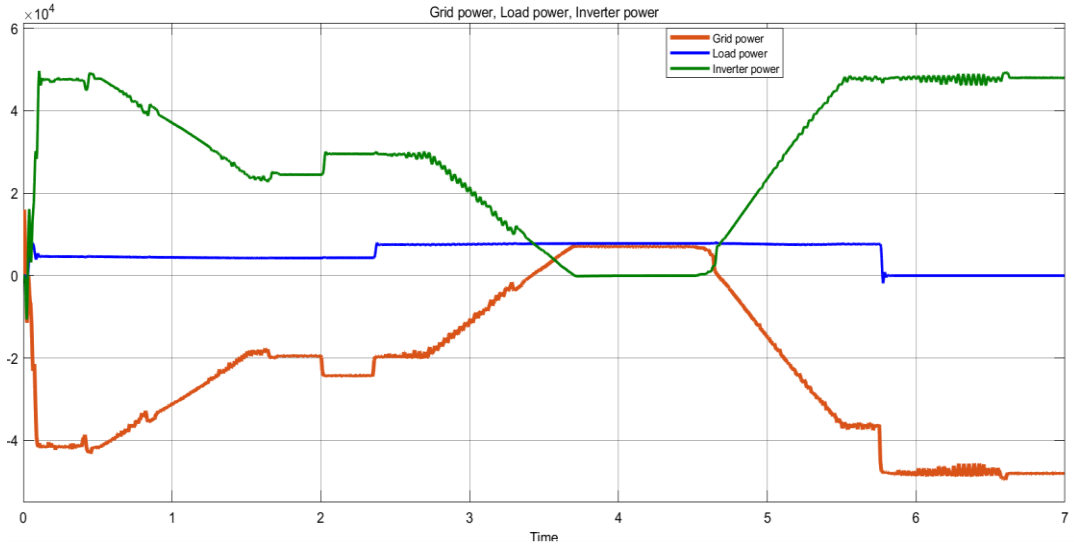

Figure 4. 7: Active power curves of source, load and inverter during the simulation time using classical inverter

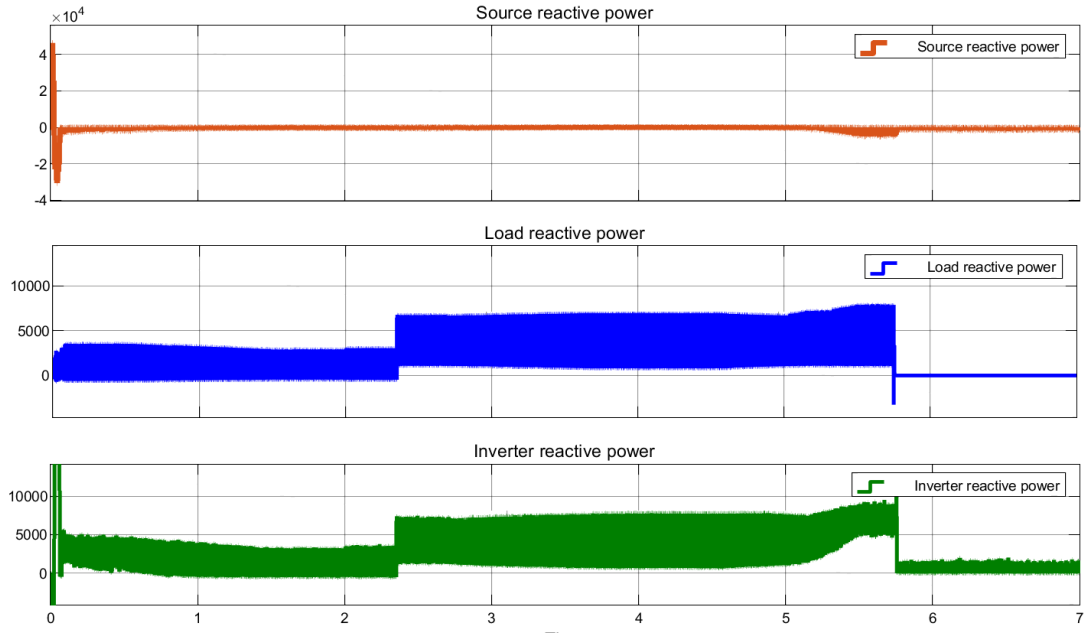

Figure 4. 8: A) Source, load and inverter reactive power in all the simulation using classical inverter

4.3.1.1 System under STC

From the simulation starting time until t=0.5s, the breaker B1 initially is closed while the breaker B2 is opened. In this way, the nonlinear load is connected to the PCC whereas the Solar-AF is supplying current. The irradiance is at 1000W/m^2 (STC) which allows a generation of a maximum output power by the PV array about 50 kW (Figure 4.2), whereas the inverter is transferring only 47.81 kW because of power loss.

The DC link voltage is stable around 1000V in all the simulation time (Figure 4.6), we can say that PID controller is tuned effectively to perpetuate constant DC bus voltage.

As is noticed in Figure 4.8, which shows the reactive power curves in all the simulation, the grid reactive power is efficiently compensated by the Solar-AF, where Q_{grid} is zero while $|Q_{solar\text{-}AF|}$ is equal to $|Q_{load}|$.

As can be seen in Figure 4.9, the harmonics effect is demonstrated in the load current however the grid current is felicitously kept sinusoidal. The Solar-AF is producing current of 75 A, which is sufficient to supply the whole load demand of 10 A while surplus of this current is sent to the grid**.**

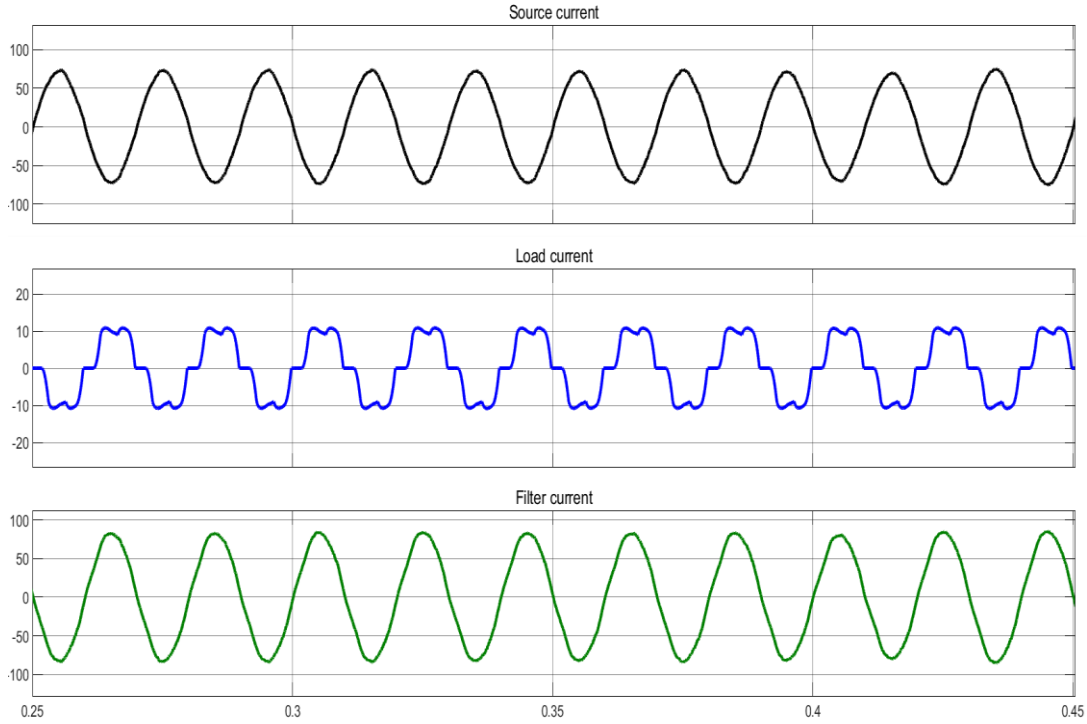

Figure 4. 9: Display of grid current, load current and filter current under 1000W/m^2

As far as the harmonic content is concerned, a fast Fourier transform (FFT) analysis of signals is performed during the whole simulation under every condition, as well as showing the frequency representation and the THD value of the grid current. For the present condition, the THD is 1.82 % (Figure 4.10) which is relatively low (less than 5% according to IEEE 519-1992).

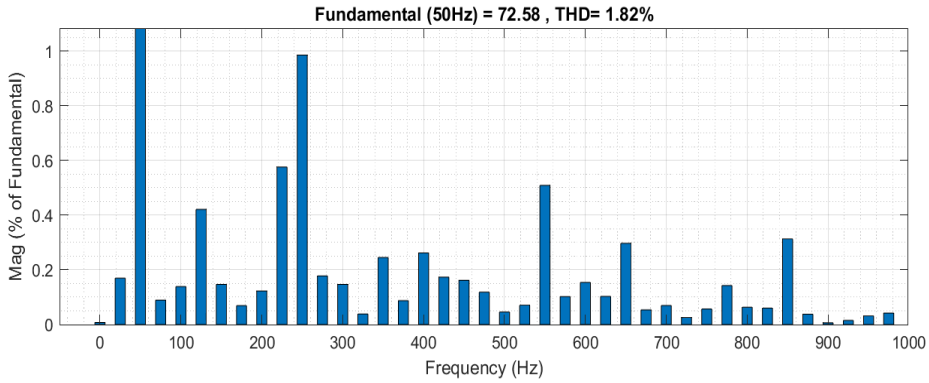

Figure 4. 10: FFT analysis tool for the source current under 1000W/m^2

4.3.1.2 System performance under decreasing of irradiance

From t=0.5s to t=1.5s, the irradiance is constantly decreased with a ramp function to 500W/m^2. As result, the PV power has steadily decreased as well as the grid injected power. That is what verifies the MPPT merit in the maximum power tracking despite the irradiance variations. The P&O MPPT controller determines the appropriate current corresponding to the irradiation level therefore forcing the inverter to extract the maximum PV output power accordingly.

Although the DC voltage has temporarily passed through a small dip, its level has not changed significantly.

4.3.1.3 System performance at irradiance of 500 W/m^2

From t=1.5s to t=2s, the irradiance is stable at 500 W/m^2, the power flow behavior is similar to the previous time interval, except that the amount of power supplied by the Solar-AF is reduced to 25.7 kW, and the inverter will deliver only 24.51 kW (power loss) by which the non-linear load demand of 5 kW is fulfilled, the remaining 19.48 Kw is injected into the grid (Figure 4.8). Thanks to MPPT, the system is capable of extracting the maximum power from the PV array under different values of irradiance.

Also, as depicted in Figure 4.11**,** the source current keeps its sinusoidal waveform, which indicates the system ability in harmonic mitigation.

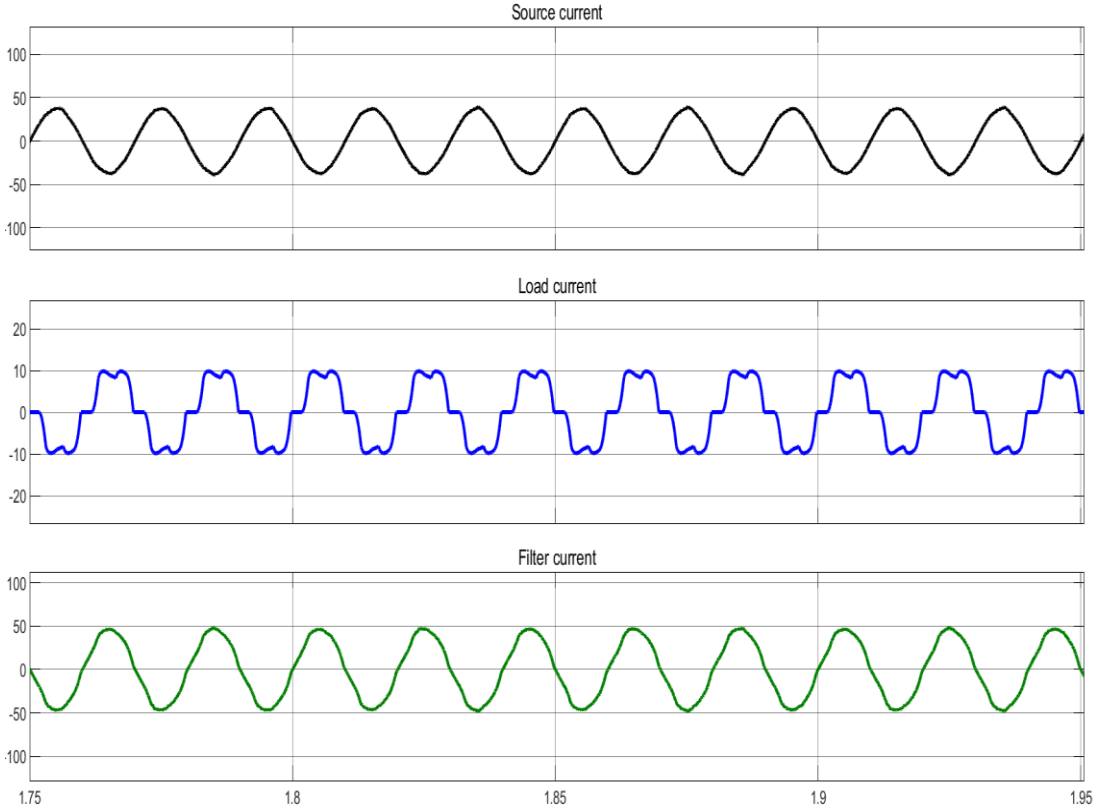

Figure 4. 11: Display of grid current, load current and filter current under 500W/m^2

The THD of a phase current to 2.34%, which is less than 5% according to IEEE 519-1992 (Figure 4.12)

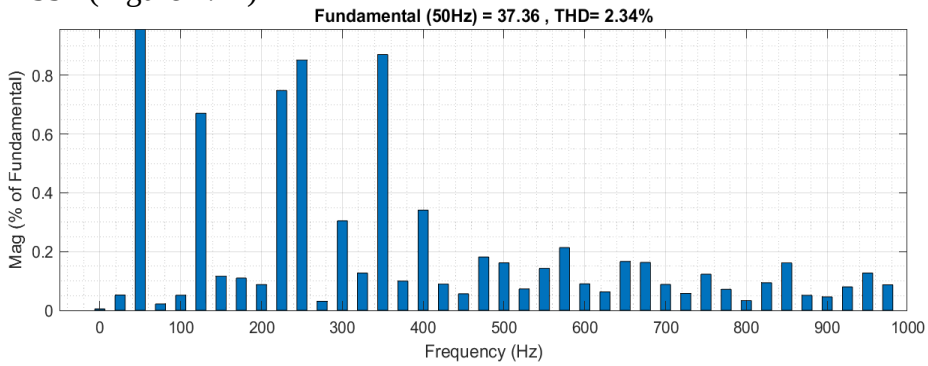

Figure 4. 12: FFT analysis tool for the source current under 500W/m^2

4.3.1.4 System performance at irradiance of 600 W/m^2

From t=2s to t=2.7s, the irradiance is slightly raised to 600 W/m^2. As was expected, a modest growth is noticed in the amount of the extracted power, the inverter is now delivering 29.53 kW (24.51 kW under 500 W/m^2). Consequently, the grid tends to absorb the extra available power reaching 24.5 kW.

Although the sudden surge in irradiance, the system is able to respond by providing such more power. This stage ensures again the effectiveness of the P&O MPPT algorithm.

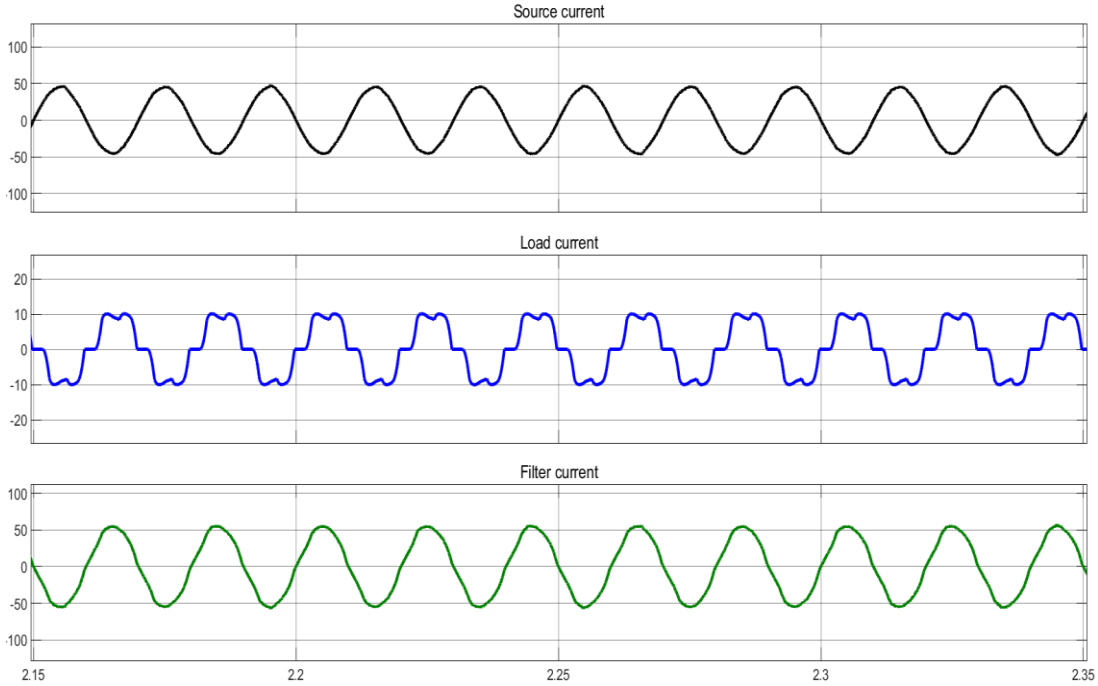

Figure 4. 13: Display of grid current, load current and filter current under 600W/m^2

The THD of current of phase a is equal to 1.99% which is less than 5% according to IEEE 519-1992.

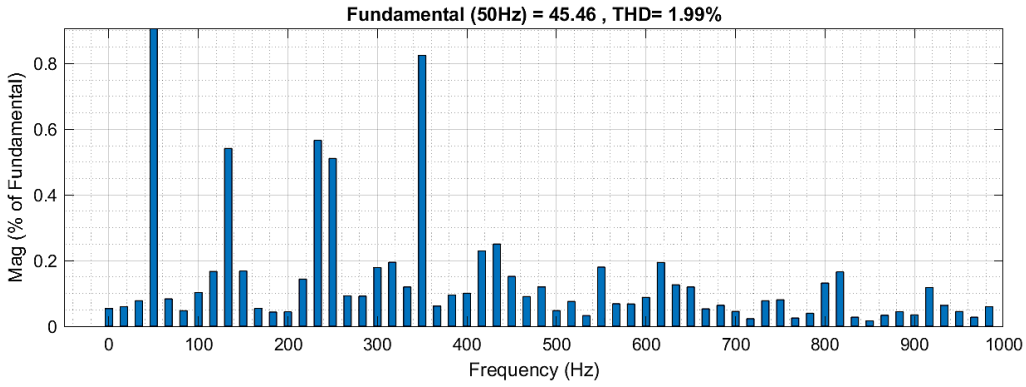

Figure 4. 14: FFT analysis tool for the source current under 600W/m^2

4.3.1.5 System performance under increased load demand

At t=2.35s, while the irradiance is maintained constant at 600W/m^2, the breaker B2 is closed causing the load demand to increase abruptly from 5 kW to 7.8 kW**.** As can be noticed from Figure 4.7, the inverter keeps delivering the same amount of power which equals 29.53 kW. The growing load demand is taking a

larger amount of power; therefore, the grid injected power is reduced to 19.91 kW. As displayed in Figure 4.8, the compensation of reactive power is also kept under control despite of the load perturbation.

Figure 4.15 gives information about currents in the system, where the increased load current reached 19.7 A and a grid current of 37.1 A.

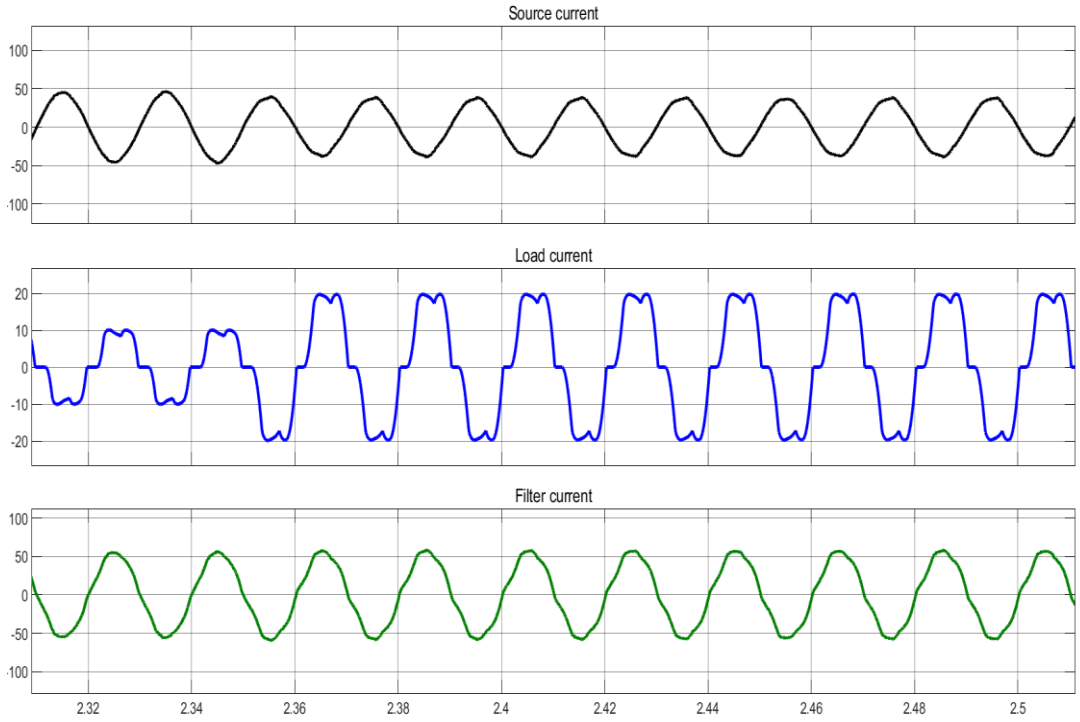

Figure 4. 15: Display of grid current, load current and filter current with additional load demand

The THD of phase A current to 2.68%, which is less than 5% according to IEEE 519-1992 (Figure 4.16)

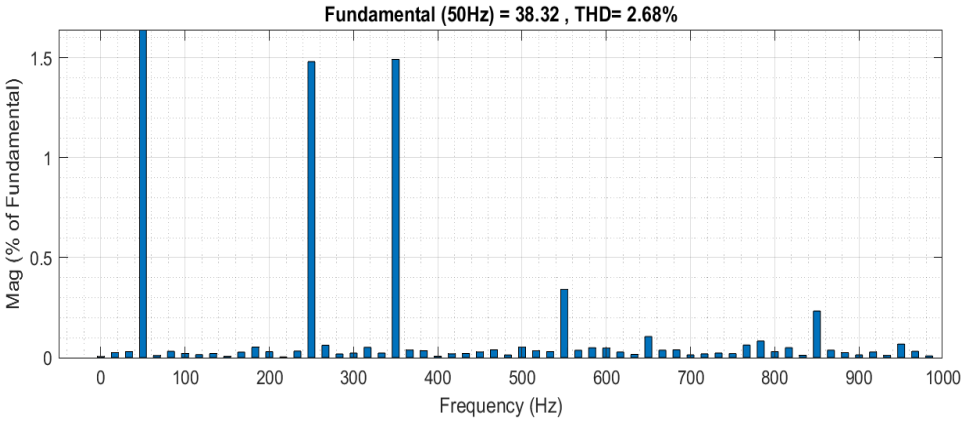

Figure 4. 16: FFT analysis tool for the source current under 600W/m^2 with extra load demand

4.3.1.6 System performance during a decreasing irradiance

From t=2.7s to t=3.7s, the irradiance is decreased again with a fixed ramp from 600 W/m2 to 0 W/m^2. Consequently, the PV power is reducing with time until there is no power generated from the PV system.

Also, it is noticed that the DC link voltage is well balanced, and this, for any case during the operation (Figure 4.6).

4.3.1.7 System performance at irradiance of 0 W/m^2

From t=3.7s to t=4.5s, the system is working under night mode condition that means there is no irradiance, thus, there is no power generated from the PV system. The load demand is completely supplied by the utility grid. In this way, the proposed system behaves as SAPF, it generates only the necessary compensating harmonics component to keep a sinusoidal source current.

The required reactive power is also provided by the Solar-AF to fulfill the load needs, and the reactive power of the grid is eliminated, which implies a unity power factor, as is shown from t=3.7s to t=4.5s in the reactive power measurements (Figure 4.8**).**

The V_{dc} is efficiently following its 1000 V reference, which significate that the PID controller-based voltage regulator is worthy.

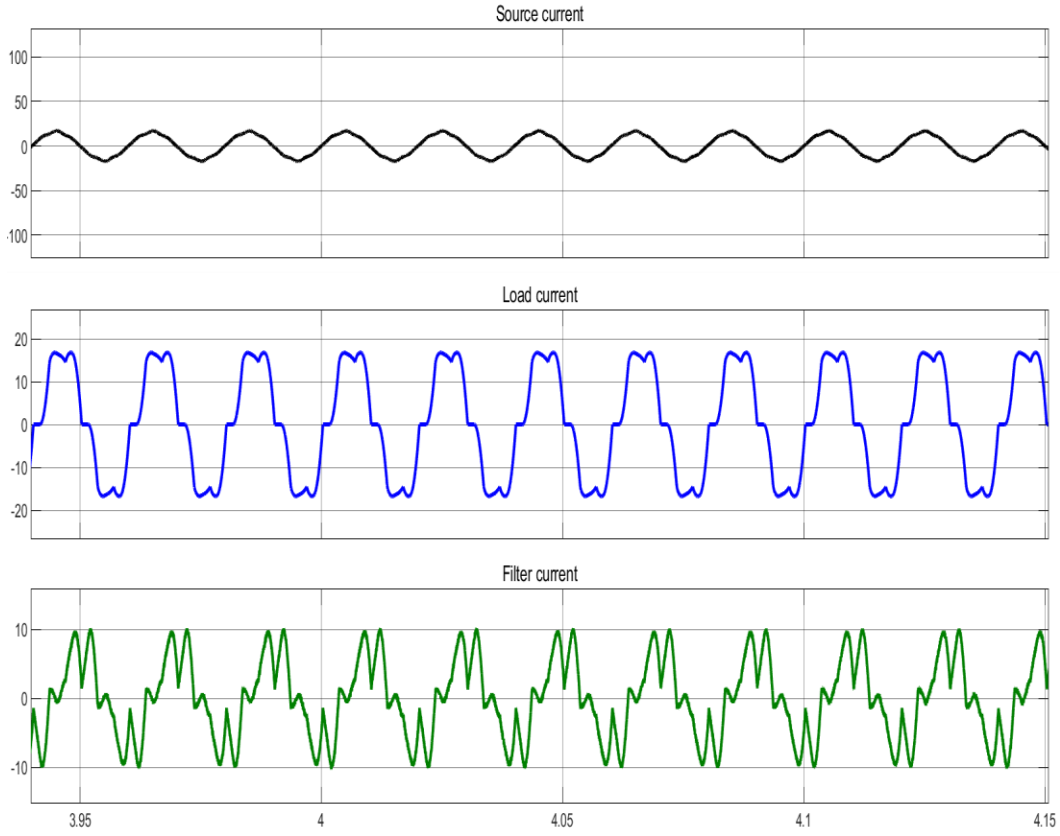

Figure 4. 17: Display of grid current, load current and filter current under zero irradiance.

The THD of phase A current under zero irradiance is 3.38%, which is less than 5% according to IEEE 519-1992 (Figure 4.18)

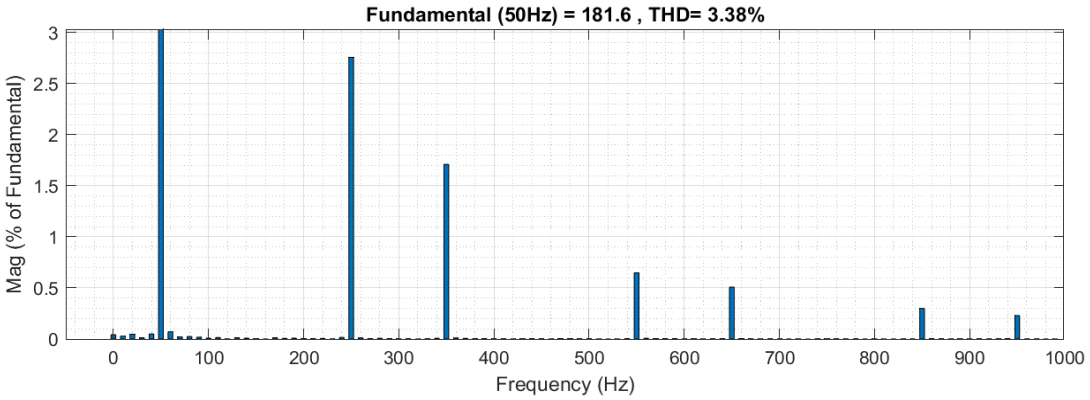

Figure 4. 18: FFT analysis tool for the source current under 0 W/m^2

4.3.1.8 System with an increasing irradiance

As is illustrated in the irradiance profile, from t=4.5s to t=5.5s the irradiance increases gradually from 0 W/m^2 to 1000 W/m^2 by the pace of a ramp function. As is displayed in Figure 4.19 during the concerned interval of time, the MPP is continuously being tracked, thus the power transmitted by the inverter is being enhanced again toward its maximum, synchronously the grid is turning from supplying into absorbing power (from positive to negative flow).

The inverter current is steadily increasing its magnitude. The grid current is reversed in direction and is growing as time passes while even keeping a sinusoidal waveform, due to the filtering that stills undergoing.

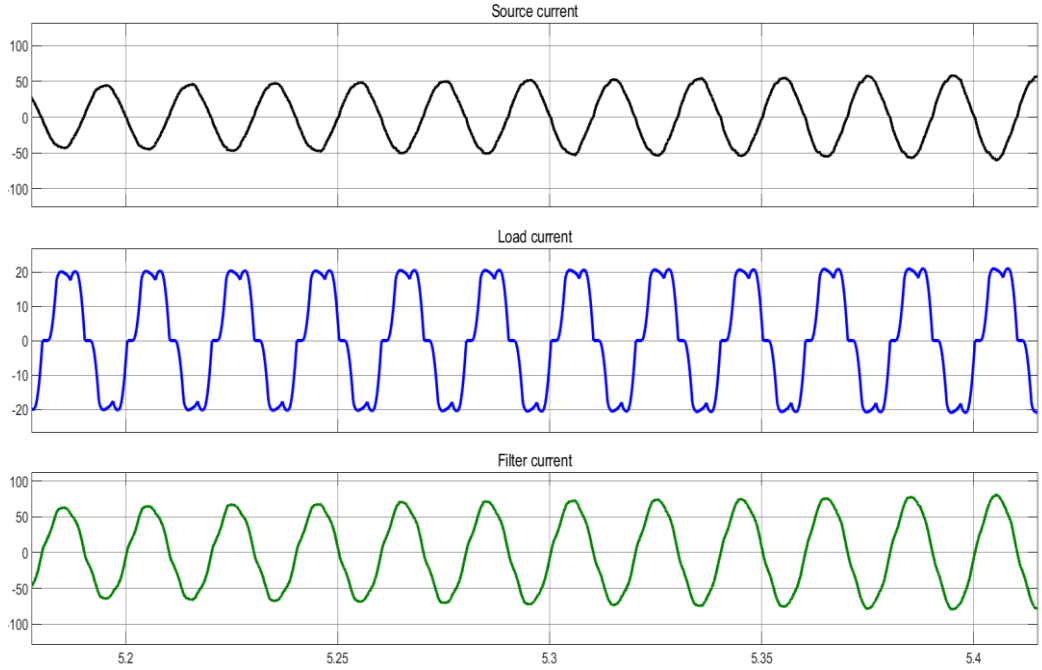

Figure 4. 19: Display of grid current, load current and filter current during increasing irradiance condition.

The investigation into this interval proves the dynamic performance of the system and its adaptiveness during the continuous change in irradiance. Even tough under the mentioned condition, the voltage regulator successfully maintains V_{dc} at

1000V, the maximum possible power is being tracked by MPPT and an accurate harmonics mitigation.

4.3.1.9 System performance at irradiance of 1000 W/m^2 with extra load demand

From t=5.5s to t=5.75s, the system is tested again at STC (1000 W/m^2) but with increased load demand. As can be noticed in Figure 4.7**,** the inverter is now delivering amount of power as much as before (from t=0s to t=0.5s), however the more power the load is consuming, the less power will be injected into the grid.

Similarly, the system stills viable, the grid source is sinusoidal, the DC link voltage is kept at 1000 and the filtering is well performed resulting in low THD level of 3.94% which is less than 5%.

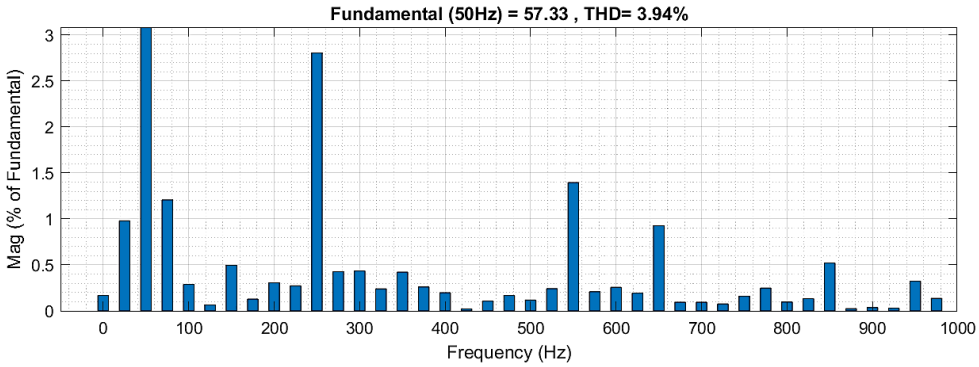

Figure 4. 20: FFT analysis tool for the source current System under 1000 W/m^2 with extra load demand

4.3.1.10 System performance without load

At t=5.75s, the breaker B1 is opened, therefore the non-linear load is completely disconnected from the system, while the irradiance is steady at 1000 W/m^2. Hence, the power produced by the PV system will be totally injected into the grid, from t=5.75s till the end of simulation the load draws zero power, the grid reactive power is zero (unity power factor).

In this case the proposed system behaves only as a grid connected PV system injecting the full available power into the grid.

As is clear in Figure 4.22, the load drains no current, on the other hand, the Solar-AF current is equal to the grid current in magnitude.

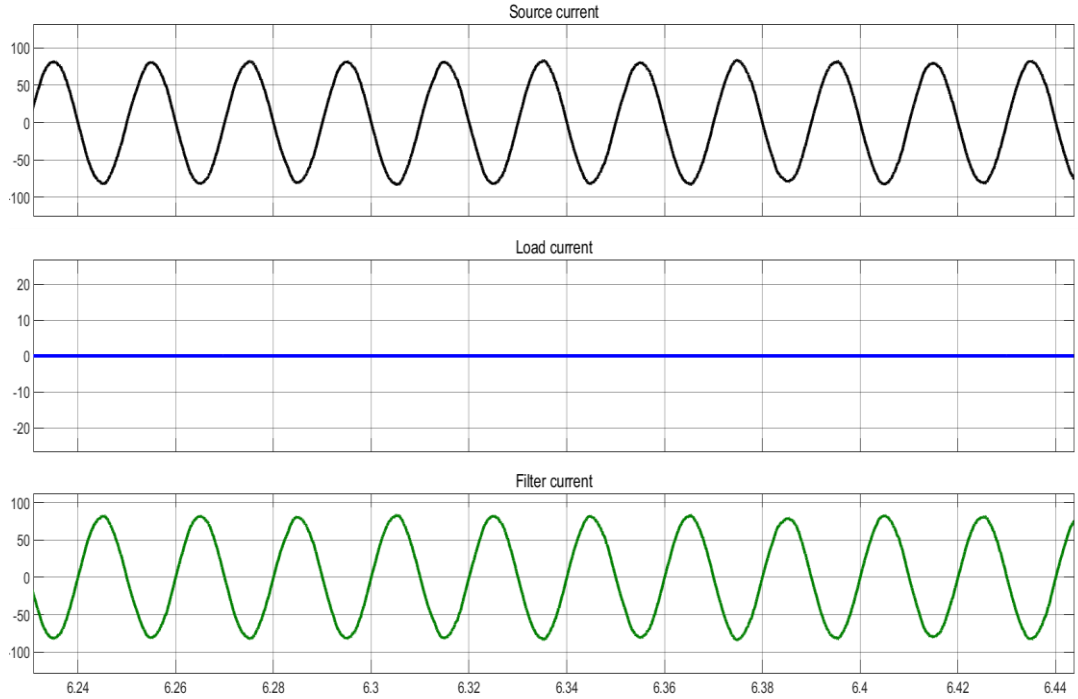

Figure 4. 21: Display of grid current, load current and filter current under no load condition.

The THD measurement of the current is shown the figure below which is equal to 1.24% which is less than 5% according to IEEE 519-1992

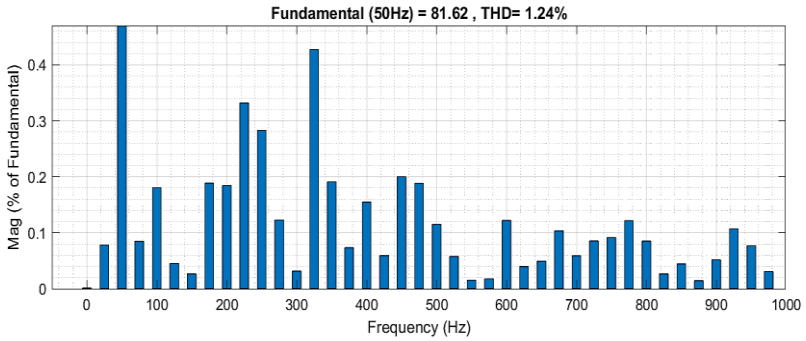

Figure 4. 22: FFT analysis tool for the source current of the system without load

4.4 PUC5 Three-phase inverter-based Solar-AF

In this section, the PUC5 inverter is compared in terms of number of components, switching frequency, voltage rating and THD etc. The three-phase configuration of the system using the PUC5 inverter has been illustrated in Figure 4.23, It is composed of 3 single-phase PUC5 units including 3 isolated PV arrays as DC sources and 18 switches, unlike the classical one which has 1 isolated DC source 6 switches. Three similar PV arrays, each array feeds one phase of the inverter at a rated power of 17 kW which is extracted at voltage of 290 V and at current of 58.8 A (STC), and it is constructed of 10 modules connected in series and 8 modules connected in parallel.

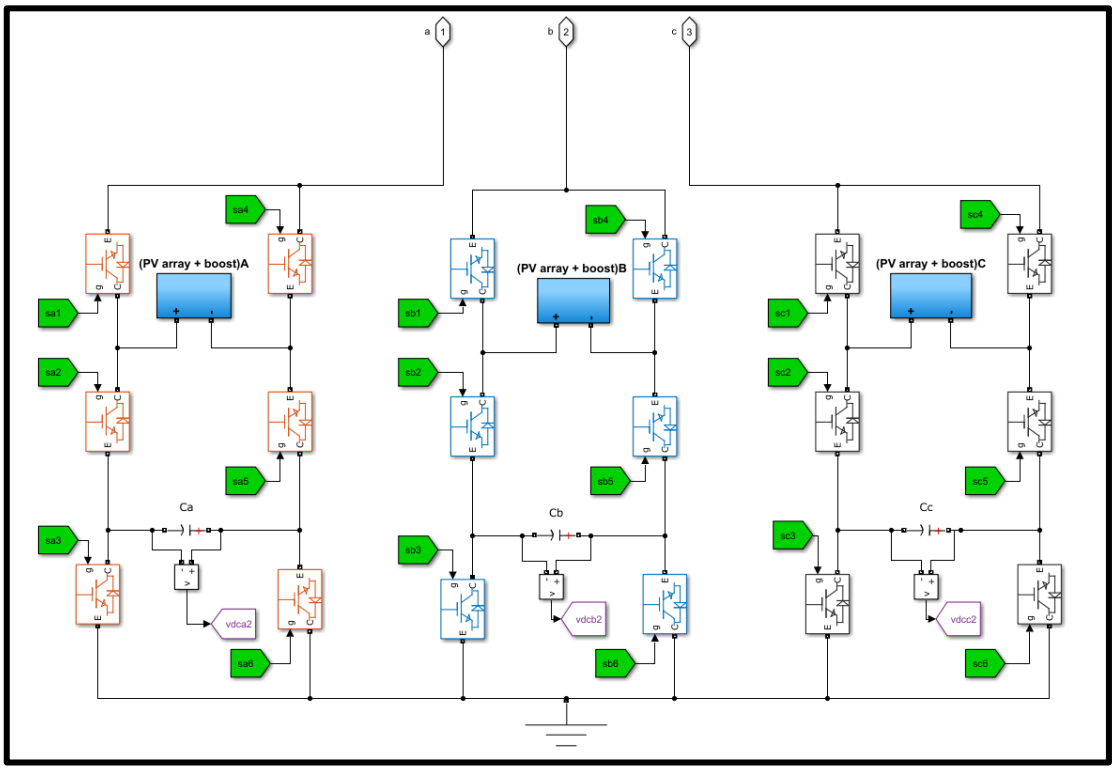

Figure 4. 23: the simulated system of the three phase PUC5 inverter-based Solar-AF

The 3-phase PUC5 inverter testing has been simulated under the same irradiance and load demand conditions, means the same perturbations have been applied in order to perform ulteriorly a fair comparison between both the inverters. The obtained curves of active power and reactive power are shown in the figures below (Figure 4. 26 and Figure 4. 27). As is noticed, the power behavior is similar to the earlier results, however, this time the smoothness of the power curves makes a noticeable difference as well as a fewer fluctuation.

4.4.1 Simulation Results

The results of PV output voltage (V_{PV}), current (I_{PV}), power (P_{PV}) and the DC link voltage (V_{dc}) are demonstrated in Figure 4.24.

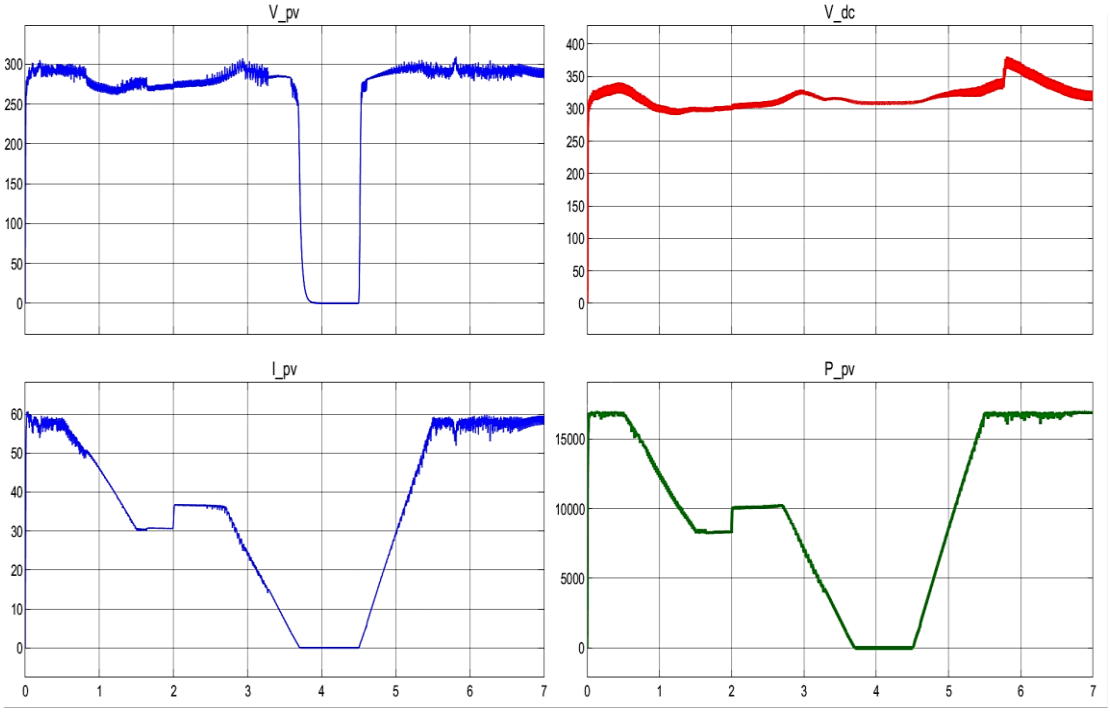

Figure 4. 24: Demonstration PV Output Voltage, Current, Power and The DC Link of phase A for All the Simulation using PUC5.

The output power of the three groups (phases) are displayed in Figure 4. 25, it can be noticed that the three phases power curves are almost identical means the phases produce the exact same amount of power, this is what significates the well balancing of the system and its control accuracy.

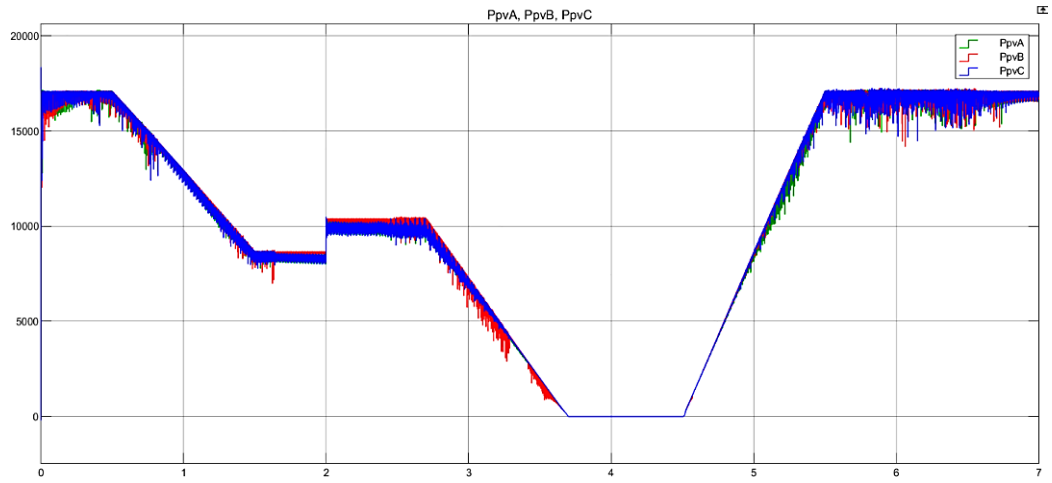

Figure 4. 25: Display of the output power of phases A, B and C

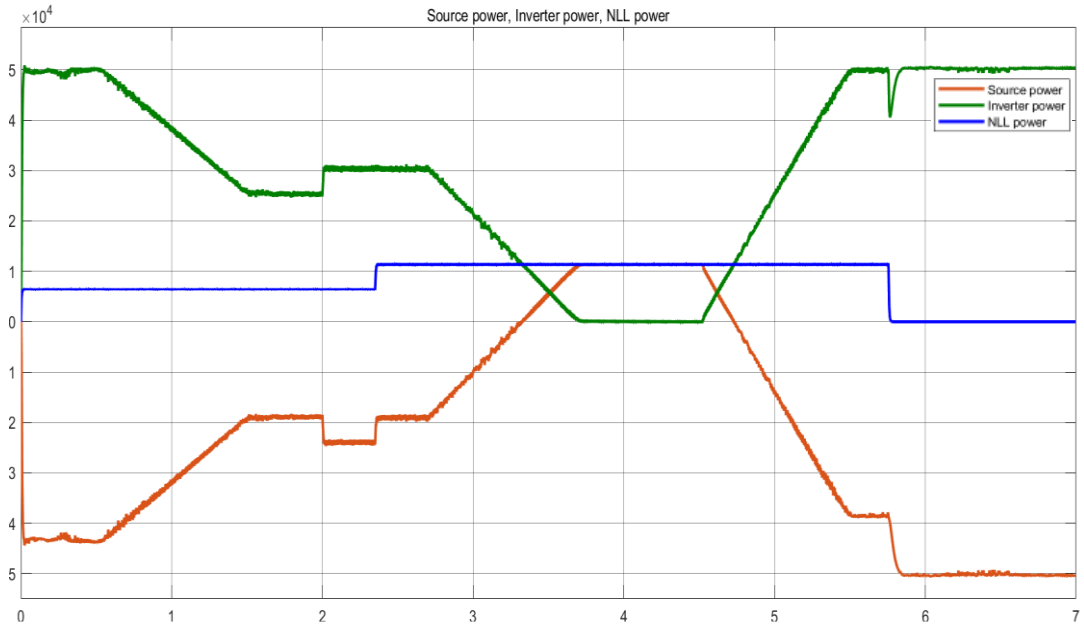

Figure 4. 26: Active power curves of source, load and inverter during the simulation time using PUC5 inverter

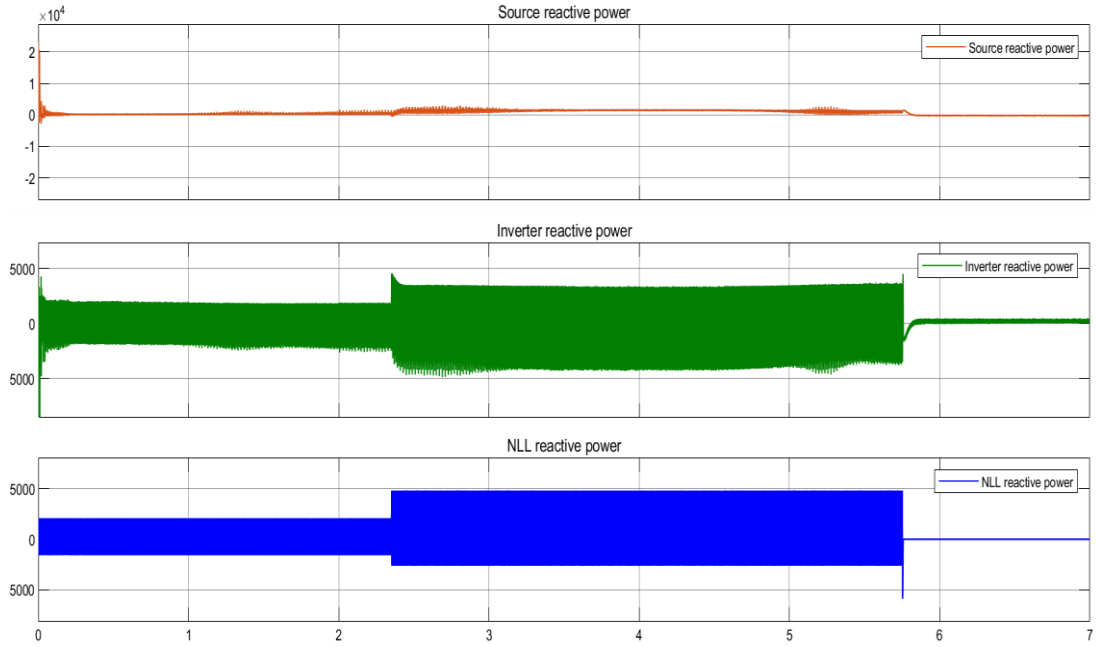

Figure 4. 27: Source, nonlinear load and inverter reactive power in all the simulation using PUC5 inverter

The high accuracy of active and reactive power compensation is obvious on its curves. Moreover, a sample of the grid voltage and current is shown in Figure 4. 28, here it is possible to take a closer look on the phase angle between voltage and current. The phase shift is exactly 0^{o} which implies a zero reactive power is generated by the source besides a unity power factor is achieved.

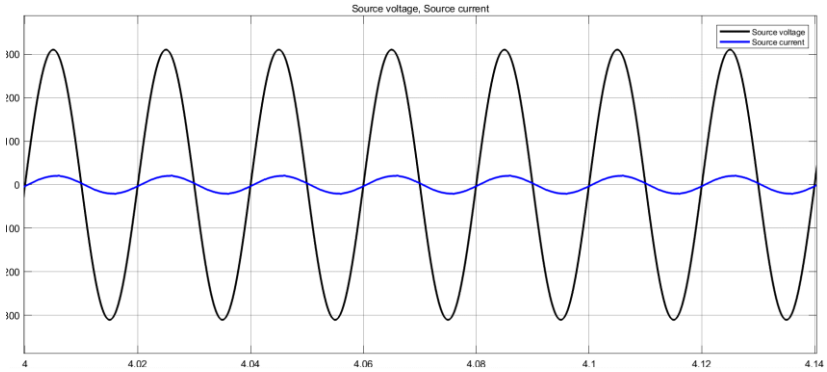

Figure 4. 28: Source current and source voltage

At each phase, a stable DC voltage source of 311V is needed to feed of the PUC inverter at V_{bus}. Each of these voltages is supplied by an isolated PV array output voltage which are continuously perturbed by the MPPT P&O algorithm and the conditions variations. A PID controller-based voltage regulator is used to provide the three DC link voltages. Figure 4.29 shows the DC link voltages at each phase.

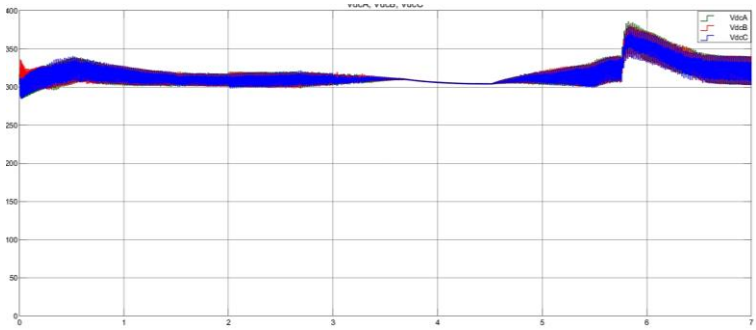

Figure 4. 29: The DC link voltages at each phase in all the simulation

As mentioned before three isolated DC sources are needed, each DC source has been set at 311V, so the capacitors voltages are regulated at half the DC sources which is 155.5V. The three phase PUC5 inverter could generate a 5-level voltage waveform at each phase. As shown in Figure 4. 30.

The output phase voltage is 5-level ($\pm$ 311 V , $\pm$155.5 V and 0 V).

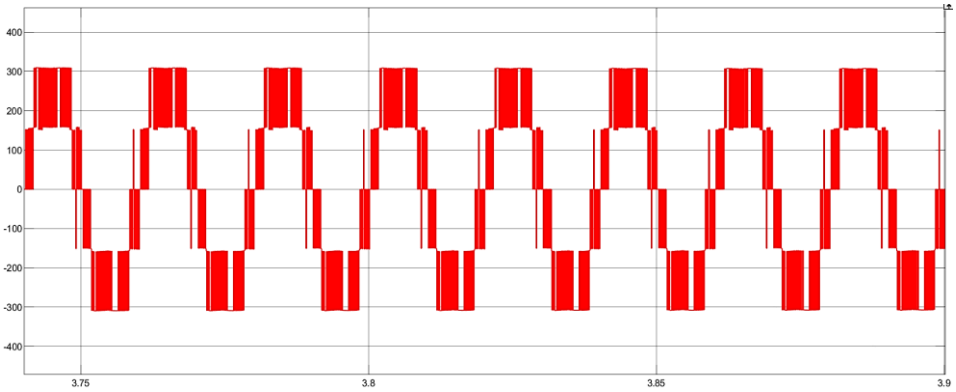

Figure 4. 30: demonstration of a one phase output voltage of PUC5 inverter

To validate the above analysis a detailed investigation has been performed only into the most significant sections of the simulation (involving the main modes of

operation), mainly the demonstrations of currents and FFT analysis of source current (THD) levels are considered.

4.4.1.1 System performance at irradiance of 1000 W/m^2 [0s,0.5s]

By keeping the irradiance on the first array constant at 1000 W/m2 (STC), It is clear from Figure 4. 25 that the proposed controller is capable of extracting the MPPT from each PV array (phase A is demonstrated in figure below). Besides, the inverter generated current that contains also the compensating harmonic components (mode of power injection and harmonics mitigation). Therefore, the source is absorbing a pure sinusoidal current.

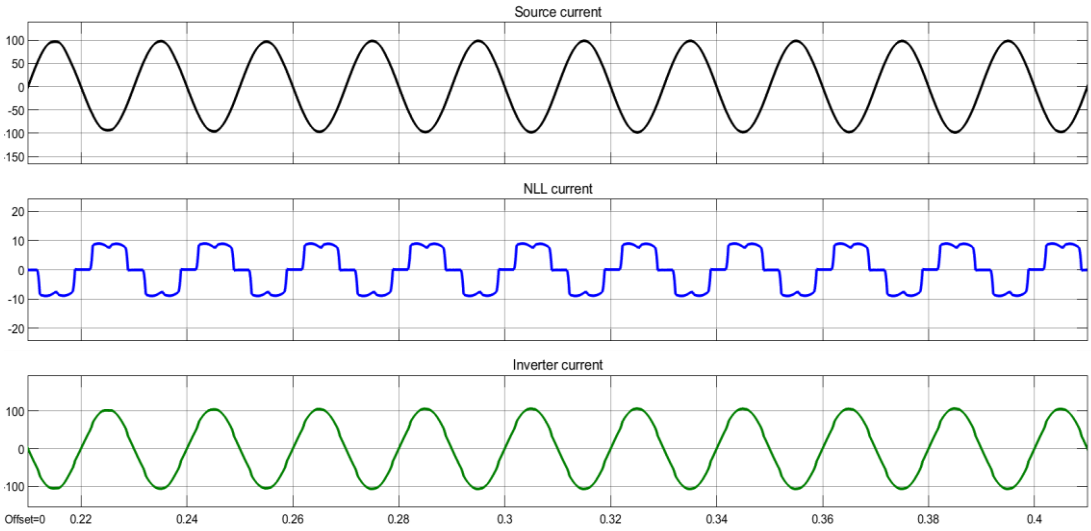

Figure 4. 31: demonstration of grid current, load current and filter current under 1000W/m^2 (PUC5 inverter)

The THD measurement of phase A current shows an excellent result of is 0.40 %, which is less than 5% according to IEEE 519-1992

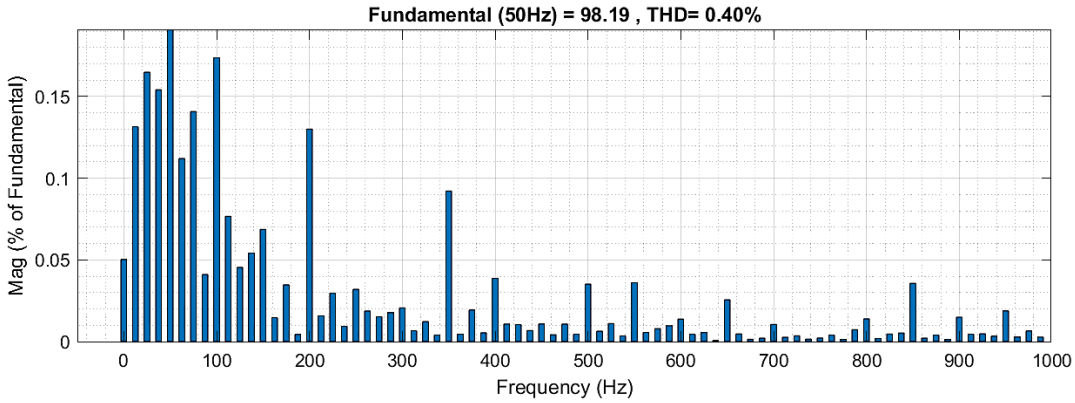

Figure 4. 32: FFT analysis tool for the source current of the system under 1000 W/m^2(PUC5 inverter)

4.4.1.3 System performance at irradiance of 0 W/M^2 [3.75s,4.5s]

In night conditions, the system behaves as an APF where it produces only a harmonic mitigating current.

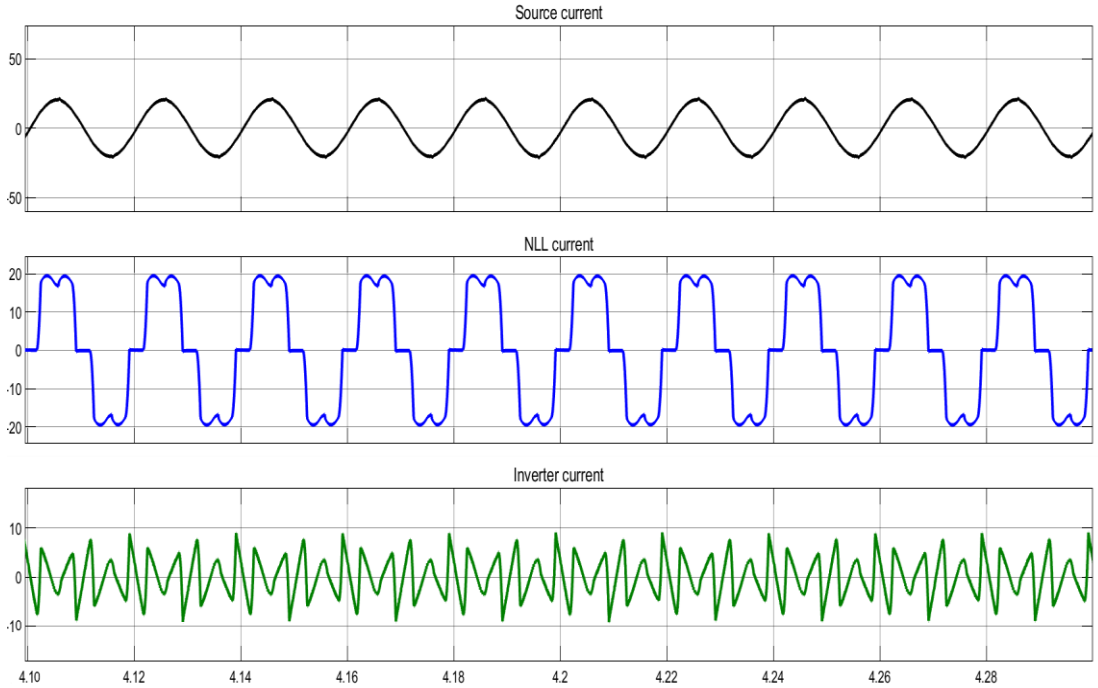

Figure 4. 33: Demonstration grid current, load current and filter current under 0 W/m^2 (PUC5 inverter)

The smoothness of the source current sinewave can be evaluated through the FFT analysis tool for the source current, the THD under zero irradiance is 1.48%, which is less than 5% according to IEEE 519-1992.

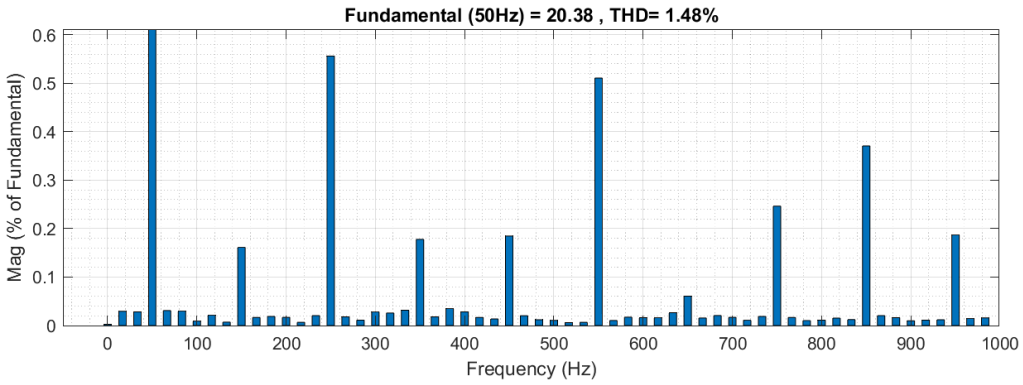

Figure 4. 34: FFT analysis tool for the source current of the system under 0 W/m^2 (PUC5 inverter)

4.4.1.2 System performance at irradiance of 1000 w/m^2 with additional load demand [5.5s,5.75s]

The system is working under the same irradiance condition (same mode) but with extra load demand, the current shape is so identical to be seen with the eye, however The THD of phase A current have sightly increased to 0.86%, which is even typical compared to 5% according to IEEE 519-1992.

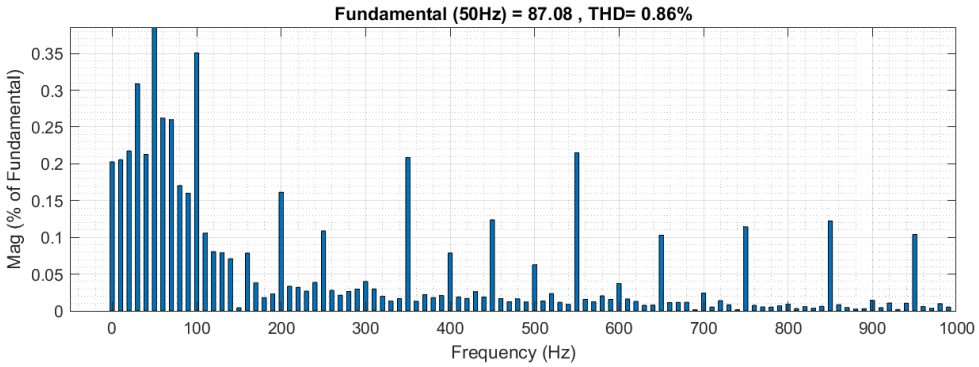

Figure 4. 35: FFT analysis tool for the source current of the system under 1000 W/m^2 (PUC5 inverter)

4.4.1.4 System performance without Load [5.75s,7s]

After the disconnection of nonlinear, the inverter current is totally directed to the grid injection with no harmonic compensation is needed. The system is analogous to a grid connected PV system.

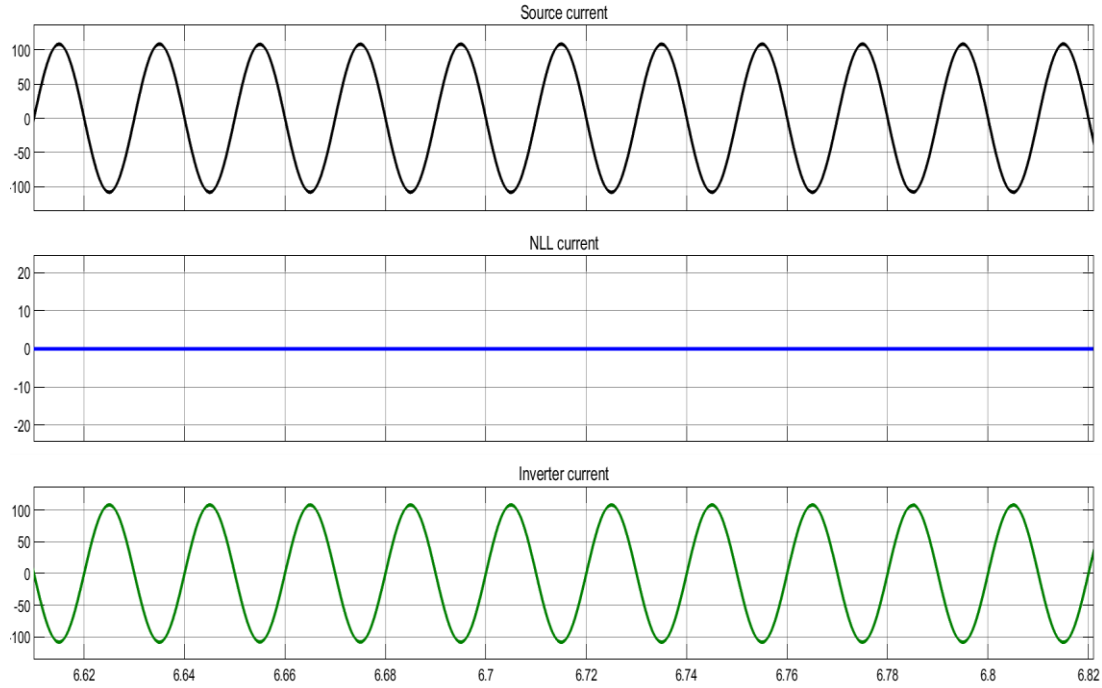

Figure 4. 36: Demonstration grid current, load current and filter current without load (PUC5 inverter)

The THD of phase A current with disconnected nonlinear load is 0.19 %, which is less than 5% according to IEEE 519-1992.

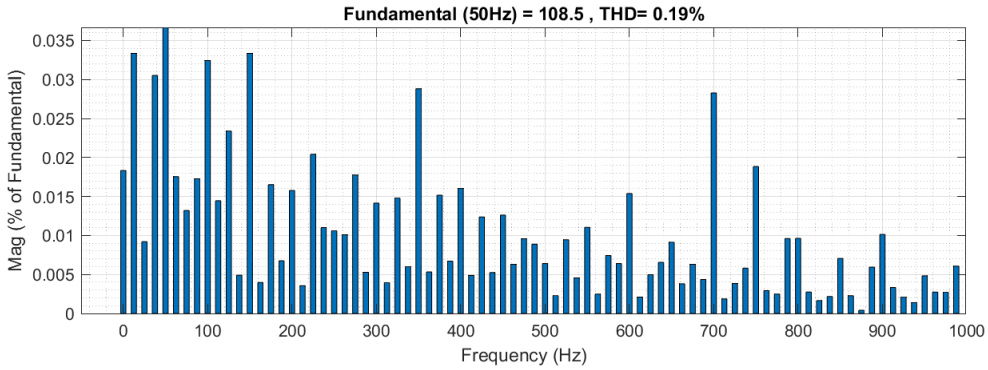

Figure 4. 37: FFT analysis tool for the source current of the system without load (PUC5 inverter)

4.5 Comparison and Evaluation

In the aim of evaluation, the simulation results of the system when using the PUC5 inverter are compared to those when using the classical inverter in terms of THD, power factor and Power losses. The results are in Table 4. 2.

Table 4. 2: Comparison in terms of THD, power factor and power loss between Classical inverter and PUC5 inverter-based Solar-AF systems.

		Main time intervals			
	Inverter type	From 0s to 0.5s	From 3.75s to 4.5s	From 5.5s to 5.75s	From 5.75s to 7s
THD (%)	2 level	1.82	3.38	3.94	1.24
	PUC5	0.40	1.48	0.86	0.19
Power factor	2 level	-0.99975	0.99870	-0.99211	-0.99999
	PUC5	-0.99998	0.98865	-0.99953	-0.99999
L filter size	2 level	Lf_load= 10 mH; Lf_inv= 15 mH;			
	PUC5	Lf_load= 1.5 mH; Lf_inv= 3 mH;			
Efficiency (%)	2 level	99.96			
	PUC5	99.92			

- As it is clear, PUC5 achieved amazing THD levels compared to the Classical inverter. Thus, giving more evidence to that adding extra levels to the voltage waveform diminishes the THD.
- The reactive power compensation is done using the same technique, based on the p-q theory extracts the fundamental and harmonics information from the polluted load current in to estimate a compensating reference current. Consequently, a very close power factor unitary is performed. It is noticed that in cases other than 0 W/m^2, the power factor is negatively signed this refers to that the grid is absorbing power.
- Due to generating more voltage levels at the output, PUC5 inverter is expected to generate lower harmonic current waveform injecting to the grid compared to

classical inverters. As result, the load voltage and current are nearly sinusoidal. An additional investment in any filters is barely needed.

- Similarly, both inverters are working at the same power and voltage ratings and under the same MPPT technique, therefore, they are working at almost the same efficiency.

4.6 Results Discussion

- Figure 4.7 and Figure 4.26 display the curves of active power, we deduce that the proposed system can work in different modes; shunt AF mode and/or power injection mode, depending on the load demand, harmonic distortions and the available irradiance.
- For a high enough irradiance (1000 W/m^2,500 W/m^2…), the PV generated power is greater than the load the demand, thus the Solar-AF delivers power to the load and the excess is injected into the grid. However, under 0 W/m^2, the grid supplies the load with its power demand, while the reactive power and harmonics are still composited by Solar-AF. Therefore, the proposed system can guarantee a unity power without being affected by the irradiance deviations.
- The proposed Solar-AF system is capable of eliminating harmonic currents, reactive power compensation, grid currents balancing, and adaptive DC link voltage regulation in addition to peak power extraction from a photovoltaic (PV) array.
- PUC5 inverter has proved its merit to generate lower harmonic current waveform at extremely low THD injecting to the grid compared to classical e grid-connected inverter due to generating more voltage levels at the output. The PUC multi-level inverter is used in this work which has low switch, capacitor count and L filter size as compared to other multilevel inverters. Moreover, using more switching components can produce more power losses.
- Results validate the efficiency of the 5-level PUC Solar-AF in eliminating the nonlinear load harmonics and also prove the good dynamic performance of the implemented controller.

4.7 Conclusion

The simulation of Solar-AF using either the classical inverter or the PUC5 inverter was successfully investigated in this chapter. In both cases, the Solar-AF is equipped with the P&O algorithm which was efficiently able to track and delivering a maximum PV power, and the reactive power and harmonics compensation was fulfilled properly. The presented simulation results validated the superior performance of the 3-phase PUC5 inverter, specially reducing the total harmonic distortion rate far less than 5% compared with the classical inverter.

General conclusion and future works

In this report, the proposed Solar-AF is used as an interconnection between the renewable energy generation and the utility electric grid. the Solar-AF do not only manage the power injection, but also offering additional power quality improvement features including harmonic currents mitigation, reactive power compensation, power factor unitary, and grid currents quality improvement.

For a maximum power extraction from the PV array, the DC-DC boost converter is provided with a maximum power point tracking (MPPT) as control technique which is based on perturb and observe (P&O) algorithm. The results of simulation prove that it works with a dynamic response and a stability in its performance even under the variable atmospheric conditions.

The proper work of an active power filter (APF) based on a voltage source inverter (VSI) necessitates the availability of reference signal. This later affords the necessary components of compensation the instantaneous p-q theory is applied for the generation of the reference signal. It is very common for the control of APFs due to its precise reference calculation besides that it offers a separate control for instantaneous active and reactive powers.

In this work, the three phase APF was proposed to reduce harmonic current at the PCC point caused by nonlinear loads. This was achieved by considering suitable controls of the three-phase grid interactive inverters. Hysteresis current control (HCC) method has been used for generating gate pulses for the classical inverter control with simple and good transient response. In the other hand, a model predictive control (MPC) has been considered for 5-level PUC inverter, offering a fast response with sinusoidal line currents at very low THD, besides, a perfect balancing of the DC-link capacitor voltage.

For further works, we suggest:

- To improve the MPPT technique by adopting particle swarm optimization (PSO), which can work under non-uniform irradiance conditions (partial shading).
- The 5-levels packed U-cell inverter can be upgraded into 7-level through some adjustments on its control strategy, or into 25-level by using two converters in cascade.
- To use fuzzy logic control instead of PID for additional accuracy in the DC voltage regulations.
- To extend the application of PUC5 to other types of renewable energies such as wind energy.
- To employ the PUC5 inverter in different situations where it works in rectification mode.

Appendix

Appendix A: Sim power diagram of solar-AF

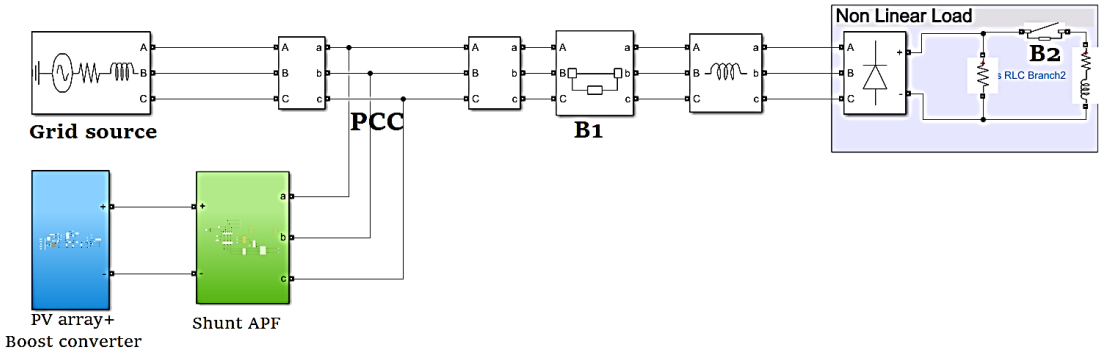

Figure A. 1: Shunt active power filter scheme

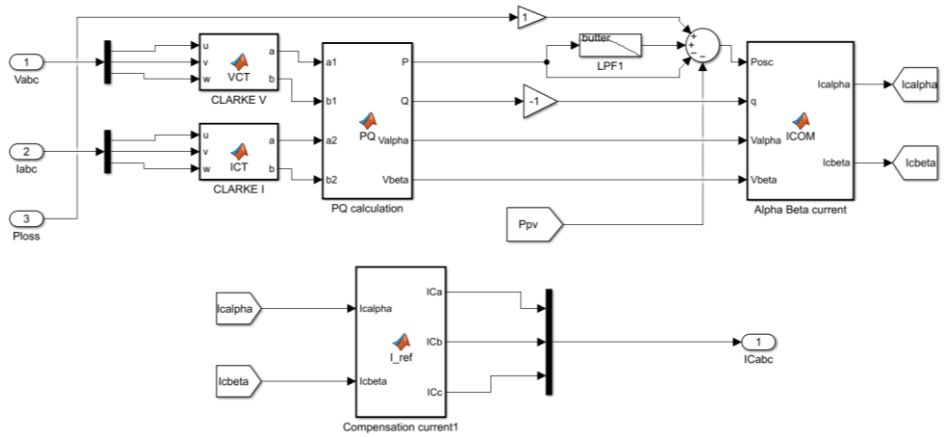

Figure A. 2:P & Q and compensating current calculation

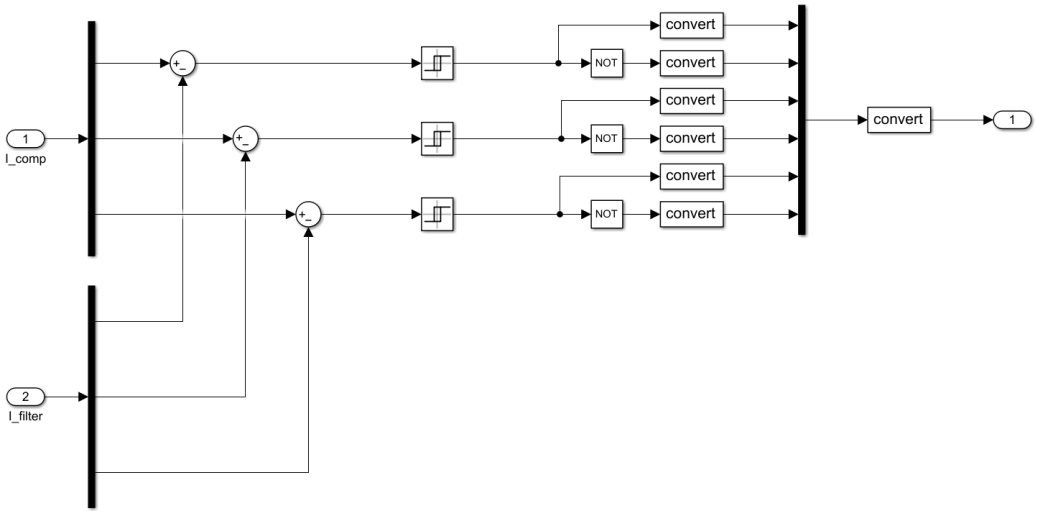

Figure A. 3: Hysteresis Current Control

Appendix B: MPC of solar-AF

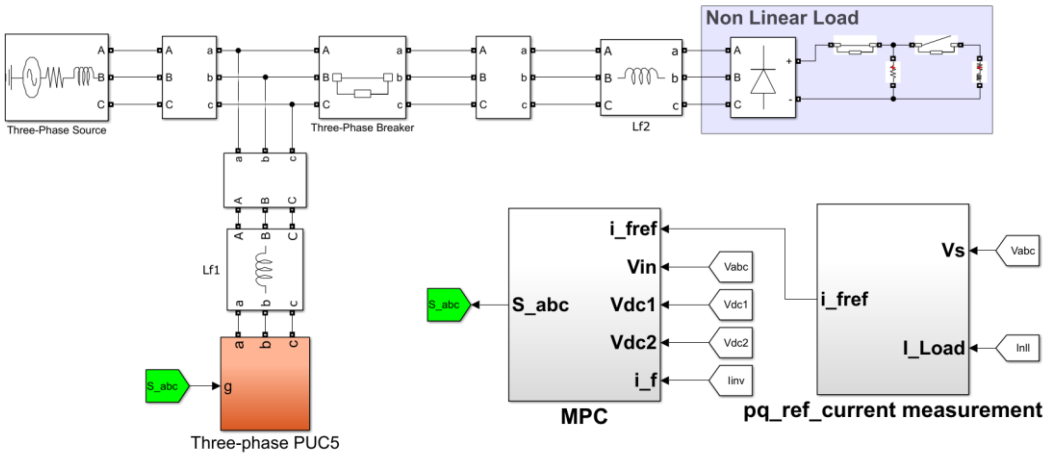

Figure B.1: Overall system diagram of PUC5 Three-phase inverter-based Solar-AF

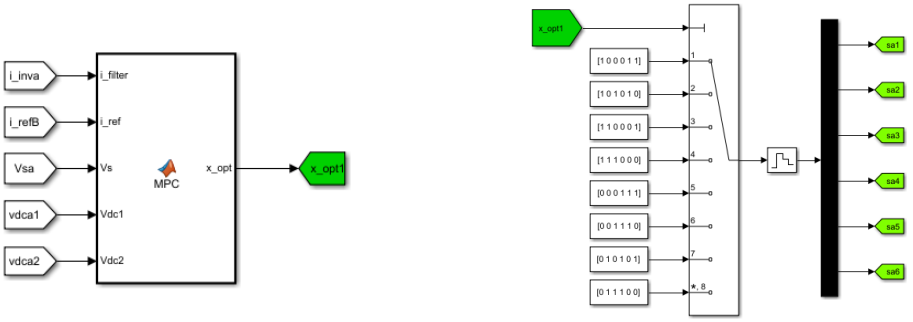

Figure B. 2: MPC scheme per phase

Appendix C: PV module datasheet

PV Panel specification	
PV model	1STH-215-P
Short circuit current (Isc)	7.84 A
Open circuit voltage (Voc)	36.3 V
Maximum Voltage (Vmpp)	29 V
Maximum current (Impp)	7.35 A
Maximum power (Pmpp)	213.15 W
Number of cells in series (Ns)	60
Temperature coefficient of Isc	-0.36099%/°C
Temperature coefficient Voc	0.102%/°C
Diode ideality factor (A)	0.98117
Series resistance (Rs)	0.39383Ω
Shunt resistance (Rsh)	313.3991Ω

Figure C.1: Soltech 1STH-215-P PV module specifications

References

[1] M.C. Falvo, F. Foiadelli, "Preliminary analysis for the design of an energy-efficient and environmental sustainable integrated mobility system", IEEE PES Gen. Meet. PES (2010) ,pp.1–7, 2010.

[2] T. C. Kandpal and L. Broman. "Renewable energy education: A global status review", Renewable and Sustainable Energy Reviews, vol. 34, pp. 300-324, 2014.

[3] A. Tripathy, "Renewable energy at a glance", Akshay Urja, vol. 6, no. 5, pp. 103, 2013.

[4] W. William, A. Lunnan, E. Nybakk and B. Kulisic "The role of governments in renewable energy: The importance of policy consistency", Biomass and bioenergy, vol. 57 pp. 97-105, 2013.

[5] N Dahlan, Mohd Jusoh and W Abdullah, "Solar grid parity for Malaysia: Analysis using experience curves", IEEE Power Engineering and Optimization Conference (PEOCO), 2014, pp.46l-466.

[6] Recommended Practice for Harmonic Control in Electric Power Systems, IEEE Std. 519-1992, 1992.

[7] Limits for Harmonic Current Emission, IEC 61000-3-2, 2001.

[8] P. Salmeron and S. Litran, "Improvement of the Electric Power Quality Using Series Active and Shunt Passive Filters", IEEE Transactions on Power Delivery, vol. 25, no. 2, pp. 1058-1067, 2010.

[9] Rahmani, S., Mendalek, N., and Al-Haddad, K., "Experimental design of a nonlinear control technique for three-phase shunt active power filter", IEEE Trans. Ind. Electron., Vol. 57, No.10, pp. 3364–3374, 2010.

[10] Chaoui, A., Gaubert, J.-P., Krim, F., and Champenois, G., "PI controlled three-phase shunt active power filter for power quality improvement", Electr. Power Compon. Syst., Vol. 35, pp. 1331–1344, 2007.

[11] Yacine Ayachi Amor, Farid Hamoudi, Aissa Kheldoun, Gaëtan Didier, Zakaria Rabiai, "Fuzzy logic enhanced control for a single-stage grid-tied photovoltaic system with shunt active filtering capability", p.3, 21 June 2021

[12] International Energy Outlook 2019 with projections to 2050, pp.1– 169.U.S. Energy Information Administration and U.S. Department of Energy, Washington, DC 20585 ,2019

[13] Renewable Energy Policy Network for 21st Century (REN21). Renewable 2018 Global Status Report, (2018)

[14] Yacine Ayachi Amor, Farid Hamoudi, Aissa Kheldoun, "Three-phase Three-level Inverter Grid-tied PV System with Fuzzy Logic Control based MPPT", ALGERIAN JOURNAL OF SIGNALS AND SYSTEMS (AJSS), p.101, September 2018

[15] Kulkarni Kedar S, Bhosale Yash S,Thorat Rutuja D, Shinde Tanmay A, Shruti Nema, Power Quality Improvement Using Unified Power Quality Conditioner, p01, APRIL 2022

[16] J Sreedevi, Ashwin N, M Naini Raju, A Study on Grid Connected PV system, p01, April 2022.

[17] Edvard, Oct 20 2014, "9 Most Common Power Quality Problems", https://electrical-engineering-portal.com/9-most-common-power-quality-

problems#:~:text=The%20most%20common%20types%20of,Long%20interruptions (accessed: May,15,2022)

[18] Zia Hameed, Muhammad Rafay Khan Sial , Adnan Yousaf , Muhammad Usman Hashmi, “Harmonics in Electrical Power Systems and how to remove them by using filters in ETAP", p02, 26 January 2020.

[19] IEEE Std 141-1993 IEEE Recommended Practice for Electric Power Distribution for Industrial Plants. The Institute of Electrical and Electronics Engineers, New York, 1993.

[20] FRANCISCO C. DE LA ROSA, harmonics and power systems, p93, 2006.

[21] Hussein A. Kazem, Harmonic Mitigation Techniques Applied to Power Distribution Networks, pp[1-3], 2013.

[22] J. C. Das, Power System Analysis, Short-Circuit Load Flow and Harmonics, Marcel Dekker, New York, NY, USA, 2002.

[23] D. Alexa, A. Sˆırbu, and D. M. Dobrea, “An analysis of three phase rectifiers with near-sinusoidal input currents”, IEEE Transactions on Industrial Electronics, vol. 51, no. 4, pp. 884–891, 2004

[24] B. Singh, B. N. Singh, A. Chandra, K. Al-Haddad, A. Pandey,and D. P. Kothari, “A review of three-phase improved power quality AC-DC converters”, IEEE Transactions on Industrial Electronics, vol. 51, no. 3, pp. 641–660, 2004

[25] P. J. A. Ling and C. J. Eldridge, “Designing modern electrical systems with transformers that inherently reduce harmonic distortion in a PC-rich environment”, in Proceedings of the Power Quality Conference, pp.166–178, 1994.

[26] J. C. Read, “The calculation of rectifier and inverter performance characteristics”, Journal of the Institute of Electrical Engineers, vol. 92, no. 2, pp. 495–509, 1945.

[27] E. J. Cham and T. R. Specht, “The ANSI 49 rectifier with phase shift”, IEEE Transactions on Industry Applications, vol. 20, no. 3, pp. 615–624, 1984.

[28] R. Hammond, L. Johnson, A. Shimp, and D. Harder, “Magnetic solutions to line current harmonic reduction”, in Proceedings of the Europe by International Power Conversion Conference (PCIM ’94), pp. 354–364, San Diego, Calif, USA, 1994.

[29] S. Kim, P. N. Enjeti, P. Packebush, and I. J. Pitel, “A new approach to improve power factor and reduce harmonics in a three-phase diode rectifier type utility interface”, IEEE Transactions on Industry Applications, vol. 30, no. 6, pp. 1557–1564,1994.

[30] S. Choi, P. N. Enjeti, and I. J. Pitel, “Polyphase transformer arrangements with reduced kVA capacities for harmonic current reduction in rectifier-type utility interface”, IEEE Transactions on Power Electronics, vol. 11, no. 5, pp. 680–690,1996.

[31] B. M. Bird, J. F. Marsh, and P. R. McLellan, “Harmonic reduction in multiplex converters by triple-frequency current injection”, Proceedings of the Institution of Electrical Engineers, vol. 116, no. 10, pp. 1730–1734, 1969.

[32] Hussein A. Kazem, “Harmonic Mitigation Techniques Applied to Power Distribution Networks”, p05,2013

[33] G. W. Chang and T. C. Shee, “A novel reference compensation current strategy for shunt active power filter control”, IEEE Transactions on Power Delivery, vol. 19, no. 4, pp. 1751–1758, 2004.

[34] H. Akagi, “Control strategy and site selection of a shunt active filter for damping of harmonic propagation in power distribution systems”, IEEE Transactions on Power Delivery, vol.12, no. 1, pp. 354–362, 1997.

[35] A. Cavallini and G. C. Montanari, “Compensation strategies for shunt active-filter control”, IEEE Transactions on Power Electronics, vol. 9, no. 6, pp. 587–593, 1994.

[36] H. Akagi, H. Fujita, and K. Wada, “A shunt active filter based on voltage detection for harmonic termination of a radial power distribution line”, IEEE Transactions on Industry Applications, vol. 35, no. 3, pp. 638–645, 1999.

[37] H. Fujita and H. Akagi, “A practical approach to harmonic compensation in power systems—series connection of passive and active filters”, IEEE Transactions on Industry Applications, vol. 27, no. 6, pp. 1020–1025, 1991.

[38] F. Z. Peng, H. Akagi, and A. Nabae, “A new approach to harmonic compensation in power systems—a combined system of shunt passive and series active filters”, IEEE Transactions on Industry Applications, vol. 26, no. 6, pp. 983–990, 1990.

[39] D. Basic, V. S. Ramsden, and P. K. Muttik, “Hybrid filter control system with adaptive filters for selective elimination of harmonics and inter harmonics”, IEE Proceedings: Electric Power Applications, vol. 147, no. 4, pp. 295–303, 2000.

[40] S. Senini and P. J. Wolfs, “Hybrid active filter for harmonically unbalanced three phase three wire railway traction loads”, IEEE Transactions on Power Electronics, vol. 15, no. 4, pp. 702–710, 2000.

[41] P. Salmeron, J. C. Montano, J. R. V ´ azquez, J. Prieto, and A. ´Perez, “Compensation in non-sinusoidal, unbalanced three- ´ phase four-wire systems with active power-line conditioner”, IEEE Transactions on Power Delivery, vol. 19, no. 4, pp. 1968– 1974, 2004.

[42] H. Akagi, “New trends in active filters for power conditioning”, IEEE Transactions on Industry Applications, vol. 32, no. 6, pp.1312–1322, 1996

[43] H. L. Jou, J. C. Wu, and K. D. Wu, “Parallel operation of passive power filter and hybrid power filter for harmonic suppression”, IEEE Proceedings: Generation, Transmission and Distribution, vol.148, no. 1, pp. 8–14, 2001.

[44] X. Zha and Y. Chen, “The iterative learning control strategy for hybrid active filter to dampen harmonic resonance in industrial power system”, in Proceedings of the IEEE International Symposium on Industrial Electronics, vol. 2, pp. 848–853, 2003.

[45] energyresearch.ucf.edu,’ Cells, Modules, Panels and Arrays’, https://energyresearch.ucf.edu/consumer/solar-technologies/solar-electricity-basics/cells-modules-panels-and-arrays/#:~:text=Photovoltaic%20panels%20include%20one%20or,of%20PV%20modules%20and%20panels.(accessed : May,25,2022)

[46] Modeling of Photovoltaic Module,” https://www.intechopen.com/chapters/75972” (accessed: May,25,2022).

[47] K.A. Ibrahim, P.M. Gyuk, S. Aliyu,"THE EFFECT OF SOLAR IRRADIATION ON SOLAR CELLS",Science World Journal Vol 14(N o1),p20, 2019

[48] M.Tampubolon, I. Purnama, P. C. Chi, J. Y. Lin, Y. C. Hsieh, H. J. Chiu," A DSP-Based Differential Boost Inverter with Maximum Power Point Tracking," 9th International Conference on Power Electronics ECCE Asia, pp. 309 – 314, 1-5 June 2015.

[49] components101, "Boost Converter: Basics, Working, Design & Operation", https://components101.com/articles/boost-converter-basics-working-design.(Accessed: May,27,2022)

[50] Mohan, N, Undeland, TM, Robbins, WP. Power Electronics: Converters, Applications, and Design. Third Edition. New Jersey: John Wiley & Sons, Inc. 2003.

[51] Zhang, S, Yu, X. Control strategy to achieve minimum/zero input current ripple for the interleaved boost converter in photovoltaic/fuel cell power conditioning system. IEEE Energy Conversion Congress and Exposition 2012; 2012: 4301-4306.

[52] B. Singh, M. Kandpal, and I. Hussain, "Control of grid tied smart PVDSTATCOM system using an adaptive technique," IEEE Trans. Smart Grid, vol. 9, no. 5, pp. 3986–3993, Sep. 2018.

[53] tntech.edu, 'CHAPTER4: Model of three-phase inverter', "https://www.tntech.edu/engineering/pdf/cesr/ojo/asuri/Chapter4.pdf". (Accessed: May,28,2022)

[54] K. Al-Haddad, Y. Ounejjar, and L. A. Gregoire, "Multilevel Electric Power Converter," US Patent 20110280052, Nov 2011.

[55] G. V. V. Nagaraju, G. Sambasiva Rao," Three phase PUC5 inverter fed induction motor for renewable energy applications", International Journal of Power Electronics and Drive System (IJPEDS)Vol. 11, No. 1, March 2020, pp. 1~9,2020

[56] M.Gowtham, J.Gowri Shankar, M.Balasubramani," A Seven Level Packed U Cell (Puc) Multilevel Inverter For Photovoltaic System", International Journal of Applied Engineering esearchISSN 0973-4562 Volume 10, Number 6 (2015) pp. 15237-15250,2015

[57] Hani Vahedi, Mohammad Sharifzadeh, Kamal Al-Haddad Topology and Control Analysis of Single-DC-Source Five-Level Packed U-Cell Inverter (PUC5), pp. (2,3),26 December 2017.

[58] H. Vahedi, P. A. Labbé, and K. Al-Haddad, "Sensor-Less Five-Level Packed U-Cell (PUC5) Inverter Operating in Stand-Alone and Grid Connected Modes", IEEE Trans. Ind. Informat., vol. 12, pp. 361 370, 2016.

[59] Y. Ounejjar, K. Al-Haddad, and L. A. Gregoire, "Packed U Cells Multilevel Converter Topology: Theoretical Study and Experimental Validation," IEEE Trans. Ind. Electron., vol. 58, pp. 1294-1306, 2011.

[60] automationforum.co, "Why synchronizing is required in an electrical power system?",https://automationforum.co/why-synchronizing-is-required-in-an-electrical-power-system/.(Accessed May,14,2022)

[61] brighthubengineering.com, Nonlinear Loads and Harmonics in Power Systems'. https://www.brighthubengineering.com/power-generation-distribution/89979-nonlinear-loads-on-electric-power-systems-cause-problems-for-local

utilities/#:~:text=A%20nonlinear%20load%20in%20a,These%20components%20are%20called%20harmonics, (Accessed: May,14,2022)

[62] AGN 025 ISSUE B, "Non-Linear Loads", Generator technologies, p1.

[63] C. Khomsi, M. Bouzid, K. Jelassi, A New Efficient Technique for Disturbing Current Extraction to Improve the Grid Current Quality in a Three-Phase Grid Connected PV System supplying a Non-Linear Load, p1,2016.

[64] M. Singh, and S. Mahapatra, "Implementation of passive filters for harmonics reduction", Intl Journal of Advanced Science and Technology, vol. 78, pp. 1-12, 2015.

[65] Quin, C., Mohan, N., Active Filtering of Harmonic Currents in Three-phase Four-Wire Systems with Three Phase and Single-Phase Non-Linear Loads, APEC, 1992, pp. 829-836.

[66] Edson H. Watanabe, Hirofumi Akagi, Maurício Aredes, THE P-Q THEORY FOR ACTIVE FILTER CONTROL: SOME PROBLEMS AND SOLUTIONS, p79, 2004.

[67] Amir A. Imam, R. Sreerama Kumar and Yusuf A. Al-Turki, Modeling and Simulation of a PI Controlled Shunt Active Power Filter for Power Quality Enhancement Based on P-Q Theory, p5, 13 April 2020.

[68] Reza Noroozian, Gevorg B. Gharehpetian, An investigation on combined operation of active power filter with photovoltaic arrays, p.5 30 November 2012.

[69] A. B. Plunkett," A current controlled PWM transistor inverted drive," in Conf. Rec. IEEE-IAS Annu. Meeting, 1979, pp. 785–792.

[70] Reza Noroozian , Gevorg B. Gharehpetian,"An investigation on combined operation of active power filter with photovoltaic arrays", International Journal of Electrical Power & Energy Systems, Volume 46, March 2013, Pages 392-399

[71] Zakaria Mohamed Salem Elbarbary, "Review of maximum power point tracking algorithms of PV system''Frontiers in Engineering and Built Environment, p 70, 2021

[72] S. Kouro, P. Cortés, R. Vargas, U. Ammann, J. Rodríguez, "Model predictive control—a simple and powerful method to control power converters", IEEE Trans. Ind. Electron. 56 (2009) 1826–1838.

[73] J. Rodriguez, P. Cortes, Predictive Control of Power Converters and Electrical Drives, John Wiley & Sons, 2012.

[74] Abdeslem Sahli, Fateh Krim, Abdelbaset Laib, Billel Talbi, "Model predictive control for single phase active power filter using modified packed U-cell (MPUC5) converter", Electric Power Systems Research, p3, 2020